TRMM Science Operations Plan

Executive Summary

The atmosphere gets three-fourths of its heat energy from the release of latent heat by precipitation. Two thirds of global precipitation falls in the tropics and rain variability in low latitude affects the weather around the world. Precipitation is the most difficult atmospheric variable to measure, mainly because of its concentration into a few cloud systems. The most important impact of rain and its variability is on the biosphere, including humans. The "average' rainfall is rarely observed. Instead, several seasons of drought and starvation are often followed by a year or two of torrential downpours and disastrous floods. Tropical rainfall and its variability impact upon the structure of the upper ocean layer by the fresh water from rain and by the wind squalls produced by the large rain cloud systems.

Cloud and rain processes are now simulated fairly well on the scale of cloud ensembles (50-100 km). However, global models for prediction of weather and climate have much coarser resolution, Therefore they must "parameterize" cloud processes. Most of these parameterizations are extremely crude. In the tropics particularly, it is vitally important to have rain and its latent heating in the initialization of global weather and climate models as well as in their prediction stage. Presently there are large discrepancies among the results of the different models. All of these models do badly in predicting precipitation and soil moisture. The poor simulation of cloud properties is one of the factors causing the models to differ so widely regarding the amount of global warming with doubled carbon dioxide. Scarcity of quantitative precipitation information has been a frustrating long-time bottleneck for atmospheric science. This gap in the centerpiece of the hydrologic cycle has had negative impacts on nearly all Earth sciences and their applications. Since the tropics are 75 per cent covered with ocean, precipitation over the global tropics can be measured satisfactorily only from space.

Based upon a proposal by Goddard scientists, the Tropical Rainfall Measuring Mission (TRMM) pre-phase A study was completed in 1985 and presented to the Goddard Center Director as well as the new business committee. In 1988, a formal phase A study outlining a cooperative mission between the U.S. and Japan was completed. Also in 1988, the Science Steering Group report was published under the title "TRMM: A Satellite Mission to Measure Rainfall." It contains the science background, requirements, goals, and specific questions the mission is to address. It spelled out specifications of the rain instruments and suggested how they were envisaged to complement each other. Accuracy requirements and error analyses were included. Congress finally passed a congressional initiative to budget for the TRMM new start in 1991. TRMM was designated as one of the first in NASA's Earth Probe Series, which is part of Mission to Planet Earth. Starting in 1991, the TRMM Project got staffed and organized, the in-house design for the spacecraft got underway and the first Science Team of 31 scientists was selected from over 100 proposals submitted in response to a NASA Research Announcement. Between 1991 and 1994, the instrument complement was finalized. Table 1 shows the final instrument complement.

Table 1
TRMM SENSOR SUMMARY - RAIN PACKAGE
_____

ORBIT: 35° inclination, 350 km altitude, 3 year duration

MICROWAVE RADIOMETER (TMI)	RADAR (PR)	VISIBLE/INFRARED RADIOMETER (VIRS)
10, 19*, 21, 37, 85.5 GHz	14 GHz	0.63 µm & 10 µm
(dual polarized)	4 km footprint	also 1.6, 3.75 &12 µm
*21 km resolution	250 m range res.	@ 2.2 km resolution
760 km swath	220 km swath	720 km swath

Additional (EOS) instruments: CERES (Cloud & Earth Radiant System) & LIS (Lightning Imaging Sensor)

An extensive validation by 10-12 cooperative surface radar sites was further specified at this time.
_____

An official Memorandum of Understanding between the U.S. and Japan was signed on October 20, 1995 by Mr. Goldin for NASA, and Mr. Matsui for NASDA. The agreement calls for NASA to provide the spacecraft, the TMI, VIRS and EOS instruments as well as the primary data processing facility. Japan will contribute the PR and the launch vehicle. A launch data in late 1997 is expected.

A more complete history of the TRMM mission in presented in Chapter 1 of this document. This is followed by the detailed role of the TRMM Science Team (TST) to insure that the overall goals of the TRMM project can be met. Chapter 2 describes the activities needed to insure that the satellite data are properly calibrated and validated. Chapter 3 describes the satellite algorithms selected by the TST and the physical assumptions that underlay these algorithms. Chapter 4 then describes the approach to obtain and calibrate ground based rainfall measurements from around the globe. Chapter 5 deals with ground based radar rainfall algorithm development, their physical assumptions and some validation strategies. Chapter 6 details the plans for the data system including plan for updating existing algorithms during the TRMM flight mission.

Chapter 7 reports on activities related to the error analysis models. Part of the error model can be constructed using existing data sources. Those quantities which are yet unknown will be explored in chapter 8 which deals with TRMM validation field campaigns planned for the 1st and 2nd years of the mission. The report ends with a description of some of the modeling and data assimilation efforts already underway in advance of the TRMM data.

1. TRMM Background and instrument selection

As early as 1981 (Atlas and Thiele, 1981), a group of scientists met at Goddard to discuss the feasibility and challenge of spaceborne missions to measure tropical rainfall. Since the diurnal and semi-diurnal variability of tropical rain is large, the orbit would have to precess. The orbit of the proposed satellite would further have to be inclined in order to maximize sampling in the tropics. An inclination of about 30 degrees was considered. To utilize the microwave part of the spectrum with both adequate resolution and modest antenna sizes, as well as to accommodate the large power requirements of the precipitation radar, the orbit would need to be low altitude also. A major question at that time was whether a low altitude (about 300 km), inclined orbit could adequately sample the rainfall.

Available data at that time came from the GATE experiment. The GATE shipboard radars provided an excellent rain data set over a substantial area in the inter tropical convergence zone off the west coast of Africa. A test orbit was selected to precess through the 24 hours in a month. Extrapolating the area of the GATE data up to boxes about 5° by 5°, studies showed that the sampling error for monthly rain over 5° by 5 boxes should be less than 10 percent. The crucial feature of the GATE rain that allows the low sampling error is that it self-correlates adequately over 12 to 14 hours. North and colleagues have shown similar autocorrelations in other parts of the ITCZ and in the SPCZ. For whole seasons, their analyses show sampling errors of 10 per cent or less over all the tropical oceans. This would allow the TRMM satellite to meet the requirement accuracies needed by the climate modeling community. However, away from the tropical convergence, the observed autocorrelations appeared lower, leading to sampling errors from the TRMM orbit as large as 20-25 per cent, which is not acceptable. Later studies have confirmed that sampling errors appear inversely related to the amounts of rain. Thus, while sampling errors appear to meet accuracy requirements in the inter-tropical convergence zone, further sampling studies using TRMM in combination with other satellite data sources were being conducted. It now appears that sampling errors in those parts of the tropics where "TRMM alone" data show excessive sampling noise can be overcome by blending TRMM data with polar orbiting SSM/I and geostationary data.

At about the same time, some scientists from the U.S. and Japan were advancing the hypothesis that rain measurement from space would be optimized by combining passive microwave sensors with radar measurements. Early in 1984, the NASA headquarters' atmospheric Program Manager held an informal competition for an inexpensive small space mission that could answer focused science questions about the atmosphere and Earth environment. The winner,

TRMM, was proposed by Goddard Scientists North (sampling statistics), Wilheit (microwave) and Thiele (management of space science activities). In 1985, joint aircraft flights with Japan using radar to relate to rainfall showed a common interest in rain measurement from space. The TRMM phase A study was approved at Goddard and formal letters between NASA and NASDA (Japan) were exchanged, starting the official partnership. The agreement was that Japan would build the precipitation radar and provide the launch vehicle, while the U.S. would provide the spacecraft, passive microwave and VIS/IR sensors.

The 20 person TRMM Science Steering Group (SSG), chaired by E. Rasmusson had several joint workshops in both countries, from which two books and numerous research papers were published (see TRMM bibliography). During the SSG deliberations, it was recognized that the vertical profiles of precipitation and related profiles of latent heat release were needed to understand the Madden-Julian waves in the tropics that modulate rain and also those waves which then propagate from the tropics, affecting global weather features far away (teleconnnections). It was also recognized that the profiles of precipitation-sized hydrometeors and of latent heating are not the same, and use of a cloud process simulation would be required to obtain the latent heating profile from that of the TRMM-measured hydrometeors.

In 1987 the phase A study was near completion. The proposed four sensors were a dual frequency, cross track scanning radar, a conically scanning SSM/I and a rehabilitated existing ESMR for the passive microwave, and an AVHRR (slightly modified) for the VIS/IR measurements. The ESMR was included primarily to provide coincident cross-track scanning capabilities to match the radar geometry). It was anticipated that the superior TRMM results could be used, through the visible and infrared measurements, to calibrate the long existing record of geostationary VIS/IR observations, thus leading to the concept of TRMM as a "flying rain gauge". The budget estimate of this configuration considerably exceeded the NASA Headquarters ceiling for the U.S. contribution of $150 million. The Japanese were also having problems funding the radar. As a result, many descoping scenarios for TRMM were investigated. The agreement of the SSG at the end of Phase A was to omit one of the two proposed radar frequencies. This reduction hurt the profiling capability, especially over land, but greatly decreased the weight and power requirements of the radar. The Program Scientist at NASA Headquarters also agreed to cover the science support portion of the mission as well as considerable parts of the Ground Validation program[1] under Research. Further savings resulted from the

---

[1]The final U.S. TRMM Project budget was $240 million, which proved to be extremely tight. Further descoping was required. Those parts of the descoping important to the rain products are listed in Appendix 1.

agreement of the Goddard Space Flight Center to build the TRMM spacecraft[2] in house.

In 1988 the SSG report was published under the title "TRMM: A Satellite Mission to Measure Rainfall." It contains the science background, requirements and desirements[3], goals, and specific questions the mission is to address. It spelled out specifications of the rain instruments and suggested how they were envisaged to complement each other. Accuracy requirements and error analyses were included. This report contains the physics upon which the rain retrieval algorithms are based. Algorithms for the passive microwave were farthest advanced in application. Numerous radar retrieval methods were outlined for different ranges of rain rate, including a class of algorithms that use the Area-Integral and probability matching concepts. A means for getting precipitation profiles over the oceans, using the passive microwave to constrain the radar equation was described. The use of TRMM with other satellite products to obtain rainfall was mentioned, but not outlined in detail. The validation plan and how the ground based radar sites would be used was described in considerable detail. Finally the SSG report defined the levels of the data and presented a preliminary design for the TRMM Information and Data System (TSDIS).

TRMM did not get a "new start" for nearly three years after completion of the Phase A and SSG reports. Finally in late 1990, the pressure exerted by the science community on NASA Headquarters and on Congress led to a congressional initiative to budget for the TRMM new start in 1991. TRMM was designated as one of the first in NASA's Earth Probe Series, which is part of Mission to Planet Earth. At this time, the TRMM Project got staffed and organized, the in-house design for the spacecraft got underway and the first Science Team of 31 scientists was selected from over 100 proposals submitted in response to a NASA Research Announcement.

Between 1991 and 1994, several important changes were made in finalizing the instrument complement to their present flight configuration. The most significant changes to the rain package were the enhancement of the SSM/I copy - renamed the TRMM Microwave Imager (TMI) while the ESMR was deleted. The most significant enhancement to the TMI was the addition of the 10 GHz channel which has a much more linear relationship between brightness temperature T_B and rain rate. Additional modifications of the TMI included moving the water vapor channel from 22.235 GHz to 21.3 GHz in order to avoid saturation in the tropics and changing the instrument look angle in order to exactly match the SSM/I despite the lower altitude of the satellite. The loss of the ESMR, predicated by budget constraints, leads to more complexity in the coregistration of the cross-track scanning PR and VIRS data with the conically

_____

[2]The TRMM spacecraft is the largest that has ever been built in house at Goddard.
[3]A requirement is regarded as essential to a successful mission; a desirement is something that the scientists would like to have to improve the products, if the available resources permit.

scanning TMI data. This complexity has been absorbed into the science algorithms. Changes in the radar consisted primarily in a loss of sensitivity from the desired 0.5 mm hr^{-1} to 0.7 mm hr^{-1}, which will lose the very light rain as well as reflectivity near the tops of clouds which is related to the latent heating. The VIRS has more channels than specified earlier, adding 1.65, 3.75 and 12 μm to the basic VIS and IR. The additional channels are to help identify warm rain and to use split window techniques. Note that the footprint of the VIRS is roughly twice that of the AVHRR. This change was made to reduce the immense load on the data system that the finer resolution would have imposed. Two additional instruments were added to the TRMM spacecraft by EOS. These are a CERES to measure upwelling radiation from the earth and the cloud tops and LIS to measure lightning. While the data from these two instruments will go to other NASA Centers for processing, they both will contribute to the value of the science from TRMM. The CERES will permit obtaining the atmosphere's radiative heating/cooling component which, in addition to latent heating/cooling is the total diabatic heating/cooling. The LIS will help identify strong updrafts in cumulonimbus thunder clouds and add to understanding of cloud electrification.

During 1991-1993 the entire Science Team met twice. The whole team divided up into 6 subteams, namely: Passive microwave, Radar, Combined algorithms from TRMM instruments, Combined algorithms using TRMM retrievals with other satellite products, Ground validation, and Modeling & Analysis. There were several meetings each of the various subteams, particularly those teams involved with developing algorithms for rain retrievals. TRMM algorithm development was greatly helped by three factors: The flying of the passive microwave SSM/I instruments on military satellites, the collection in Darwin, Australia, of good surface radar and rain gauge data for four rainy seasons and flying airborne versions of the TRMM instruments in the TOGA COARE experiment in 1993.

Significant progress was made during this time on virtually all aspects of TRMM science. Particularly noteworthy were 1) the rapid development of retrievals using geosynchronous products (GPI) adjusted by SSM/I (as a TRMM proxy) to obtain monthly rain maps over the global tropics by Adler and colleagues, thus "beating" the TRMM sampling limitations and the physical limitations of the GPI at the same time. 2) the development by Simpson, Tao and colleagues of an algorithm to obtain latent heat profiles from hydrometeor profiles using simplified versions of the Goddard Cumulus Ensemble (GCE) model. The resulting profiles are highly dependent on the ratio of convective to stratiform rain and 3) the demonstration by Krishnamurti that a global tropical model initialized with rain and associated latent heat (again using SSM/I and gauge data as proxies for TRMM data) gives far better initial and 24 hr forecast rain patterns than the large-scale models with conventional initialization.

In February 1994 a new TRMM Science Team was selected in both the U.S. and Japan, based on a joint NASA/NASDA Research Announcement. These will comprise the TRMM Science team for 4 years, until the TRMM satellite is launched in August 1997. The U.S. selected 38 PIs to be divided into the same subteams as was the first Science Team. The Japanese NASDA has selected a comparable number of TRMM PIs. To coordinate activities, an executive body referred to as the Joint TRMM Science Team (JTST) has been chosen which consists, from both countries, of the Project Scientist, Deputy Project Scientist and the Team Leaders, as well as the Headquarters TRMM Program Scientist and his counterpart in NASDA.

An official Memorandum of Understanding between the U.S. and Japan was signed on October 20, 1995 by Mr. Goldin for NASA and Mr. Matsui for NASDA.

2. Instrument Calibration/Validation Plan

2.1 TRMM Microwave Imager (TMI)

The TMI calibration plan covers both the pre-launch and post-launch activities. It provides for continuous validation of the radiometric accuracy of the radiances and for spot checks of the earth location.

2.1.1 Pre-launch activities

During the construction phase of the TMI, a math model for the radiometer calibration was programmed. Before the critical components were integrated into the system, their losses were measured and incorporated into the math model. During the thermal/vacuum (T/V) testing of the instrument, known targets were used to validate the math model and to provide a basis for system level refinements. The agreement between the refined math model and the T/V observations to the 1K level were achieved.

Corrections for the antenna pattern, particularly the part that will miss the earth entirely, are critical for converting the measured antenna temperatures into brightness temperatures. A requirement that the antenna patterns be measured to the same resolution as for the SSM/I instrument were therefore maintained. Since TRMM will fly at a lower altitude, the earth will subtend a slightly larger solid angle so that the same measurement resolution will permit a better correction for the fraction missing the earth. The antenna patterns will also permit validation of the pointing of the main beam for each of the frequencies.

2.1.2 Post-launch activities

The TMI instrument is a self calibrating radiometer. For each scan, the radiometer views cold sky (with a well known radiometric temperature of 2.7K) and an internal hot load (~300K) monitored independently by three thermistors. This design, used in the current SSM/I sensor has proved extremely reliable. Nonetheless, it is critical to verify that TMI is performing within specifications. A three phase calibration/validation effort has therefore been identified. The three activities are: 1) Initial reasonableness checks (IRC), 2) Intensive Field Experiment (IFE), and 3) long term performance monitoring and quality control(QC)

The IRC phase will include:

> Comparisons of Tbs with radiative model calculations for typical tropical conditions.

Examination of images for artifacts and for proper location of major geographic features

Long term averages (about a week) of Tbs as a function of scan position to check for scan position dependent biases.

Comparisons of retrievals of Sea Surface Temperature (SST), Surface Wind Speed (WS) and Precipitable Water (PW) with climatology.

The IFE phase:

Two major field experiments are planned as part of a general TRMM validation program. In this section, only those aspects that deal directly with the calibration/validation of the TMI radiances are discussed. The details of how these subcomponents fit into the overall validation experiment cannot be decided until the field campaigns are better defined. For the calibration and validation portions, measurements with an airborne set of radiometers matching the TMI in frequency and polarization are essential. Ideally, they should also match in view angle but an airborne platform permits some adjustment for a few minutes at a time. (i.e. the aircraft can be rolled a few degrees if necessary to match the view angles). The aircraft should underfly the satellite over uniform clear ocean and a reasonably uniform vegetated land area such as the tropical rainforest to calibrate the radiances. The aircraft should fly along the satellite swath and turn so that the radiometer beams match the TMI beams in incidence angle and azimuth. The airborne radiometers should be calibrated with wingovers in flight before and after the satellite pass and with warm calibration targets before takeoff and after landing.

Since retrievals of wind speed (WS) and sea surface temperature (SST) are being used to validate and monitor the performance of the TMI, ground truth for these variables are necessary. Low level flights of the aircraft can be used for this purpose. Aircraft flights for this purpose, however, must be considered nice-to-have, not critical, since there are other sources of ground truth. Retrievals of precipitable water (PW) are also being used to validate the radiances. Since PW measurements will be needed in the rainfall algorithm validation, it is further important to get some clear-uniform condition PW measurements (i.e. dropsonde launches).

The QC phase:

The QC phase requires monitoring of many parameters to detect any drifts. Under non-raining conditions the radiances can be used to retrieve PW, CLW, WS & SST. The behavior of these parameters is reasonably well understood,

so by monitoring them some drifts can be detected. Similarly, in the subtropical highs, the radiances would be expected to be fairly stable; they will be monitored.

If a drift is suspected from the above measurements, it will not be clear which channel has drifted and how much. However, by taking a measurement which is coincident with a radiosonde launch from an oceanic location under clear sky condition, we can compare the measured radiances with computed radiances that have a high degree of confidence. These computations must also be performed early in the satellite lifetime to establish a baseline.

Earth location has been a problem that has plagued many spacecraft experiments; it must be monitored. Small isolated islands can be used as landmarks. Approximately circular islands (not atolls) with a diameter of about 10 km are ideal. Their locations will initially be located in the data manually, but if errors are frequent, an automated procedure for the long term monitoring of geolocation quality can be implemented. With an automated program, rain can cause some false alarms for mislocation; a human will have to double check any indications of bad earth location.

Additionally, it is expected that there will be 2 SSM/I's on DMSP spacecraft during the TRMM period. For the channels common between SSM/I and TMI the coincidences between TRMM and DMSP will provide an additional monitor of drift.

2.2 Visible Infrared Radiometer (VIRS)

The VIRS calibration plan covers both the pre-launch and post-launch activities. It provides for continuous validation of the radiometric accuracy of the radiances and for spot checks of the earth location.

2.2.1 Pre-launch activities

Pre launch tasks included system characterization and calibration. Characterization will establish baseline sensor performance, verify system specifications such as signal-to-noise, spectral bandpass and MTF and determine any responses that require correction and/or adjustments in the level-1 algorithm. Examples of the latter include temperature dependence, non-linear effects and coherent noise.

VIRS pre-launch radiometric calibration consists of establishing a radiance scale for both the VIS/NIR and (thermal) IR bands. The VIS/NIR bands are calibrated via a NIST-traceable Spherical Integrating Source (SIS) with numerous quartz iodide lamps that are turned on or off sequentially to construct the radiance to

digital counts transfer curve. The IR bands are calibrated by transferring the radiance scale from a laboratory blackbody (BB) to the onboard BB, thereby enabling a two-point inflight calibration using the BB and a view of space each scan line. Pre-flight calibration was monitored by the VIRS instrument scientist throughout the TRMM Design Reviews and Calibration Reviews.

Inflight stability of the VIS/NIR bands is determined via a solar diffuser that is exposed to the sun on command. Any change in system response is used with the pre-launch calibration to establish the new radiometric scale. The reflectivity of the diffuser is measured pre-launch and can be checked in flight by occasional views of the moon. Transfer of the pre-launch calibration to post-launch can be performed by exposing the diffuser to the sun pre-launch, performing atmospheric corrections and then comparing the pre- and post-launch results. The technique has been used with SeaWiFS and is planned for MODIS. Its use with VIRS is to be determined.

As part of the development by SBRC, a radiometric math model of VIRS will be generated and delivered with the sensor. The model can be used for tracing anomalies post-launch and possibly for generating Level-1 corrections.

2.2.2 Post-launch activities

Earth location accuracy will be monitored by noting the apparent locations of land features such as islands.

VIRS will be cross-validated against AVHRR (during the early part of the TRMM Mission) and against MODIS (following Eos AM launch) using co-registered pixels. Specifically, this cross-validation would try to verify the calibration of the VIRS radiances. This requires identifying either standard targets or particular days. As an example, ERBE collected AVHRR data from NOAA-9 every fifth day and made a special validation product which contained ERBE, AVHRR, and HIRS from the same satellite. The members of the Science Team could use this to intercompare their interpretations of various kinds of data.

Much of the current work on standardizing AVHRR for ISSCP data involves observing particular portions of the Earth where the albedo (or perhaps the surface temperature) is known. The sites have usually been desert targets, although there has been some intercomparison work with selected targets for the standardization of GOES data, where targets are more widely dispersed. For this kind of work, the particular targets and the frequency of measurement need to be identified. Because the targets used for this work need to be fairly broad and because the satellite will not see the sites with the same solar or viewing geometry, some form of angular model is needed as well.

Calibrate Sea Surface Temperature retrievals against ground truth to validate 11 & 12 micron split window retrievals. There are a number of buoys that can be used as ground truth. During the IFE additional ground truth will be obtained. This exercise is quite similar to part of the TMI plan, the ground truth would serve two purposes. In this case, the location and frequency of the ground truth sites need to be specified. A plan is needed to monitor the calibration of these channels. The specific work that must be done for each site includes:

a) Obtain measurements from surface site.
b) Identify the time and space window of the satellite swath that contains the surface site.
c) Locate the surface site within the satellite swath.
d) Identify the cloud conditions and continue only if the site is reasonably clear.
e) Decide on the amount of correction for this observation.
f) collect a number of such corrections and estimate the necessary gain change (probably some form of least squares estimate for example).
g) Apply correction to gain.
h) Check that gain was properly applied by re-running the data with the revised gains.

2.3 Precipitation Radar (PR)

As with the other instruments, the radar will have an internal calibration mode to detect short term drifts so they can be removed from the data. The external reference will be an active radar calibrator (ARC) which can measure the transmitted signal and respond with a known signal at a delayed time . The goal is to determine and maintain the calibration to 1 dB. To develop the PR calibration algorithm, variation and drift of the PR system parameters have been modeled to have "intermediate-term", and "long-term" components. The former is caused by the temperature change inside the PR and roughly has a period of one revolution of the satellite (about 91 min.). Thus, the correction for this term can be done by monitoring the temperatures. The latter may occur due to gradual degradation of system performance (gain, loss, etc.) and/or failure of some active array elements. Since this term may involve changes in antenna characteristics and telemetry sensors, calibration using an external reference target is required.

2.3.1 Pre-launch Activities

In the PR Proto-Flight Model development phase, a large volume of data will be obtained in order to establish the database for the post-launch PR calibration. The data set will include the temperature dependence of various parameters (e.g. gain, loss, phase) in the PR, and the antenna pattern measured at Toshiba and Tsukuba Space Center (TKSC), NASDA. Also PR sensitivity will be verified at TKSC using

the Active Radar Calibrator (ARC) of CRL. These activities will serve as the baseline for the post-launch PR calibration and validation.

2.3.2 Post-launch Activities

Two types of activities are necessary to calibrate/validate the PR measurements following the TRMM launch: Radar calibration and routine monitoring. To have confidence in the radar measurements, the internal calibration needs to be examined to insure that it is working properly. The calibration of the radar (i.e. radar constant) must be determined and verified using external sources, and the antenna patterns need to be specified. Additionally, it is important to validate the PR observations by using direct comparisons with airborne radars as well as monitor the long term stability of the system.

Internal calibration
The internal calibration algorithm has been developed using a detailed PR system model which describes the temperature dependence of all system parameters related to the conversion process from the count value to the radar received power or to the radar reflectivity factor. The error analysis presented at the PR system CDR indicates that an error (3 sigma) of less than 1 dB can be achieved in the estimation of the radar reflectivity factor. The internal calibration using the temperature telemetry will be implemented in the Level-1 processing algorithms, so that no off-line calibration activity will be required.

External calibration and internal-loop calibration
External calibration of the PR will be performed using an ARC placed at a ground calibration site in Japan. The ARC will have three functions: radar transponder, radar receiver and beacon transmitter. In order to reduce the error caused by the uncertainty of PR antenna beam pointing, a special over-sample antenna scan will be used in the PR external calibration mode. ARC echo levels obtained from the multiple beam directions allow a precise estimation of PR antenna pointing and "peak" ARC echo level corresponding to the PR antenna beam center position. One problem in the ARC calibration is that an ARC calibration can provide the calibration factor only at a specific angle bin. The internal loop calibration is performed by invoking the PR internal calibration mode, which is intended to measure the overall I-O characteristics of PR receiver IF and data processing units. Since this requires the interruption of science observation, this calibration would be performed in series with the external calibration using the ARC. The external calibration and the internal-loop calibration will be performed every 2 to 4 weeks by NASDA. The results will be accumulated to monitor the long-term trend of the PR system parameters. Updates of PR calibration factors will be based upon a statistical analysis of the trend data. The updated calibration coefficients should be sent to TSDIS so as to keep Level-1 products generated at TSDIS and NASDA consistent. The amount of reprocessing should also be taken into account in defining the strategy of the calibration coefficient updates.

Antenna pattern measurement
Post-launch measurement of the PR antenna pattern is important to assess the in-orbit performance of PR. The measurement of the along-track pattern is relatively easy because the time trends of the ARC received power and of the PR received power in the normal ARC calibration can be used to generate the transmit pattern and 2-way pattern, respectively. Similarly, the PR receive pattern can be obtained using the ARC beacon mode. On the other hand, measurement of cross-track (antenna scan plane) pattern is much more difficult in spite of the importance to assess the overall amplitude/phase stability of 128 active array elements. To make this measurement possible, a special spacecraft attitude (90-degree Yaw maneuver) will be employed, in which the time trends of the received powers in the ARC calibration now provide the antenna scan plane pattern. The cross-track pattern measurement using the 90-deg yaw maneuver will be conducted at least once in the initial check-out period and about once per year after that (to be reviewed).

Airborne validation experiments
An important component of the validation plan for the TRMM Precipitation Radar (PR) is the use of airborne rain radars which will underfly the TRMM PR. At present, there are two such airborne radar systems that are ideally suited for the validation experiments. They are the Airborne Rain Mapping Radar (ARMAR) from NASA/JPL and the CRL Airborne Multiparameter Precipitation Radar(CAMPR) from Japan/CRL(Takahashi et al. 1995). Major characteristics of the ARMAR of JPL are described by Li *et al.* (1993). These radars were developed with the same operation frequency and downward-looking geometry as the TRMM PR. These radars provide several unique data sets for the validation of the TRMM PR:

The direct reflectivity measurements from the surface as well as rain cells can be compared with the TRMM PR results. For regions that are not raining, the surface cross sections as measured by the TRMM PR can be compared with the airborne radar results after appropriate spatial averaging. This will give additional calibration information for the TRMM PR. The airborne radar reflectivity measurements from raining regions can also be compared with the TRMM PR since the radars operate at the same frequency and, with appropriate spatial averaging, should show similar reflectivity and attenuation characteristics as the results from the PR at least for nadir pointing observations. This step can provide information for the validation of the TRMM PR level 1 data products.

Routine Monitoring
The ARC will be used over the life of the instrument to monitor the calibration although probably not on every pass over the ARC site. Within the planned TRMM satellite coverage, the TRMM PR will make frequent observations over a number of natural targets whose radar cross-sections are spatially

12

homogeneous and temporally stable. Because of these key characteristics such natural targets can be used to monitor the PR stability.

(1) Ocean Surface at 10-degree Incidence: It has been well-established through theoretical modeling and airborne experiments that the rain-free normalized radar cross-section of the ocean surface is insensitive to the sea state and the wind condition at incidence angles of approximately 10 degrees. At the PR frequency of 13.8 GHz, the experimental results obtained by the NASA/JPL Airborne Rain Mapping Radar (ARMAR) during the TOGA COARE field campaign show a statistical mean of 8.5 dB and a standard deviation of +/- 0.5 dB over a two month period. Since the TRMM PR will make continuous observations over a +/-17 degree scan throughout the entire mission, the rain-free ocean backscatter measurements collected at 10 degrees incidence by the PR can be used to monitor the stability of the radar system and to determine the radar calibration constant.

(2) Amazon Rain Forest: Because it is homogeneous and its normalized radar cross section is relatively insensitive to the change in incidence angle, the Amazon rain forest has frequently been used as a primary external calibration target for many spaceborne radar missions. Using the SEASAT Scatterometer data set, Birrer et al. (1982) and Kennett and Li (1989 a, b) have demonstrated that the normalized 14.6-GHz radar cross-sections of the rain forest at incidence angles between 20 and 70 degrees are quite uniform (with standard deviation of ~+/-0.5 dB) at a specific local time. Since the Amazon rain forest will be visited frequently by the TRMM satellite, it can be used as an external target to determine the long-term drift of the TRMM radar system parameters. Previous analyses were performed at large incidence angles. The suitability of this region as a standard TRMM radar calibration target, therefore, must be verified through prelaunch airborne observations with ARMAR.

2.4 CERES and LIS

The CERES and LIS are EOS instruments and as such do not fall under the purview of the TRMM science team. Their calibration and validation, although certainly of great interest to TRMM science community are discussed in the appropriate EOS documents.

3. TRMM algorithm selection

Rainfall products, their error budgets and the vertical structure of latent heating form the cornerstone of TRMM science. In designing the data systems to generate these products under the very tight budget constraints, it was necessary to minimize the set of products that would satisfy the mission requirements. This section presents an overview, by algorithm team, of the algorithms deemed critical to the mission success. A summary of these products is presented in Table 3-1 for reference.

Table 3-1: TRMM Satellite Products

Type of Product	TSDIS Ref. no.	Name	Purpose
(a) Basic data	1B-01	VIRS radiances	Unaltered basic data
	1B-11	TMI brightness temperatures	Unaltered basic data
	1B-21	PR power/ noise level	Unaltered basic data
	1C-21	PR Reflectivities	Basic reflectivity data (omitted if no rain in FOV to reduce data load)
(b) Correlative data	1B-21	Surface cross-section	Radar surface scattering cross-section/total path attenuation.
(c) Qualitative	2A-52	Qualitative rain information	Type of rain, Existence and height of bright band.
(d) Surface rainfall	3A-11	TMI monthly rain map	Monthly 5° rainfall maps - over ocean only.
	3A-26	PR monthly rain map	Monthly 5° rainfall maps over both land and ocean.
(e) Vertical structure of rainfall	2A-12	TMI Instantaneous 3-D structure	Profiles of hydrometeors and heating from wide TMI swath.
	2A-25	PR Instantaneous 3-D structure	Profiles of hydrometeors and heating from PR swath.
	2B-31	PR/TMI Monthly 3-D structure	Best instantaneous product based on merger of instrument data
	3A-25	PR Monthly, 5° 3-D structure	Profiles of hydrometeors and heating from PR swath.
	3B-31	PR/TMI Monthly, 5° 3-D structure	Profiles of hydrometeors and heating from combined TMI/PR retrievals.
(f) TRMM and other data sources	3B-42	Adjusted AGPI	Geostationary precipitation index calibrated by TRMM. Rain at 5 day, 1° resolution
	3B-43	Merged Satellite & gauge products	TRMM, AGPI and gauge data merged into single rain product. 5 day, 1° res.

This section deals with the generation of geophysical parameters (Level 2 and higher products). Insuring that the calibrated, Earth located radiances are available to these algorithms is the responsibility of the TRMM data system in coordination with the instrument scientists. Coding of the algorithms is described in chapter 6 dealing with the TRMM data system TSDIS. The responsibility for insuring the quality of the level 1 products was discussed in the previous chapter.

3.1 TMI Team

Present planning calls for two TMI algorithms, a level 2 (satellite coordinates) profiling algorithm for use over both land and ocean, and level 3 (5°x5°, monthly) oceanic rain mapping algorithm. Very close analogs for both of these algorithms exist today. Christian Kummerow is currently running an experimental version of the profiling algorithm on SSM/I data at GSFC. A minimal solution would be to port the algorithm to the TSDIS environment and modify it to match the TMI data format. Similarly, Alfred Chang is running a level 3 oceanic algorithm using SSM/I data for the Global Precipitation Climatology Project (GPCP).

The key to improvement and selection of the algorithms lies in the various rainfall algorithm intercomparison projects supported by various entities outside of TRMM. These intercomparisons also serve to widen the community participation in the TRMM algorithm development. Several intercomparisons have been performed. They have served to focus the questions and to narrow the range of reasonable views within the community. Although it is conceivable that these workshops will produce clear winners and losers, it is unlikely. In any case, the range of participants in a position to produce the programs needed by TSDIS on the required schedule is quite limited. A more likely result is that the workshops will show that certain features are advantageous and others unnecessary or even degraded. The results of the Kummerow or GPCP algorithms will be modified accordingly. The TMI team is small and a consensus is likely. If however a consensus cannot be reached, a majority vote of the Joint US-Japan TMI team will decide among specific proposals.

The proposed algorithms will be tested to the extent possible using SSM/I data. The SSM/I data are central to the development of these algorithms. For TMI characteristics not found in SSM/I, a synthetic data set will be used. Minimal resources will be expended on this synthetic data set since it will only catch a small subset of the possible range of problems.

3.1.1 TMI Profiling Algorithm - (TSDIS ref. 2A-12)

Profiling techniques being considered all make use of cloud dynamical models in order to constrain an otherwise ill-posed problem. The primary technique is

based upon a Bayesian approach. Here, many realizations of the Goddard Cumulus Ensemble model are used to establish a prior probability density function of rainfall profiles. Detailed three dimensional radiative transfer calculations are used to determine the upwelling brightness temperatures from the cloud model to establish the similarity of radiative signatures and thus the probability that a given profile is actually observed. It has been shown by Kummerow *et al*., 1995, that good results may be obtained by weighting profiles from the prior probability density function according to their deviation from the observed brightness temperatures. This method, by avoiding iterative radiative transfer computations, is computationally very fast compared to traditional inversion solutions. A representative example, obtained from 4 channel airborne radiometer is shown in Figure 3-1.

Figure 3-1: Top panel: EDOP measured reflectivity structure. Center panel: AMPR observed brightness temperatures, at nadir, coincident with EDOP measurements. Bottom panel: Retrieved radar reflectivity from GPROF algorithm. Reflectivities are determined from cloud model prescribed drop-size distributions.

While these results appear quite good, the solution does not work well when the data base of possible cloud structures is not sufficiently populated. In this case, a secondary approach developed by Smith et al., 1995, will be employed. Here, the profiles are adjusted in an iterative technique aimed at minimizing differences between observed and modeled brightness temperatures. While computationally much more intensive, this solution will only be employed if no satisfactory result can be found by the primary method.

The product consists of the surface rainfall rate and a confidence parameter, as well as the 3-D structure results, with 4 hydrometeor classes and the associated latent heating derived at 14 vertical layers. While the structure information may not be as detailed as that which can be obtained from the PR instrument, the much wider swath of the TMI makes this product important for climatological purposes. Good surface rainfall and structure retrievals should be possible with the TRMM resolution over oceans. Over land, where the emission signature cannot be detected directly, the precipitation will have a strong model dependence. The horizontal resolution of this product will be 10 km. Additional information will be supplied to determine if the primary or secondary algorithm was used for each pixel.

Instantaneous errors can be rather large (~80%) for individual footprints. The largest component of this error estimate is due to random variations.   (Random errors reduce as 1/sqrt(N) where N is the number of pixels in the area. Random errors therefore disappear almost entirely over areas as small as 1°x1°). The magnitude of the systematic errors is of much greater concern but almost impossible to estimate quantitatively on a global scale. The TMI team goal is an estimate with errors in the 10% range for retrievals over ocean. Immediate uses of this product are foreseen in the area of data assimilation.

3.1.2 TMI Monthly Rain Mapping Algorithm - (TSDIS ref. 3A-11)

Figure 3-2 is a flow diagram of the Level-3 algorithm which is intended to produce monthly totals of rainfall for 5°x 5° boxes over the ocean areas. The data are first passed through a land mask to eliminate all radiances contaminated by significant amounts of land in the field of view. The data are then filtered to determine if rain is possible using the 85 and 37 GHz channels. This filter must be fairly conservative in that it must not conclude that rain is not possible when it is, in fact, raining, at least, not any significant portion of the time. A small percentage of errors on light rain cases would, however, not have a large impact on the monthly totals. The data are not discarded when it is determined that rain is impossible; this determination is itself a rainrate estimate of zero that must be included in the averages. The rain-free oceanic data can also be used as input to a monitor of instrument drift as discussed in Chapter 2.

Figure 3-2: Flow diagram of algorithm 3A-11 intended to produce monthly totals of rainfall over 5°x5° grid boxes.

For the purposes of the oceanic rain-mapping algorithm the brightness temperatures are considered to be a function of only two variables, the rain rate and the height of the 0°C isotherm (freezing level). The freezing level is associated with the total integrated water vapor content (TIWV) through our modeling assumptions. These assumptions, while weak in the general case, are reasonably robust when restricted to raining conditions. Since the TIWV impacts the 19 and 21 GHz channels very differently whereas the rain impacts them rather similarly, the two channels can be used to solve for the TIWV and, by implication, the freezing level. This freezing level is then used for several independent estimates of the rain rate. The rain rate can then be derived using several channel combinations. The lowest frequency used in any rainfall retrieval determines the spatial resolution and the dynamic range of each retrieval.

3.2 PR Team

The standard TRMM PR algorithms for the estimation of rain parameters are summarized in Table 3-1 according to the levels of data processing. In the Table 3-1, the names of the algorithms, the contact person of the algorithm and product

18

names are listed. The flow diagram of the total algorithm system is shown in Figure 3-3. The algorithm 1B-21 converts the output of log-detector (A/D converted count value) to the total received power (Signal + Noise) or noise power. These are the most fundamental data for the Level 2A algorithms. Algorithm 1B-21 includes a routine to detect minimum echo (rain/no rain) in the instantaneous field of view (IFOV). A data flag indicating whether or not the power threshold has been exceeded is added to the output of the algorithm 1B-21. The algorithm 1B-21 also includes a routine to estimate storm height. When rain is present in the IFOV, algorithm 1C-21 outputs the radar reflectivity factor Z without rain attenuation correction. The output data from algorithm 1B-21 is used as input to algorithm 2A-21.

Figure 3-3: Flow diagram showing the relation among Precipitation Radar algorithms.

Table 3-1 TRMM Radar Algorithms and Contact Persons

Product No.	Name	Contact Person	Product
1B-21	PR Calibration	NASDA	Total Received Power, Noise.
	Minimum Echo Flag	H. Kumagai	Min. Echo Flag First Echo Range
1C-21	PR Reflectivities	NASDA	dBZ when rain in IFOV
2A-21	σ^0	R. Meneghini	σ^0_R, Averaged σ^0_{NR}
2A-23	PR Qualitative	J. Awaka	Bright Band, Rain Type
2A-25	PR Profile	T. Iguchi	Range Profile of Rain Rate
3A-25	Space, Time Average	R. Meneghini	Space, Time Avg. of Rain Param. of 1C-21, 2A-23 & 2A-25
3A-26	Statistical Method	R. Meneghini	Space, Time Avg. of Rain Rate

----

When rain is absent, 2A-21 updates the library of the averaged surface scattering coefficient σ^0 over ocean or land. When rain is present, an estimate of Path Integrated Attenuation is made. The output of the algorithm 1C-21 is the input to the algorithms 2A-23 and 2A-25. Algorithm 2A-23 tests for the presence of a bright band and, if detected, determines its height. This information is also used to classify the rain type (stratiform type, convective type or so called warm rain). The height of the bright band will be input to the TMI algorithms. Algorithm 2A-25 is a deterministic algorithm to retrieve rain parameters over each resolution cell by applying a profiling method using the total attenuation as determined by 2A-21. The outputs of 2A-25 are the profiled rain rate and its path averaged value. Output o f algorithm of 3A-25 gives statistics of rain parameters over the space-time domain (5° x 5°, 1 month) as obtained from the high resolution data of 1C-21, 2A-23 and 2A-25. Algorithm 3A-26 gives the space-time averaged rain rate by the use of a statistical method.

3.2.1 PR Calibration - (TSDIS ref. 1B-21)

Objectives:
(a) To convert the count values of radar echoes and noise levels into engineering values and to subtract the noise level from the total received power.
(b) To append geodesic information (latitude and longitude data on the Earth surface) and equations or tables to calculate the locations of each range bin.
(c) To find the first echo range and clutter range. To find the highest range bin where the received power exceeds the lower threshold for the minimum echo test. This range bin represents the PR observable storm height. Also the range bin positions, where the ground clutter originated both from antenna mainlobe coupling and antenna sidelobe coupling may appear, are calculated based on antenna pattern and surface scattering cross section.
(d) To test at each angle bin whether the received power exceeds certain threshold levels and generate flag. The physical meaning of this flag is to indicate whether or not rain is present at each angle bin. The flag will express the three states of rain/no-rain conditions, that is, low, medium, and high probabilities of

raining. The threshold levels will correspond to confidence levels based on the radar signal statistics.

Method:
(a) To exclude special mode data (such as external calibration mode).
(b) To average HK temperature data in the calibration period (tentatively 3 minutes).
(c) To correct the temperature dependence of antenna gain, beam width, transmit power of 128 SSPAs (Solid State Power Amplifier), receiver chain gain of 128 LNAs (Low Noise Amplifier) paths and logarithmic amplifier input/output characteristics at the FCIF (Frequency Converter & I/F) unit using averaged temperature data of each element obtained at item (b).
(d) To calculate the antenna beam direction vector by using ACS (Attitude Control System) ancillary data and to calculate latitude and longitude data on the Earth surface and the spacecraft height by using definitive orbit data every 1 minute.
(e) To calculate latitude and longitude data on the Earth surface within one scan plane by interpolating the 1-minute latitude and longitude data or to provide a conversion formula to calculate them by using observation time, angle bin number and so on. Similarly, equations or tables are provided to calculate the location (latitude, longitude and height) of each range bin.
(f) To confirm the range bin number which corresponds to the surface echo position by searching maximum echo level with the range bin decided by onboard searching.
(g) To convert the count value of the radar echo into engineering values and to obtain calibrated received power.
(h) To make oversampled dataset with 125m range bin for angle bin number of 11-39.
(i) To determine the height range bin between 0 and 20 km above sea level at each angle bin. This height range is checked whether or not rain is present.
(j) From the surface position, the database of PR antenna pattern, and the surface scattering coefficients, to calculate the range bins at which the ground clutter is significant. The surface clutter can arise either from the antenna mainlobe or sidelobes. The range bin numbers where the clutters appear are the outputs of the clutter ranges.
(k) The two threshold levels are calculated based on the confidence levels of signal detection probabilities. The confidence levels are selectable.
(l) The received signal power at each range bin is compared with predetermined threshold levels. A flag is generated at each range bin within the range determined in (i). To minimize the probability of a false alarm, N continuous range bins are checked simultaneously. A flag indicating presence of rain is turned on only when the signal at all N range bins exceeds the threshold level. Then the largest flag level (highest probability of raining) within one angle bin represents the flag level within that angle bin. This procedure is repeated for every angle bin.

(m) The highest range bin height where the signal exceeds the threshold is defined as the first echo height.

3.2.2 PR Reflectivities - (TSDIS ref. 1C-21)

Objectives:
To calculate the radar reflectivity factor (measured Z-factor) when rain is present. The attenuation correction is not applied to the measured Z-factor.

Method:
When rain is present:
        (a)   A system noise is subtracted from the total received power.
        (b)   To convert received power, which is the output of 1B-21, into radar reflectivity factor Z by applying the radar equation.
When rain is absent:
        (a)   To delete all radar echo data including over sample data.
        (b)   Other data (ancillary data, surface echo, and so on) are not deleted.

Output Data:
Radar reflectivity factor Z in the same range area defined at 1B-21 in case of rain with surface range bin number, various flags including minimum echo flag (rain/no rain), first echo range (storm height), clutter range and so on calculated at 1B-21. In case of no rain, surface echo (including over sample), surface range-bin number, various flags and so on calculated at 1B-21.

3.2.3 Surface Cross Section - (TSDIS ref. 2A-21)

Objectives:
The primary objective is to compute an estimate of the path attenuation and its reliability by using the surface as a reference target. Secondary goals are to compute the spatial and temporal statistics of the surface scattering cross section, and classify the cross sections into land/ocean, rain/no-rain categories.

Method:
The path attenuation is estimated by comparing the apparent surface cross section measured in the presence of rain with the averaged surface cross section measured in the absence of rain. A reliability parameter will be computed based on the variability of the surface cross section in the absence of rain.

Input Data:
The primary inputs will be from 1B-21 from which we will obtain the noise-corrected radar powers at the surface and earth location information. The input data volume will be similar to the output volume of 1B-21. A rain/no-rain

determination will be made in 2A-21 which will be identical to the method used in 2A-23. TSDIS will supply information as to the background type: land, ocean, and indeterminate. Internal memory requirements (to store the statistics of the surface cross sections) is about 40 M bytes.

Output Data:
In the presence of rain, the output products are the estimate of the path attenuation and its reliability. The output data volume will be less than 300 bytes per scan. In the absence of rain, the statistics (the running mean and standard deviation) of the surface cross sections will be updated and stored internally with a spatial resolution of 0.25 deg. x 0.25 deg.

3.2.4 *PR Qualitative* (Bright band and rain type classifier) - (TSDIS ref. 2A-23)

Objectives:
The algorithm 2A-23 has the following five objectives.
    (a) to detect bright band
    (b) to determine the height of bright band when it exists,
    (c) to classify rain types
    (d) to output storm height
    (e) to output rain/no rain information

Method:
Detection of bright band is carried out by searching a peak of Z-factor with respect to range. This peak search is made by using a spatial filter, which is basically based on a second derivative concept. When the peak is prominent and appears around the expected height of freezing level, it is determined that the bright band exists. When the bright band exists, the height where the peak occurs is regarded as the height of bright band.

Rain is classified into three types, i.e. (a) stratiform, (b) convective, and (c) others. When the bright band exists, rain is classified as stratus. When the bright band does not exists but any one value of Z along the range exceeds a predetermined value, rain is classified as convective. When the bright band does not exist and all values of Z along the range are less than the predetermined value, rain is classified as others. In the case of convective type rain and other type of rain, detection of "warm" rain is also carried out. When the storm height appears lower than the height of freezing level, the rain is judged as "warm" rain. The storm height itself is determined by a Level-1 algorithm by using the first range echo flag from 1C-21.

Input Data:
All the input data, except temperature data, are handed down from 1C-21.

Output Data:

The output data of 2A-23 are mainly flags, which indicates (a) existence of bright band, (b) three rain types, (c) existence of "warm rain", and (d) status flags indicating the quality of output data. The rain/no-rain flag, which is handed down from 1C-21, is also included in the output of 2A-23. In addition to these flags, 2A-23 outputs the height of bright band and the storm height, the latter of which is handed down from 1C-21.

3.2.5 *PR profile* - (TSDIS ref. 2A-25)

Objective:
The objective of 2A-25 is to produce the best estimate of the vertical rainfall rate profile for each radar beam from the TRMM PR data. The rainfall rate estimate is given at each resolution cell (4 km times 4 km times 250 m) of the PR.

Method:
This algorithm basically uses a hybrid method described in Iguchi and Meneghini (1994) to estimate the true vertical radar reflectivity (Z) profile. The vertical rain profile is then calculated from the estimated true Z profile by using an appropriate Z-R relationship. One major difference from the method described in the above reference is that in order to deal with the beam-filling problem, a non-uniformity parameter is introduced and is used to correct the bias in the surface reference arising from the horizontal non-uniformity of rain field within the beam. The Z-R relationship may be adjusted according to the rain types, the altitude, the correction factor in the surface reference method when applicable, and the non-uniformity parameter. In more detail, a range-dependent non uniformity parameter has to be defined, though the details of the procedure have not been decided at present and remain a subject of future investigation.

Input Data:
The primary input data will be the Z-factor profile from 1C-21 and the surface reference data from 2A-21. Most of the output products from 2A-23 are also required in this algorithm. They include the rain/no-rain flag, the storm height, the existence of bright band and its height, and the rain type. The ancillary input data required are the land/ocean/intermediate information and the height of 0 degree isotherm.

Output Data:
The primary output data will be the rainfall estimate given at each radar resolution cell above the surface. The estimate will be given only in the presence of rain. This algorithm will also output an integrated rainfall rate along the radar beam between the two fixed altitudes. Other output products include the parameters and coefficients used in the calculation of rainfall rate from the measured Z-factor. The output data volume will be similar to that of 1C-21.

3.2.6 Space-Time Accumulations of Level 2 Radar Products - (TSDIS ref. 3A-25)

Objective:
The primary objective is to compute the statistics over a space-time region for the output products of level 2 radar algorithms.

Method:
In most cases the method of computation is a simple sample mean of the measurements made over the appropriate space-time domain. In other cases, histograms or the correlation coefficients will be computed from the data.

Input Data:
The input data will be obtained from the outputs of algorithms 1C-21, 2A-21, 2A-23, and 2A-25. The input data volume will be approximately 30 kbytes per scan.

Output Data:
The most important output products are the monthly rainfall accumulations and monthly average rain rates over 5 deg. x 5 deg. boxes at fixed heights of 2 and 4 km. Other products include histograms of radar and meteorological parameters, probabilities of rain and bright-band, and correlations among the various radar and meteorological parameters. The output data volume per month is expected to be on the order of 1 Mbyte.

3.2.7 Space-Time Accumulations using Statistical Methods - (TSDIS ref. 3A-26)

Objectives:
The objective is to compute rainfall accumulations and rain rate averages over 5 deg. x 5 deg. x 1 mon. boxes using a statistical method.

Method:
The technique employed is a multiple threshold method. Measured rain rates over an area (intersection of the radar swath and a 5 deg. x 5 deg. region) that are within the 'effective dynamic range' are used to construct a partial histogram of the instantaneous area-wide rain rate. To estimate the distribution at all rain rates, a log-normal or gamma distribution model is assumed, the unknown parameters of which are determined by the measured data. As part of the method, the fractional areas over which the rain rate exceeds certain threshold values will be computed and stored. The histograms of the instantaneous area rain rates will be output for each overpass of each 5 deg. x 5 deg. box; they will also be used to estimate the rainfall accumulations and rain rate averages over monthly periods.

Input Data:
The algorithm will probably use data only from 2A-25. This will be approximately 10 k bytes/scan when rain is present. Information from 2A-21 as to the magnitude

and reliability of the path-attenuation estimate may be needed, however, if these data are not contained in the 2A-25 output data set .

Output Data:
Tentatively, the data sets (generated each month) will consist of 4 types of output:
(a) Monthly rainfall accumulations and monthly averaged rain rates at each 5 deg. x 5 deg. box (5 kbytes)
(b) Parameters of the fitting function at each 5 deg. x 5 deg. box (0.54 Mbytes) for each TRMM overpass
(c)   Histogram, mean and variance of the rain rates at each 5 deg. x 5 deg. box over a 1 month period (51 kbytes)
(d) The fractional areas above selected rain rate thresholds for each overpass of each 5°x 5° box (0.54 Mbytes)

The total output volume per month is approximately 1.2 Mbytes.

3.2.8 PR post launch algorithm development

There are some reasons to believe that radar (spaceborne or ground based) algorithms based upon first principles such as those described above, have shortcomings which can only be overcome by altering the retrieval philosophy towards an entirely statistical approach. Whether or not this is the case for the PR will be tested once data become available. A comprehensive review of the foundations of these statistical algorithms is contained a publication by Atlas *et al*., (1995). The review attempts to diagnose the reasons for the failure of a variety of approaches and highlights those which now show promise. It begin with the characteristics of rain drop size distributions and the foundations for the relations between radar reflectivity Z and rainfall rate R. These are shown to be statistical in nature. In addition there are a large number of factors related to the radar measurements and the variability of the rain which make it necessary to treat radar rainfall measurements in a probabilistic manner. Approaches such as the Area Time Integral (ATI) and Probability Matching Method (PMM), particularly when used with the classification of precipitation type, appear to be especially appropriate to the measurement of average rainfall over space time domains because they are generally free of the corrupting influences on point measurements. Polarimetric methods are also reviewed; they are especially useful for identifying the nature of the hydrometeors and estimating rainfall because they are generally independent of the absolute radar calibration.

3.3 Combined TRMM instruments Team

Combined algorithms represent a new generation of mission qualified rainfall retrieval schemes that utilize a combination of instruments, i.e. measurements obtained from separate instruments, to improve upon single instrument-based

algorithms. This is accomplished by blending the strengths of different types of instrument approaches to overcome weaknesses inherent to all single instrument approaches. There are no restrictions as to the possible combination of instruments that can be used for this purpose once TRMM is launched, as the satellite will carry a radar, a passive microwave radiometer, an optical-infrared radiometer, a lighting detection system, and a cloud-radiation budget radiometer.

Since a main objective of TRMM is to commence soon after launch with rainfall estimates derived from a hierarchy of physically-based algorithms whose design avoids ad hoc relationships and empirical calibration schemes, the first generation of algorithms (referred to as Version 1 or Day One algorithms) will be principally based on measurements from the precipitation radar (PR) and the TRMM Microwave Imager (TMI). These are the only TRMM instruments that can explicitly detect rain signatures over a meaningful dynamic range, and for which algorithms can be designed which need not employ empiricism. From near the beginning of the project, the Project Scientists, Deputy Project Scientists, and rainfall algorithm developers from both the U.S. and Japan felt that it was crucial to include one or more combined algorithms as part of the Version 1 algorithm hierarchy to take advantage of the active-passive PR-TMI configuration, and to explore means to overcome known weaknesses with single instrument techniques. It was within this context that for Day One algorithm purposes, two PR-TMI combined algorithms were configured into the Version 1 plan, one to generate rainfall profile products on an instantaneous basis, the other to generate rainfall profile products on a monthly-averaged basis. Therefore, this section of the SOP focuses on the design and validation plan for the two Version 1 PR-TMI combined algorithms, referred to a 2B-31 (the Level 2 combined instantaneous rainfall structure algorithm), and 2B-31 (the Level 3 combined monthly-averaged rainfall structure algorithm).

The guiding principle in the design of the Day One combined algorithms was to demonstrate progress could be made by either extracting one or more parameters from the PR measurements for use in a TMI-based algorithm in which the TMI measurements were clearly at a disadvantage (e.g., unlike the TMI, the PR will be able to retrieve an unambiguous estimate of the freezing level, an essential parameter for both 2A-12 and the 3A-11 monthly-averaged surface rainfall algorithm), or alternatively, by extracting one or more parameters from the TMI measurements for use in a PR-based algorithm (e.g., the TPA as discussed). Both of these options were deemed equally viable at the time of the CAWG meeting. The deadlock was broken by recognizing that the TMI measurements could come to the aid of a PR algorithm over the entire PR swath (the narrow swath), whereas the PR measurements could not aid a TMI algorithm over its entire swath (the wide swath), and therefore a modified 2A-12 algorithm supported by say freezing level information from the PR, would represent an incomplete solution for the TMI. Furthermore, it was clear that once the alternative 2B-31 retrievals were available, the 2B-31 products could be used

to re-calibrate the 2A-12 products within the narrow swath, and by applying the calibration across the wide swath and then re-calculating an alternative TMI-based solution on a monthly basis over the wide swath, the pre-conceived specifications of the 3B-31 combined algorithm could be met. In so doing, the modified-PR approach will provide a means to test both the original 2A-25 instantaneous product against the modified instantaneous products from 2B-31, it will also provide a means to test the modified 2A-12 products accumulated on a monthly-averaged basis, against the 3A-11 products averaged at that same time scale.

3.3.1 Combined PR/TMI Profiling algorithm - (TSDIS ref. 2B-31)

Computations of the Total Path Attenuation:
This sub-section addresses a needed component of the 2B-31 Day One algorithm. In essence, a technique is needed to obtain total path attenuation at 13.8 GHz, the frequency of the TRMM Precipitation Radar (PR), independent from the radar measurements. This will be done using brightness temperature measurements from the TRMM Microwave Imager (TMI), a 9-channel passive microwave radiometer in which none of the channels match the frequency of the PR. However, because low frequency brightness temperatures are well correlated with total path attenuation in the first place, and because there is good correlation between 13.8 GHz total path attenuation and similar quantities at nearby frequencies, this study investigates how well the lower frequencies of TMI, specifically 10.7 and 19.35 GHz, can be used to estimate 13.8 GHz total path attenuation over oceans. The attenuation parameter will be used in conjunction with a modified version of the Day One PR profile retrieval algorithm which is currently under development.

Scatter diagrams of total path attenuation A/μ, as a function of upwelling brightness temperature at the four TMI window frequencies are presented in Figure 3-4. Results are shown for both vertical (VPol) and horizontal (HPol) polarizations. The view angle $_v$ is taken at 49°, while μ represents the cosine of $_v$. Thus, A/μ is the slant-path attenuation and will be henceforth referred to as A when referring to a fixed view angle. The ocean SST is set to 303 K, while the surface wind speed U is set to 20 m s^{-1}. For the imposed variations in cloud, ice, and rain microphysics, the 10.7 GHz T_B's exhibit only small scatter about the mean T_B-A relationship up to a 10 dB slant path attenuation (equivalent to 6 dB at nadir). The higher frequency 19 GHz T_B's might be useful for estimating path attenuation, but only up to about 1 dB, since the relationship becomes sensitive to the rain and ice DSD variations. Beyond 2 dB, the relationships saturate, and render virtually no useful information. At 37 GHz, scattering from ice becomes dominant in controlling the T_B's for path attenuations beyond a fraction of a dB, and since total atmospheric transmission is so small in precipitating atmospheres

at this frequency, the surface becomes virtually obscured to the extent that the VPol and HPol components are indistinguishable.

Figure 3-4: Scatter relations between total path attenuation in dB for vertically (VPOL) and horizontally (HPOL) polarized brightness temperatures in degrees Kelvin for 10.7, 19, 37 and 85 GHz. Results are presented for 49° view. Calculations are for an SST of 303K and a U of 20 m s^{-1}

Radar rain retrieval:
We use a parameterization of the drop size distribution (DSD) using three mutually independent parameters: a quantity parameter R (the rainrate), and the two shape parameters D' and s', the first representing essentially the mass-weighted mean drop diameter and the second representing essentially the relative standard deviation of diameters about this mean ("essentially" signifies that these variables are modified slightly in order to be mutually independent). This parameterization produces Z-R and k-R relationships, where Z = a(s',D')R$^{b(s',D')}$ and k =   (s',D')R $^{(s',D')}$.

In summary, the problem can be stated as follows. One has profiles of measured radar reflectivities represented by the vector Z_n (the components of each vector are the reflectivities from the various range bins, and the index n refers to the n'th radar beam), along with SRT estimates of the path-integrated attenuations A_n in each of N radar beams constituting a radiometer beam (so n = 1, ..., N), and an associated measured 10.7 GHz brightness temperature T_B^m. One wants to get out of it an estimate of the rain rate profile R_n (again, the components of each

vector are the rainrates at the various range bins, and the index n references to the n'th radar beam) and of the shape parameters of the associated DSD and of the uncertainties in R and the DSD shape parameters, assuming the DSD shape parameters are uniform in altitude and, to a certain extent (described below), within the radiometer beam (this uniformity assumption will not apply to the resulting $, \mu, $ as they will be expected to vary from range bin to range bin and from one radar beam to another.

The approach taken by the combined algorithm is, for a given radiometer beam:

(1a) Input Z_n measured in the n'th radar beam within the given radiometer beam, along with the additional parameters that the current 2A-25 radar-only profiling algorithm uses, namely the SRT estimate of the total path attenuation An, its uncertainty, and the type of rain within the radar beam.

(1b) For every value of the DSD shape parameters (s',D') whose a priori probability pr(s',D') is non-zero, run a modified version of the radar-only algorithm and store its intermediate estimated rain profile R_n(s',D') and the estimated integrated attenuation k_n(s',D').

(2) When all values of (s', D') have been considered on all the radar beams, combine the corresponding attenuation estimates k_n(s', D') to form the corresponding predicted brightness temperature T_B^P(s',D') within the radiometer beam, using the inverse of the FSU T_B-PIA formula.

(3) Quantify, with conditional probabilities, the degree to which the TBp predicted by different (s',D')'s matches the measured TBm. The average of the (s',D')'s, weighted by this probability, is the combined radar-radiometer estimate of the DSD shape parameters (s',D'). The uncertainty in this estimate is given by the variance of the probability.

(4) Go back to the individual radar beams n = 1, ..., N, and for each one, calculate the average of R_n weighted by the probability calculated in (3), and its variance.

3.3.2 Combined Instrument Monthly Rain Profiles - (TSDIS ref. 3B-31)

This algorithm will use rainfall and vertical structure output from 2B-31 over the PR narrow swath and use it to calibrate the rainfall-vertical structure results from TMI algorithm 2A-12 product on monthly time scales. This is accomplished by sub-sampling the 2A-12 product to the 2B-31 product scale, with calibration coefficients calculated at 5° grid elements based upon their comparison within the inner swath. For Day One purposes, an individual calibration coefficient within a grid box will be obtained by determining the scale factor that transforms the average of 2A-12 pixels to the average of 2B-31 pixels over the narrow swath

intersection. After launch, the calibration procedure may be upgraded to a histogram matching scheme, if after analyzing operational products, the bulk statistical properties warrant an upgrade.

The calibration transform will then be applied to the entire 2A-12 product over the with (TMI) swath. The calibrated 2A-12 product will then be accumulated on a monthly time scale for 5°x5° grid elements. The output will consist of surface rainfall, confidence limits on surface rainfall, the number of satellite visits to individual grid positions as well as structural information concerning 4 classes of hydrometeors (precipitating liquid, precipitating ice, suspended cloud water and suspended ice crystals) and latent heating in 14 vertical layers.

3.3.3 Post-launch Algorithm Development

The approach that has been described in section 3.3.1 is, by any measure, a conservative and safe approach. Although it is safe to say that such an approach will be at least as good as the 2A-25 approach, as 2B-31 is essentially a modification of solving the radar equation along the same lines as 2A-25, it is possible that it will not lead to a substantive improvement over 2A-25. In that event, the riveting question will be the relative accuracies of 2A-25 and 2A-12. Current thinking by various science team members is that 2A-12 will outperform 2A-25, at least initially, since the PMW methods have been around longer and are a more matured class of algorithms.

It is from this perspective that a new class of algorithms is under development, in which radar reflectivity measurements will be used to augment the TMI brightness temperature measurements, largely in the framework of the radiometer-based profile-type inversion schemes. These schemes incorporate both emission and scattering frequencies, and are quite robust in that they receive attenuated forward emission and scattering signals which are sensitive to the total column liquid water path, rather than radar-type backscattered signals which are sensitive to the 6th power of the drop size and thus become dominated by only the largest drops.

In essence, the technique involves extending the brightness temperature measurement vector, which in a TMI-based inversion scheme would be used as a solution target by a forward radiative transfer model, with reflectivities from the PR at range gates above, below, and in between those levels in the rain column where the passive channels of the radiometer peak (thereby augmenting the TMI measurements with rain signatures from vertical levels to which the passive instrument is not sensitive). This concatenation of brightness temperatures with reflectivities is what is meant by a tall "vector". The inversion process is conducted in much the same fashion as with the radiometer-only algorithms, i.e. attempting to reproduce with forward modeling the entire "tall vector", except that now the forward model has to include both steady-state radiative transfer of

the passive case, and pulsed radiative transfer from specific range gates for the active case. Such models have been developed at both FSU (Smith et al., 1995) and GSFC (Olson et al, 1995). "Tall vector" algorithms have been tested using combinations of Advanced Microwave Precipitation Radiometer (AMPR), see Spencer et al., (1994) and the Airborne Rain-Mapping Radar (ARMAR), see Durden et al., (1994) by Xiang et al., (1996) and Farrar et al., (1996). Olson (1995) employed AMPR data in combination with the ER-2 Doppler Radar (EDOP) see Heymsfield et al., (1994).

3.4 Combined TRMM & Other Satellite Team

The TRMM and Other Satellite Team (TOST) is responsible for two standard TRMM algorithms to be produced by TSDIS. In the first product (TSDIS ref. no. 3B-42), the TRMM satellite rain estimates are used to calibrate (or adjust) estimates from geosynchronous satellites using the GOES Precipitation Index (GPI; Arkin and Meisner, 1987). The second product (TSDIS ref. no. 3B-43) will use 3B-42 plus information from other polar-orbiting microwave sensors and raingauge analyses to produce a merged satellite/gauge product. Both products are designed to maintain the small biases inherent in the TRMM instantaneous rainfall estimations and bring in the enhanced sampling available in the additional sources of rainfall information. This approach will allow production of TRMM-based products on finer time and space scales.

3.4.1 GPI Calibration Product - (TSDIS ref. 3B-42)

Although different approaches are being investigated (e.g., by M. Desbois), the current draft TSDIS algorithm and code for Product 3B-42 is based on the Adjusted GPI (AGPI) technique described by Adler et al. (1994). The technique uses accurate instantaneous rain rates inferred from low-orbit satellite observations (currently SSM/I, in the future TRMM Combined Instrument, or TCI, which is product 2B-31) to objectively adjust rain rates inferred from geo-IR satellite observations to produce monthly total rain maps for the region 40°N to 40°S. The adjustment is based on the spatially variable ratio of rainrate estimates from coincident TCI (currently SSM/I) and infrared data (VIRS, currently cutouts of geosynchronous IR data) which is then applied to the full geo-IR data set. The resulting "adjusted geo-IR rain estimate" has the (usually low) bias of the TCI (currently SSM/I) estimates, together with the smoothness and temporal coverage of the geo-IR data.

We expect variations in the adjustment ratios to be meaningful only on relatively large space and time scales, so we smooth each field before computing the ratio. The current smoother is an evenly weighted 3x3 grid-cell filter, with cyclic boundary conditions on the east and west edges and "missing" boundary conditions on the north and south edges of the domain.

Verification in Adler et al. (1994) against rain gauge analyses over water and land and subjective examination of the resulting maps and zonally-averaged fields show that the AGPI estimates are superior to either the microwave or the GPI estimates by themselves for a four-month period of August-November, 1987. A seven year data set using this procedure has recently been produced for the Global Precipitation Climatology Project (GPCP)

In its current version the algorithm produces a monthly product on a 2.5° lat./long grid. The temporal and spatial resolutions are dependent on the resolutions available in the GPI data sets supplied to the Global Precipitation Climatology Project (GPCP) by the geosynchronous-satellite operators. The GPI data sets already have a five-day resolution, but currently occupy a 2.5° lat./long grid. Therefore, in order to meet the 3B-42 specifications (5-day, 1° lat./long), the GPCP data set specifications will have to be changed. This modification is being considered by the GPCP, with a reasonable chance of implementation before TRMM launch. The change in the temporal and spatial resolutions will require minor modifications in the draft software.

3.4.2 *Merge Satellite and Gauge Product* - (TSDIS ref. 3B-43)

The current draft of 3B-43 builds on the Satellite-Gauge-Model (SGM) technique described by Huffman et al. (1995), which makes use of the results in 3B-42. In the first stage, the Multi-Satellite intermediate precipitation product is produced from the TRMM Combined Instrument (TCI) precipitation estimate (2B-31), the Adjusted GOES Precipitation Index (AGPI) precipitation estimate (3B-42), and the SSMI estimate (3A-46). Estimates of the (spatially fluctuating) errors in each field are computed, mostly reflecting the sampling-induced uncertainty in each, then a linear combination is computed in which each estimate is weighted by the inverse of its (local) error-variance. This stage also yields the Multi-Satellite relative error estimate intermediate product. In the second stage, the Raingauge Precipitation Analysis (3A-45) and the Multi-Satellite precipitation estimate are similarly combined (using the 3A-45 raingauge relative error analysis and the Multi-Satellite relative error estimate) into 3B-43 Satellite/Gauge precipitation estimate and relative error estimate fields. The current SGM includes numerical-model estimates, a feature not included in product 3B-43. The primary limitation in the method is imperfections in the estimation of relative error for the individual fields.

Verification in Huffman et al. (1995) for one year of SGM results (July 1987 to June 1988) show important differences from the individual estimates, including model estimates, as well as climatological estimates. In general, the SGM is drier in the subtropics than the model and climatological results, reflecting the relatively dry microwave estimates used in the paper, which dominate the SGM in oceanic regions. A seven year data merged SSM/I, geosynchronous and

gauge set using this procedure has recently been produced for the Global Precipitation Climatology Project (GPCP).

An alternative to the SGM-based draft scheme for 3B-43 is the Xie and Arkin (1995) procedure, which constructs global analyses of monthly precipitation by merging estimates from three types of satellite estimates (geo-IR-based GOES Precipitation Index, or GPI; the microwave scattering-based Grody estimates; and the MW emission-based Chang estimates) and gauge-based monthly analyses from the Global Precipitation Climatology Centre (GPCC). As with the SGM, Xie and Arkin's (1995) technique includes numerical model accumulations, which would not be used in 3B-43. A 2-step strategy is used to reduce the random error found in the individual sources and to remove the bias of the combined analysis. First, the three satellite-based estimates are combined linearly based on a maximum likelihood estimate, in which the weighting coefficients are inversely proportional to the squares of the individual random errors determined by comparison with gauge observations and subjective assumptions. This combined analysis is then blended with an analysis based on gauge observations using a method that presumes that the bias of the gauge-based field is small where sufficient gauges are available, and that the gradient of the precipitation field is best represented by the combination of satellite estimates elsewhere.

Results for the original Xie and Arkin (1995) method for a seven year period showed substantial improvements relative to the individual sources in describing the global precipitation field. The large-scale spatial patterns, both in the tropics and the extra-tropics, are well represented with reasonable amplitudes. Both the random error and the bias have been reduced compared to the individual data sources, and the merged analysis appears to be of reasonable quality everywhere.

3.4.3 Post-Launch Algorithm Validation

Products 3B-42 and 3B-43 are surface rainfall products and require no vertical profile validation data. They will be validated with routinely available gauge products from different locations and special validation data sets produced at TRMM validation sites.

The adjusted geosynchronous satellite product (3B-42) will be routinely validated with surface raingauge data sets and analyses produced over the Pacific Ocean atoll gauge network (Morrissey and Greene, 1991) and over land areas (GPCC, 1992). Although some of the atoll data can be processed to 5-day 1° lat./long fields, we anticipate that most of the atoll and all of the land validation will be carried out on the monthly 2.5° lat./long scale discussed above. Validation data sets at the TRMM ground validation sites combining radars and raingauges will be used to validate at the finer scale. Other special raingauge analyses will be

used as available. One such product is the 5-day 0.5° lat./long Surface Reference Data Center (SRDC) analysis currently being produced by NOAA National Climatic Data Center for the GPCP over parts of the United States and a few foreign locations (NCDC, 1995).

The routinely available GPCC raingauge analyses will be incorporated into product 3B-43. Therefore, the validation of the "TRMM and other data sources" product (3B-43) will be limited to the TRMM ground validation sites and other special raingauge analyses that are independent of the data being used by GPCC. The SRDC gauge analysis fits this description and is therefore of particular interest.

3.4.4 Post-Launch Algorithm Improvement

The algorithms on which products 3B-42 and 3B-43 are based have already shown utility. Nonetheless, they continue to be topics of research, so it is expected that improvements will continue to be made for both products after launch. Barring catastrophic data quality or coding problems, we expect to seek reprocessing only after validation, so reprocessing should be necessary no less than six months after launch.

Both products are critically dependent on the TCI estimate of instantaneous rain (2B-31), which serves as the foundation for calibrating or adjusting the other satellite estimates. Changes in that product will immediately impact the results in 3B-42 and 3B-43. Therefore, changes in 3B-42 and 3B-43 should be coordinated with 2B-31 regarding reprocessing.

4. TRMM Validation Program

The stated requirement, as established by the TRMM science team, is to have 10 ground validation (GV) sites, representing a reasonable variety of tropical rain regimes in place at the time of TRMM launch. The 10 sites that have been identified are located in Florida, Australia, Texas, the Marshall Islands, Israel, Brazil, Taiwan, Thailand, Guam, and Hawaii. The Weather Surveillance Radar-88D (WSR-88D) participation in the continental United States (U.S.), Hawaii, and Guam requires coordination with the National Oceanic and Atmospheric Administration (NOAA). Arrangements for participation by Australia, Taiwan, Israel, and Brazil are based on the acceptance of their proposals to the 1994 National Aeronautics and Space Administration-National Space Development Agency (NASA-NASDA) joint TRMM NASA Research Announcement (NRA-94-MTPE-01). Agreements exist with the U.S. Army and Thailand for data from their radars at Kwajalein and Om Koi, respectively, including their operating a number of rain gauges supplied by the TRMM Office. Development of the GV sites, their technical description, and other details are contained in the TRMM Office GVP I&O Plan.

Due to the extremely high volume of raw data as well as logistical difficulties in obtaining and quality controlling data from radars, raingauges and disdrometers, it was felt that the TRMM data system should concentrate its limited resources on only a few radars. Therefore, the plan that is now being implemented is to focus on four of the highest priority sites, i.e., Florida, Kwajalein, Australia, and Texas, from which TSDIS will receive direct data, i.e., direct data (DD) sites. These are 4 individual radars, chosen by the TRMM Ground Validation Team to be best suited for the problem of routine satellite rainfall and rainfall structure validation. These decisions are based upon rainfall climatologies, operational availability and resource availability. Data from these radars will be processed at TSDIS. Each site has at least one investigator from the TRMM GV team assigned to insure that the data products meet TRMM standards. Only one of the multiple radars in Florida and Texas will be used for the direct data input to TSDIS. These will be the Melbourne, Florida, and Houston, Texas, Next Generation of Meteorological Radars (NEXRAD's) (WSR88-D's). Merged data products from the multiple radars will be the responsibility of the respective Principal Investigators (P.I.'s) for these two sites.

The P.I.s of the six remaining sites will utilize specified algorithms and procedures furnished by the TRMM Office to produce validation data products (DP) for direct ingest by TSDIS. These DP sites, referred to as "Special Climatology Sites" have individual or closely spaced radars which present a unique opportunity for TRMM validation but which cannot be processed by TSDIS in an operational manner. Data from these sites will be processed by selected TRMM Principal Investigators and delivered to TSDIS. The location, designation, and assigned P.I. for each GV site are summarized in Table 4.1.

Because of the great difficulty associated with routine processing, it is expected that these sites will concentrate upon 3-6 month periods during which they can generate the high quality products necessary for TRMM validation. Because of the TRMM decision to concentrate on high quality data periods instead of continuous processing, there is currently room to increase slightly the number of Special Climatology sites. To be included, a site must have a good (preferably 10 cm) radar, a network of raingauges and perhaps most importantly, an individual that will interact with the TRMM science team to insure that the products meet TRMM standards. Figure 4-1 indicates the distribution of the TRMM validation sites and identifies Primary sites (black) and Special Climatology sites (white).

Table 4-1: Location, Type, and P.I. Assigned for GV Sites

SITE	DESIGNATION	TYPE	P.I. & AFFILIATION
Melbourne, Florida	Direct Data (DD)	WSR-88 (10 cm doppler)	D. Short, GSFC
Houston, Texas	DD	WSR-88 (10 cm doppler)	M. Biggerstaff, TAMU
Kwajalein, RMI	DD	10 cm doppler	R. Houze, UWA
Darwin, Australia	DD	5 cm dual pol., doppler	T. Keenan, BMRC
Florida (multiple radars)	Direct Product (DP)	4 x WSR-88 (10 cm doppler)	P. Ray, FSU
Texas (multiple radars)	DP	4 x WSR-88 (10 cm doppler)	E. Zipser, TAMU
Israel	DP	10 cm	D. Rosenfeld, Hebrew U.
Taiwan	DP	10 cm doppler	J.-T. Wang, NCU
São Paulo, Brazil	DP	10 cm	O. Massambani, U. of São Paulo
Om Koi, Thailand	DP	10 cm doppler	D.Rosenfeld
Guam, M.I.	DP	WSR-88 (10 cm doppler)	W. Krajewski, UIA
Hawaii	DP	WSR-88 (10 cm doppler)	TBD

Figure 4-1: Worldwide distribution of TRMM ground validation sites.

4.1 Product Generation

Product generation at all TRMM GV sites will be performed using identical product algorithms. These algorithms will be chosen by the GV team. The TRMM office will integrate the individual science algorithms into a radar data processing package and make this package available to both TSDIS as well as the Special Climatology sites. It is expected that the product code itself will be identical for all sites except for the Z-R conversion parameters which must be locally adjusted based upon raingauge information. Because of the difference in resources available for Primary and Special Climatology sites, it was further necessary to develop slightly different processing scenarios for the various GV sites. For primary sites, TSDIS will archive data Level 1B-51 and higher. For Special Climatology sites, TSDIS will only archive Level 1C-51 and higher. The TRMM office has agreed to serve as a repository for the raw data tapes should it become necessary in the future to access this data again. It is fully expected that for Special Climatology sites, the individual P.I.s will retain a duplicate archive of the original data.

4.1.1 Primary site functions

Radar data from these four sites will be made available to TSDIS either directly from the P.I., the TRMM office or NCDC. TSDIS will ingest the raw radar tapes, perform some minimal data reduction[4] and archive the data as level 1B-51. Raw radar tapes will be sent to the TRMM office for storage. To produce higher level products, it is necessary to know the satellite orbit parameters (to identify overpasses and therefore full data retention periods) and Z-R relations which are derived by analyzing the raingauge record. TSDIS has satellite orbit parameters. The Z-R relations, however, are typically not yet available at the time of processing. TSDIS will therefore produce rainfall products with a default Z-R derived from either climatology or preceding months. The data products are archived in EOSDIS, but labeled as "unverified". The data products are also sent directly to the P.I. for verification. Raingauge data will be collected and quality controlled by the TRMM office and/or the P.I.s. Once the gauge data is quality controlled, it is sent to the P.I. who derives new Z-R relations and examines the gauge data further. If the new Z-R does not warrant a reprocessing of data based upon the climatological Z-R relations, then the P.I. updates the EOSDIS product with a "verified" stamp. Otherwise, the P.I. submits the new Z-R relations to TSDIS and the data are reprocessed. The P.I. then also sends the final gauge data to TSDIS for archival in EOSDIS.

4.1.2 Special Climatology site functions

---

[4]   Data beyond 230 km from the radar will nto be archived, nor will the spectral widths.

These sites must perform the same tasks as is done for the primary sites except that only the "best" data periods (3-6 mo.) are critical and that a delay in the processing is acceptable. For that reason, it is expected that these sites will collect all the radar and raingauge data first, develop Z-R relations, apply them and then send their product set to TSDIS for archival in EOSDIS as "verified". In order to determine data retention for Level 1C-51, the P.I.s must have TRMM ground track parameters. This will be supplied by TSDIS. Data volumes are such that TRMM cannot archive all the original data from Special Climatology sites. The data sent to TSDIS will therefore begin with Level 1C. P.I.s should archive their raw and Level 1B-51 data as well as making the raw data available to the TRMM office.

4.1.3 Special Climatology--multiple radar sites

These special study areas in Florida and Texas consist of more than one overlapping radar which makes it possible to generate rainfall estimates over areas commensurate with the 5° grid elements specified in TRMM. Up to Level 1C, these sites will process data the same as for individual Special Climatology radars. That is, they will generate separate Level 1C products for each radar in their grid. For level 2 and above, these sites must use specialized software to merge the data from the individual radars. All level 2 and higher products are then in a Cartesian grid over the entire area encompassed by the multiple radars. P.I.s should archive their raw and Level 1B-51 data as well as making the raw data available to the TRMM office.

4.2 Radar Calibration and Data Quality Control

At present, specific plans by the various cooperating GV sites to perform absolute or sphere calibrations for their radars have not been developed, except for Darwin, which is a research facility that performs routine sphere calibrations once or twice per year. The TO has requested the NEXRAD Operational Support Facility to perform sphere calibrations on all WSR-88D radars being used in the GV effort, to the maximum extent of their ability to do so and efforts are underway to obtain such calibrations at all sites that are of interest to TRMM.

Assuming that accurate calibration has been achieved, the next major task is radar data quality control. Radar data quality is severely impaired by several factors such as ground clutter, anomalous propagation, second trip echoes, spikes (due to radio and/or solar interference), clear air echo, and random noise. These spurious echoes must be removed from the data before reliable application of any of the subsequent GV algorithms can be attempted.

The TO has developed an automated quality control (QC) algorithm that uses the vertical structure of reflectivity in moving windows to determine whether a

given area is comprised of rain or spurious echo. A limited hand-edited data set is being developed by members of the GV science team which will then be compared to the automated algorithm to ensure that the technique is effectively removing the spurious echoes without eliminating the raining echoes.

Quality control (QC) of the rain gauge data has been an important focus of the TRMM Office. Different quality control measures occur at each level of processing. Some quality control measures are applied to all sites; others are site specific. For instance, tipping bucket data received from several sites (KSC, Om Koi, and Phuket) include records containing calibration tips. The data records need to be eliminated from the file before the 1 minute rain rates can be computed. Data received from the St. Johns Water Management District in Florida, can include multiple tip records with the same time stamp. An automated module was developed to address this particular case during the processing of the GMIN file. Currently, new algorithms are being implemented which use radar data to determine anomalous gauge inactivity. Anomalous gauge inactivity occurs due to the mechanism becoming clogged by organic materials such as leaves, insects, and bird droppings. The use of radar data to QC gauge data was successfully tested during the Algorithm Intercomparison Workshop (AIW).

4.3 Program Execution

Before launch, the TRMM Office will make necessary arrangements with each of the GV sites for processing and/or direct transfer of radar data including rain gauge and disdrometer data. When fully operational, the TRMM GV network will include 10 sites. The sites are designated Direct Data (DD) or Direct Product (DP) sites. The DD sites are the four "high priority" sites, i.e., Melbourne, Florida, Houston, Texas, Kwajalein Atoll, RMI, and Darwin, Australia. These sites will transmit raw data directly to TSDIS for processing. The DP sites will provide, through their respective P.I.s TRMM GV products to TSDIS. With the use of multiple radars (up to 5 NEXRAD's) the Florida and Texas sites are expected to merge the radar data to produce large-area (~500 x 500 km) rain fields. The remaining DP sites, Israel, Brazil, Taiwan, Thailand, Guam, and Hawaii are single-radar sites. All GV sites are associated with either operational weather radars or quasi-operational research facilities and are expected to be operated continuously throughout the TRMM mission life time. If during the mission, a GV site is expected to suffer a prolonged down time, it is possible that another GV site could be substituted for it. Substitution may also be considered for those GV sites that have prolonged dry seasons. Selection of a substitute or another site in a critical area would be based on recommendations by the GV science team and TRMM Project Scientist.

There are a series of time-critical events that are crucial in order to support operational processing of ground validation (GV) data. While a number of

scientists on the TRMM GV team are engaged in developing suitable algorithms for the 11 identified TRMM GV products, the TRMM Office must have the infrastructure to convert the individual pieces of software developed by the algorithm scientists into a single operational package for TSDIS. This package must be general enough to not only run at TSDIS, but also at each of the Special Climatology Sites discussed above.

4.3.1 Pre-Launch Operations

Beginning in August 1995, radar and rain gauge data collected at the Darwin and Melbourne GV sites will be sent to GSFC, where the TRMM Office and TSDIS will collaborate to generate all the GV products (described in the subsequent chapter) and make them available to TRMM Science Team PIs. They will continue to do this end-to-end data processing, archival, and distribution at a level commensurate with on-going development activities at TSDIS and the TO.

This procedure will systematically test all aspects of the TRMM GV methodology. By the time the satellite is launched in 1997, a steady stream of GV products should be flowing to the TRMM PIs. The goal is to work all the "bugs" out of the GV data collecting and processing system during the pre-operational phase. The TRMM GV pre-operational phase is thus a building process that goes on in parallel with the construction of the TRMM satellite itself. A key intermediate goal is to have documented procedures covering calibrations, operations, data collection and transmission and data processing, as appropriate, delivered to all participating DP sites by August 1996. At that time, end-to-end data flow testing will be extended to include all 4 primary sites. The remaining sites will be phased in during the ensuing year. Specific scheduling for participation by the remaining sites will be developed in coordination with their representatives over the next 2 years. Huge quantities of data will be arriving at GSFC every month, and all links of the processing, archival, distribution, analysis, evaluation, and modification of procedures must be smoothly and efficiently operating by the TRMM launch time.

4.3.2 Post-Launch Operations

Post launch operations are limited to gauge data QC and P.I. support. After TRMM launch, DD sites will continue to send the raw radar data to TSDIS and rain gauge data to the TRMM Office. TSDIS will reformat the raw data and produce Level 1B data. Level 1B radar data will be processed further to produce higher level data products. These products will be sent to EOSDIS to archive according to TSDIS/EOSDIS schedules. The data will contain a quality flag that shows that the data have not been validated. The TO will receive one month of rain gauge data from GV sites about 1 to 2 months after the actual measurement time. The TO will process the rain gauge data and send the data to TSDIS and to

site P.I.s. When algorithm P.I.s have validated their Z-R relationships, proposed changes will be reviewed by the science team, and, if approved, TSDIS will request the Level 1C data from EOSDIS for reprocessing, and reprocess the radar data. Once radar data are reprocessed, the quality flag will be changed according to the established procedure.

DP sites will send the Level 1B data to the TRMM office, and Level 1C and higher level data products to TSDIS. The data products delivered from DP sites are expected to include all the products listed in Appendix C. The data will be produced in the TSDIS standard format (HDF) using TSDIS-provided tool kits. It is anticipated that DP site data will be available about 3 months after actual measurement time. The algorithms to be used by the DP sites are expected to be the same as the ones used by TSDIS to produce data products from DD site data. The TRMM Office plans to provide GV Version 3.0 software with a computing facility and deliver it to the P.I.s. The TRMM Office will assist the multiple-radar site P.I.s in developing uniform merging software to provide large area rain fields.

5. TRMM Ground Validation Algorithms

The goals of TRMM drive the TRMM Ground Validation effort. The overriding goal of TRMM (Simpson 1988) is "evaluation of the four-dimensional structure of latent heating in the tropical atmosphere." To achieve this goal, the TRMM satellite must determine:

Table 5-1

> I.   the amounts of convective and stratiform precipitation,
>
> II. the vertical structure of precipitation,
>
> III. the areal rainfall over 5° x 5° deg areas for 30-day periods.

To achieve these three objectives accurately, the satellite must determine these aspects of precipitation over the diurnal cycle, which is complex for tropical rainfall.

While the TRMM satellite is flying, the GV program will address the three TRMM goals *locally*. The GV program will operate several ground validation sites on a continual basis while the satellite is in orbit. These sites will provide a climatological sample of the three aspects of precipitation represented by the three TRMM objectives listed above. Each operational GV site will be equipped with Doppler radar instrumented for precipitation measurements and a network of surrounding rain gauges. The detailed characteristics of each site are in Chapter 4. The data from the operational GV sites will be the basis of several data products that mimic as closely as possible the products based on the satellite TMI and PR data.

The resolution of the GV data from ground-based radars varies with antenna characteristics, distance of target from radar, and the elevation angle spacing of scans. As a rule of thumb the resolution of the operational GV site radar data is ~2 km in the horizontal. The slant range resolution (along a radar beam) is < 1 km. Interpolation of the slant-range data to a Cartesian grid yields a vertical resolution ~0.5-2 km in the vertical, depending on horizontal distance from the radar. These basic spatial resolutions of the satellite-borne TMI (4 km at 85 GHz to 40 km at 10 GHz) and PR (4 km jhorizontally and 250 m vertically) and of the operational GV site radars fundamentally limit the types of comparisons between the TRMM satellite data and the GV site data. Since the operational GV site data have considerably greater horizontal resolution than do the TRMM satellite data, the operational GV data will provide the better picture of the horizontal texture of the precipitation.

The PR aboard the satellite will detect only that precipitation which has radar reflectivity ~20 dBZ or greater. The operational GV site radars will detect echoes down to 0 dBZ or less. This greater sensitivity means the GV radars will give a more complete picture of the precipitation, especially its vertical structure. Above the 0° C level (about 5-km altitude in the tropics) most precipitation has reflectivity below 20 dBZ. The operational GV radars will thus provide a much better indication of the distribution of ice-phase precipitation particles. This information on the vertical structure of the radar-echo structure is essential for physical understanding and for underpinning the TMI-based algorithms, which need this information. The PR has a wavelength of about 2 cm, which is highly attenuated, especially by melting snow particles. The GV radars, with one exception, will have wavelengths of 10 cm, which suffer very little attenuation. The one exception (Darwin, Australia) has a wavelength of 5 cm, which has moderate attenuation, but not nearly as severe as attenuation at 2 cm. Moreover, the Darwin radar is polarimetric, which may allow some partial correction of the attentuation. The high attenuation rates of the PR complicate direct intercomparison of reflectivities measured by the PR and an operational GV radar viewing the same targets.

In part because of the measurement differences, the products based on the operational GV site data will be stand-alone products that will fully address all three of the TRMM goals listed in Table 5-1 for a particular site. Thus, the GV products serve as significant research data in and of themselves. In this way, they constitute the best possible comparison data set for the TRMM satellite data. The products based on the operational GV site data will be stand-alone products that will fully address all three of the above TRMM goals for a particular site. Thus, the GV products serve as significant research data in and of themselves. In this way, they constitute the best possible comparison data set for the TRMM satellite data.

The fundamental philosophy of the TRMM GV program recognizes that *we have no truth*. The TRMM GV program does not provide "truth;" rather, it provides an independent estimate, at certain locations, of the same quantities estimated by satellite. We will thus have two estimates of the three aspects of precipitation listed in Table 5-1: one estimate from the satellite, another estimate from ground sites. We will compare the two estimates. The closer the two estimates are to agreement, the greater the confidence we have in both estimates. The uncertainties in instrumentation, sampling, and theoretical interpretation of both satellite and ground-based data are so great that any other view of the TRMM GV data products or of the TRMM satellite data cannot be supported by fact.

The TRMM GV program provides for two types of validation between the satellite and operational GV data. The first type of validation is *instantaneous comparison*. The orbit of the TRMM satellite guarantees that the satellite will sample the region covered by a ground-based radar ~2 times daily. Each overpass provides an opportunity to determine whether or not the satellite and

operational GV data are consistent—taking into account the differences in resolution, sensitivity, and attenuation discussed above. Instantaneous validation consists of comparing satellite and operational GV data obtained simultaneously in an overpass region. Since the overpasses occur at intervals of many hours, the physical understanding and interpretation of the overpass data samples depend on knowing the life histories of the precipitation systems present at the overpass time. Only the operational GV radar can provide this time context since it will be scanning the precipitation in high time resolution both before and after the satellite overpass.

Instantaneous comparison will be a valuable check on the consistency of the TRMM satellite data and operational GV site data. However, limiting the comparisons of TRMM satellite data and operational GV site data to the twice daily overpasses would severely underutilize the operational GV site data, which will be obtained continually 24 h a day whether the satellite is passing over or not.

The second type of validation is *climatological comparison*. In this case, we determine whether the two data sets (satellite and operational GV data) lead to similar determinations of TRMM objectives I-III stated in Table 5-1 by making statistical comparisons. We will determine and compare ensemble characteristics of measurable precipitation parameters estimated from both satellite and ground-site data. The satellite and ground-site estimates may come from data samples that do not actually overlap in time and/or space. The basic premise of this climatological comparison is that the samples obtained by satellite and operational GV sites are drawn from the same population.

For the climatological comparisons between satellite and operational GV site data products to address the TRMM objectives I-III listed in Table 5-1, each set of instruments (satellite and ground-site) must obtain meaningful statistics of rain amount, convective-stratiform texture, and vertical echo structure for 1-month samples over regions of a few hundred kilometers in horizontal dimension. Because the diurnal cycle of precipitation in the tropics is strong and because its amplitude and phase vary strongly from one location to another, the sampling of radar echoes at an operational GV site must be done with fairly high time resolution in order to obtain the desired monthly statistics accurately. Figure 5-1 shows the uncertainty of monthly rainfall estimates as a function of time interval between samples. The spread of points at each time measures the variance of the monthly mean rain for that sampling time interval. According to this analysis, any interval less than about 1 h gives essentially the same estimate of the averaged one-month areal rainfall accumulation.

The above discussion implies that the time resolution of the operational GV data must be:

- as high as possible (~10 min) for time periods bracketing overpasses (±30 min.) in order to provide the evolutionary context of the echoes observed in instantaneous comparisons.

- about 1 hour or less for all other time periods in order to provide monthly statistics for climatological comparisons over the region covered by a ground site.

Figure 5-1: Uncertainty of monthly areal rainfall estimates as a function of the sampling time resolution. The results are based on the Darwin raingauge network data of February 1988. The dark (light) shaded area in each sampling time interval bin corresponds to the range of the mean ± 1(2) standard deviation(s). The heavy horizontal line indicates the true monthly areal mean rainfall accumulation for this particular month and site based on the continuous raingauge record (255 mm). The 50% uncertainty range is shown by the dotted horizontal lines. The sloping dashed lines indicate that decreasing the sampling time resolution increases the uncertainty of the monthly areal rainfall estimate by roughly 3.5% per hour decrease in time resolution. From Steiner et al. (1995).

5.1 Ground Validation products

5.1.1 Types of products

The data collected at the operational GV sites will be organized into five types of products, referred to as: *basic data, existence of rainfall, convective/stratiform maps, vertical structure,* and *rain maps* (Table 5-2).

The basic data products [1B-51 and 1C-51 of Table 5-2] serve two purposes. First, they serve as input to all the other products listed in Tables 5-2. Second, they are a fail-safe product for the future. TRMM is a decade-long program, and it is impossible now to predict what investigators will want to do with the TRMM data 5, 10, or more years from now. The products that we generate for convective/stratiform separation, vertical structure, and rain mapping may not be the products needed for research in the future. By saving the basic data from

the operational GV sites in a minimally processed form, we guarantee the long-term value of the TRMM GV data set.

The existence-of-rainfall product [2A-52 in Table 5-2(b)] simply indicates whether a particular site has any precipitation in its field of view at a given time. It is primarily an index to simplify the process of searching for data.

The convective/stratiform product [2A-54 in Table 5-2(c)], vertical structure products [2A-55 and 3A-55 in Table 5-2(d)] , and rain mapping products [2A-53, 3A-53, and 3A-54 in Table 5-2(e)] address directly the TRMM goals I-III listed in Table 5-1.

5.1.2 Basic data products

The product 1B-51 will consist of the complete set of volume scans of radar data from an operational GV site radar. The archived data will be the values of reflectivity, radial velocity, and differential reflectivity (for polarimetric radars) at all the azimuth and range bins containing data. Other variables from polarimetric radars may also be archived. The product 1C-51 is a mask that will identify spurious data. The mask will also include corrections for attenuation where appropriate. Chapter 4. describes the data quality control methods used to identify spurious data and make corrections for attenuation by atmospheric gases and intervening precipitation.

5.1.3 Existence of rain

The product 2A-52 will indicate the number of pixels on the lowest elevation angle scan within a 150 km radius of a GV radar that have echo exceeding a prescribed threshold at a given time. A potential user of TRMM GV data can access this number as an indicator of whether or not to proceed further with analysis of the data for this time at this station.

5.1.4 Convective/stratiform structure

Beyond the simple existence of precipitation, the next level of complexity is to subdivide the precipitation into two basic categories, convective and stratiform. These categories of precipitation are physically distinct and essential to separate if we are to understand how the precipitation relates to heating of the tropical atmosphere. In tropical precipitation, the vertical profile of heating is composed of two modes: a longer wavelength convective mode, and a shorter wavelength stratiform mode (Houze 1982, 1989). These modes are illustrated in Figure 5-2. The total latent heating profile in the tropics is a combination of these two modes. The large-scale atmosphere responds to these modes differently (Mapes

and Houze 1995). The adjustment of the large-scale circulation to the latent heating depends (critically) on the mix of convective and stratiform heating processes represented by the stratiform and convective precipitation (Raymond 1994). Separation of tropical precipitation into convective and stratiform components is therefore one of the major objectives of TRMM (objective I in Table 5-1).

Figure 5-2: Characteristic shapes of heating profiles in convective and stratiform regions. Based on Houze (1989).

Product 2A-54 is the GV product designed to separate any precipitation observed at an operational GV site into its convective and stratiform components. It is a plan view map showing all the precipitation detected at the lowest elevation angle. It identifies each pixel within 150 km of an operational GV radar as containing either convective, stratiform, or no precipitation. During the first Algorithm Intercomparison Workshop (AIW), which was held in Seattle in December 1994, GV team members tested the following five methods of convective-stratiform separation:

A. The *random* method is a completely nonphysical control method. It decides by a coin toss whether a pixel is convective or stratiform.

B. The *"Simple Simon"* method is the simplest physical method. It classifies precipitation as stratiform or convective depending on whether or not the radar reflectivity on the low-level scan exceeds a given threshold value. This method is a good approximation but is not completely adequate because radar echoes of intermediate intensity may be either convective or stratiform.

C. *Steiner et al.* (1995) proposed a method in which an echo is convective if it either is very intense (exceeds a given high threshold reflectivity) or if it forms a peak value in relation to background echo intensity. Any echo that is not convective by one of these criteria is stratiform. The method is calibrated against bright-band observations.

D. *Rosenfeld et al.* (1993, 1994) proposed a method that uses a combination of radial reflectivity gradient and reflectivity bright-band identification to locate stratiform precipitation. The remainder of the precipitation is called convective.

E. *Krajewski et al.* (1995) proposed a method that uses a rain rate threshold (rather than a reflectivity threshold) to determine if precipitation is convective or stratiform. Their algorithm is affected by the methodology used to determine the rain rate (Sec. 4.7).

Figure 5-3 (a,b) shows a map of radar reflectivity along with an example of a convective/stratiform map (product 2A-54). This example map was computed by method C. Results from the AIW showed that methods C, D & E all performed better than the random or "simple simon" methods. Methods C & E were quite similar while method D had a tendency to underestimate the convective area (possibly due to a programming error). After the workshop, the GV team adopted a slightly modified version of method C for producing the 2A-54 product.

Figure 5-3: Radar reflectivity (a) and map (b) showing convective (red) and stratiform (green) areas as determined by algorithm C discussed in the text. Reflectivity values shown by color scale in (a) are in dBZ. Range marks are at 25 km intervals. North is at top of page. The coast line of northern Australia passes through the radar site at Darwin, Australia. Bathurst (smaller) and Melville (larger) Islands are to the north of Darwin.

5.1.5 Vertical structure

Direct measurements of the vertical distribution of latent heating in the tropical atmosphere are not possible. Instead we must use model-based algorithms to estimate the vertical profiles of heating which are consistent with measurements of the vertical structure of precipitation. These retrieval techniques use either satellite measurements (e.g. Wilheit et al. 1994) or ground-based radar data (e.g. Houze et al. 1980; Braun and Houze 1995) combined with theoretical principles of cloud microphysics, radiative transfer, and fluid dynamics. The TRMM objective II in Table 5-1 provides data for use in connection with model-based methods of estimating the vertical profiles of heating in both convective and stratiform regions, as well as in "anvil" regions (regions of precipitation aloft but not reaching the earth's surface).

The vertical structure products 2A-55 and 3A-55 listed in Table 1(d) satisfy objective II in Table 5-1 by indicating quantitatively the distribution of the precipitation intensity in three-dimensions throughout the volume of observations obtained by an operational GV radar. In contrast to the convective/stratiform maps described above, which subdivide observed precipitation into its two basic physical categories—the minimal possible

subdivision of the radar data—the vertical structure products 2A-55 and 3A-55 document the texture of the precipitation more completely by subdividing the radar reflectivity data from an operational GV site into 1 dBZ-wide intensity categories and determining the frequency of occurrence of precipitation in each category. Also in contrast to the convective/stratiform maps, which only consider the radar data at the lowest altitude observed by the radar, the vertical structure products 2A-55 and 3A-55 include a histogram of the reflectivity in 1 dBZ-wide bins for each of a series of altitudes spaced 1.5 km apart, ranging from 1.5 km to echo top. Thus, the products 2A-55 and 3A-55 provide the statistical distribution of radar reflectivity values throughout the three-dimensional volume of radar-observed precipitation. These distributions of radar echo are suitable for presenting in the form of Contoured Frequency by Altitude Diagrams (or CFADs, Yuter and Houze 1995). The software for CFAD presentation of the data will be part of the product. Figure 5-4 shows an example of the CFADs for an instantaneous echo pattern (product 2A-55). Figure 5-4(a) shows the distribution of reflectivity for the whole three-dimensional echo volume. Figures 5-4(b,c) show the distributions for the convective and stratiform subregions (whose horizontal boundaries are established in product 2A-54). Figure 5-4(d) is the CFAD for the "anvil" region, which is the region for which echo exists aloft but not at the surface. Products 2A-55 and 3A-55 include total, convective, stratiform, and anvil CFADs for land and ocean areas separately as well as for the whole regions surveyed by the radar. Thus, 2A-55 and 3A-55 each include 12 CFADs for each time period. In addition to the three-dimensional Cartesian reflectivity maps and the CFADs, a vertical profile of mean reflectivity corresponding to each CFAD is computed and included as part of products 2A-55 and 3A-55.

Figure 5.4: Examples of Contoured Frequency by Altitude diagrams (CFADS) for radar data taken by the Darwin, Australia, radar at 0721 UTC, 28 Dec., 1993. CFAD bin size is 3 dBZ and the plot is contoured at intervals of 0.5% of data per dBZ per km starting at 0.5% dBZ^{-1} km^{-1}.

5.1.6 Rain maps

The rain-map products [2A-53, 3A-53, and 3A-54 in Table 5-2(e]) address the TRMM objective III listed in Table 5-1. This objective is the 30-day total rain accumulation over a 5° x 5° area. The total rain accumulation gives the net (i.e., vertically integrated) latent heating of the atmosphere, if we know the net evaporation from the earth's surface. The rain-map products thus differ from the products listed in Tables 5-2(a-d), which are relevant to determining the vertical distribution of the heating. It is only by combining the information on both vertical distribution and net amount of latent heating that we can achieve the TRMM goal of determining the climatology of the four-dimensional latent heating of the tropics.

The suite of rain-map products (2A-53, 3A-53, and 3A-54) breaks the 30-day accumulation of rain over a broad area down spatially and temporally. Each map presents the accumulated rainfall in 2 km square bins over the whole region covered by radar observations. The products 2A-53 and 3A-53 break the 30-day

patterns down into instantaneous and 5-day accumulation maps. These products thus allow the investigator to determine from which storms the large areal accumulations derive. This spatial and temporal breakdown is essential to understanding areal accumulations, which arise from highly intermittent precipitation processes.

Whereas the products relevant to vertical distribution of heating [Tables 5-2(a-d)] involve only the radar reflectivity field, the rain maps involve conversion of the measured low-level field of radar reflectivity (Z) to a pattern of estimated surface rain rate (R). This $Z - R$ conversion requires use not only of the radar data but also of the rain-gauge data from a GV site. The AIW compared rain maps produced by three different approaches to the $Z - R$ conversion. Each of these methods uses the radar data in a "window" 36 km^2 surrounding each rain gauge. The reflectivity values observed in these windows are related empirically to the rain rates observed simultaneously by the gauges. As TRMM proceeds, additional rain map algorithms may also be based on multiple polarization parameters.

This empirical relationship, between radar and rain gauge data, is difficult to obtain because the area sampled by a gauge is of the order of 10^8 times smaller than the resolution volume of the radar. Moreover, the volume of air sampled by the radar lies ~0.5-2 km above the surface of the earth. The precipitation processes of growth, breakup, evaporation, turbulent diffusion, and advection guarantee that the raindrops falling in the gauge have different characteristics than those observed by radar (Austin 1987). The exposure of a gauge is always fraught with uncertainties (e.g., Kleinschmidt 1935). In addition, it is well known that precipitation is spatially and temporally so intermittent by nature, even if measured perfectly accurately, measurements by gauges short distances apart may differ by significant amounts.

The three approaches to $Z - R$ conversion tested in the AIW are (using the same letter designations as in Sec. 5.1.4):

C) *Steiner et al.* (1995) assume that the $Z - R$ relationship is of the form $Z = aR^b$, where a and b are positive constants. They assume that b is known from previous drop-size distribution measurements, but that a may vary. They average the rain gauge and window-reflectivity data over a one-month period. Using these values for Z and R, they solve for a and then assume that this value of a applies to the instantaneous radar data.

D) *Rosenfeld et al.* (1993, 1994) plot histograms of the 3-min average values of gauge-measured R and instantaneous window-average Z. They assume that the percentile values of R and Z match. The set of matched percentile values of R and Z constitutes the $Z - R$ relation.

E) *Krajewski et al.* **(1995) plot scatter diagrams of the 5-min average values of gauge-measured** R **and instantaneous window-average** $\hat{Z}$**, where** $\hat{Z}$ **is a value of reflectivity obtained by integrating the measured** Z **values over all the low elevation angles up to about the 4 km level. A best fit line gives the** $\hat{Z} - R$ **conversion.**

Thus, the three $Z - R$ approaches tested at the AIW differ in how they organize the gauge-measured R and instantaneous window-average values of reflectivity. The AIW split the rain gauge data. Each investigator (C, D, and E) received a subset of the rain gauge data to develop a $Z - R$. Then the remainder of the gauge data served as a test data set. In general the three approaches performed similarly when compared with the test rain gauge data (Figure 5-5).

After the AIW, the GV Team decided to use a hybrid of approaches D and E to produce the rain maps for products 2A-53, 3A-53, and 3A-54.

Figure 5-5: Comparison of rain amounts taken from the rain maps produced to rain amounts indicated by gauges. Data are for the period 24 December 1993-23 January 1994 ("month 1" of the AIW Darwin test data set) for rain gauges in the field of view of the Darwin, Australia radar. The letters c-e refer to the algorithms C-E discussed in the text.

5.2 Pre-Operational Phase of TRMM GV

The TRMM GV Team will evaluate the products generated by the prototype algorithms during the pre-operational phase. In this way, the PIs will learn how to manage and study the continuous large-volume data flow from the GV sites. They will conduct further tests of the algorithm performances and recommend modifications, as necessary, to the algorithms. In particular, they will closely evaluate the performance of the rain map algorithms [Table 5-2(e) and 5-3(e)] and recommend a design for a combined algorithm that optimizes the characteristics of the algorithms D and E (Sec. 5.1.6). A workshop similar to the AIW in 1996 will evaluate the algorithm performances and make a recommendation regarding the amalgamation of algorithms D and E.

One extremely important objective of the pre-operational phase of TRMM GV is that a climatology of precipitation characteristics be in place by TRMM launch. This climatology of the TRMM products in Table 5-2 will allow climatological comparisons of the TRMM satellite data and operational GV data to be made immediately following launch. Since the operational GV sites are at fixed locations, it will take _time_ to build up a climatology of precipitation amount, convective-stratiform structure, and vertical echo structure for each site. Because it sweeps quickly over large areas of the globe, the TRMM satellite will rapidly build up a data base of the statistical characteristics of tropical precipitation. In order to have an equivalent ground-based statistical base with which to compare these satellite results by the time the satellite flies, we must have a subset of the operational GV sites operational for 2 years prior to launch.

5.3 Comparisons of GV and TRMM satellite products

The two general strategies of comparison that have been discussed are instantaneous and climatological. In this section we describe the methodologies suitable for comparing the independent estimates of TRMM variables based on data from the operational GV sites with those based on data from the TRMM satellite instruments.

5.3.1 Convective/Stratiform validation

Both the TRMM PR and the operational GV site radars lead to maps of the regions covered by convective and stratiform precipitation regions. We must compare these maps on both an instantaneous and climatological basis.

For each satellite overpass of a TRMM GV site, we will have both GV and PR maps indicating the locations of convective and stratiform precipitation. As a first step in comparing these instantaneous maps, we will overlay the operational

GV site convective/stratiform map on the PR-based convective/stratiform map. Based on this overlay, a 2-km grid will be labeled such that each grid square is flagged as GV, PR, or both depending on which radar shows precipitation for that location. In general, the operational GV radar will show a much larger region of rain because the PR has very low sensitivity (~20 dBZ minimum detectable signal).

Comparison of GV- and PR-based convective/stratiform designations may be done only within the region where both radars show precipitation, as determined by the above comparison. A further complication in comparing the GV- and PR-based convective/stratiform maps is that the horizontal resolution of the PR is ~4 km, while that of the GV radar map has a resolution of 2 km. This difference in GV radar and PR resolution must be accounted for in the comparison in determining the degree of agreement between GV- and PR-based convective/stratiform designations.

A map showing the convective pixels on the PR map will be overlaid on a map showing the convective pixels of the GV map. Within each convective pixel of the PR map the four closest pixels of the GV map will be tallied to determine how many of them are convective. The more of these four that agree with the PR map, the better the score for that PR pixel. This procedure will be repeated for each PR convective pixel. The total score will indicate the degree to which the regions of convective echo agree between the GV and PR designations of convective area for this time. A similar procedure will be followed for each PR stratiform pixel to obtain the degree of agreement between the GV and PR designations of stratiform area for this time.

In order to compare results for one overpass time to another, the scores obtained in the convective and stratiform comparisons will have to be normalized.

For climatological comparison of convective/stratiform designations, we will compile statistics on the percentage of area of precipitation echo covered by stratiform and convective rain for both GV- and PR-based maps. For this purpose, precipitation echo will be defined as radar echo >20 dBZ in intensity.

5.3.2 Vertical structure validation

When radars have greatly differing characteristics, as do the GV radars and the PR, point-by-point comparison of the radar reflectivity values are not especially meaningful and are difficult to interpret. However, the statistical properties of the echoes sampled should be similar, altitude-by-altitude. For this reason, the CFAD (Sec. 5.1.5) is the primary tool for comparing the vertical structure of radar echoes seen by the GV radars and the PR. The CFAD representation of the data displays the frequency distribution of the radar echo intensity as a function of altitude in a volume of the atmosphere. Thus, by comparing CFADS of GV and

PR data, the comparisons between GV and PR data sets will be made on the basis of similarity of the frequency distributions of radar echo values at each sampled altitude. Note that it is meaningless to subtract histograms. Therefore, CFADS are compared by measuring differences in the parameters of the distribution and determining the variation of these differences with altitude.

CFADs will serve for both instantaneous and climatological comparisons. CFADs are obtained for the GV radar for both instantaneous and climatological (30-day) sets of data (Products 2A-55 and 3A-55 in Table 5-2(d). These GV products will be compared with CFADs of the PR reflectivities both in overpass volumes and for monthly data sets of PR reflectivity values in the general vicinity of a GV site.

5.3.3 Rain map validation

TRMM algorithms will produce rain maps from the PR, TMI, IR, and combined TMI and PR data. We will compare these satellite-based TRMM products with rain maps based on the operational GV site data. TRMM objective III in Table 5-1 is the 30-day average rain accumulation over a broad area. Such averages will be determined for each of the TRMM data sources and intercompared.

To gain insight into the differences among the estimates and to gain physical understanding of the precipitation processes giving rise to the 30-day accumulations, we will also compare maps of instantaneous rain rates and rain accumulations for 5 and 30 day periods. To compare any two pairs of maps, the horizontal resolution of the higher-resolution map will be degraded to the resolution of the lower-resolution map. Comparisons will be in the form of difference maps, rms differences between maps and frequency distributions of the rain rates (or accumulations) over the regions covered by the maps. The rms errors and frequency distributions will be broken down into subclasses, especially into the categories of convective and stratiform precipitation and land and ocean areas. Tests of statistical significance of the differences in distributions will be performed by standard methods.

5.4 Summary

Both the TRMM satellite and the TRMM GV sites will produce estimates of areas of convective and stratiform precipitation, vertical structure of radar reflectivity, and rain maps. However, both the TRMM satellite measurements and the GV site measurements are subject to large uncertainties of sampling, instrumentation, and theoretical interpretation of the data. Hence, the basic premise of the TRMM GV program is that the GV program can produce an independent estimate of all the TRMM variables. In some ways the TRMM

variables produced by the operational GV sites will be better than the satellite-based products. For example, the greater sensitivity of the operational GV site radars (compared to the PR) will show the vertical structure of tropical precipitation much more completely than will the satellite. Because of its higher local sampling frequency, the GV site data will document the evolution of precipitation areas and thus provide a time context to interpret the ~2 per day satellite samples. The satellite, on the other hand, will be able to map the precipitation structure and amount over the whole tropics. By combining the two independent estimates of the TRMM variables (satellite and GV), TRMM will realize a greater overall science achievement.

This philosophy and approach to TRMM GV is complementary and constructive. The GV and satellite programs build on each other. Where the GV and satellite product sets overlap, we seek consistency and agreement. It is not possible to attach accurate error bars to either the GV products or the satellite data products. However, the degree of agreement between the two types of products will lend confidence (or otherwise) to the combined (satellite plus GV) TRMM science achievements. The products in Table 5-2(c-e), respectively, address directly the three TRMM objectives listed in Sec. 1. Comparison of these products to their counterpart satellite products (listed under "Purpose" in Table 5-2(c-e) will determine the degree of confidence in TRMM science objectives. If reasonable agreement is achieved, then *both* the satellite- and GV-based products will yield a strong TRMM science achievement.

Since both satellite- and GV-based products require physical models to convert them to parameters of the four-dimensional heating of the tropical atmosphere, TRMM must make further measurements to fill in the missing links between the data products (Table 5-2) and the heating. To this end, field campaigns (Chapter 8) will make special measurements more closely related to latent heating in order to determine if the models are making an accurate connection between the TRMM data products and the desired heating variables.

Table 5-2: TRMM Ground Validation Products

Type of GV Product	TSDIS Ref. no.	Name	Purpose
(a) Basic data	1B-51	Radar volume scans from operational GV sites	Unaltered basic data archive
	1C-51	Quality control mask for radar data	Quality control of 1B-51
(b) Existence	2A-52	Instantaneous existence of rain	Flag rain events
(c) Convective/ Stratiform map	2A-54	Instantaneous conv./strat. map	Compare to 2A-23: PR qualitative products
(d) Vertical structure of echo	2A-55	Instantaneous 3-D structure	Compare to 1C-21: PR reflectivities & 2A-12: TMI profiles
	3A-55	Monthly 3-D structure	Compare to: Rain layer thickness from TMI rain map (3A-11) Structure derived from PR 3A-25 and Combined 3B-31.
(e) Rain maps	2A-53	Instantaneous rain map	Compare surface rain to 2A-12: TMI rain; 2A-25: PR rain and 2B-31: Comb. Instr. rain.
	3A-53	5-day rain map	Compare to 3B-42: Merged TRMM & other satellites rain products.
	3A-54	30-day rain map	Compare rainfall to 3A-11: TMI rain map; 3A-35, 3A-26: PR rain maps; 3B-31: Combined rain map;

Table 5-3: Algorithms for producing TRMM Ground Validation products

Type of GV Product	TSDIS Ref. no.	Required algorithm	Prototype Algorithm
(a) Basic data	1B-51	Format conversion to HDF	None. Data will remain in native format.
	1C-51	Ground clutter removal	AIW version developed by TRMM office
(b) Existence	2A-52	Identification of echo above threshold	UW algorithm developed by S. Brodzik.
(c) Convective/ Stratiform map	2A-54	Map showing location of conv. and strat. precipitation	UW algorithm developed by Steiner et al., (1995)
(d) Vertical structure of echo	2A-55 3A-55	3-D polar to cartesian interpolation; CFADS; mean vertical profile of reflectivity	NCAR SPRINT software for interpolation; Algorithms of Yuter and Houze (1995) for CFAD and vertical profile.
(e) Rain maps	2A-53 3A-53 3A-54	Conversion of low altitude reflectivity to surface rain map	The HU algorithm of Rosenfeld et al., (1994) and UI algorithm of Krajewski et al., will run in parallel for further comparisons and testing with the goal of combining them into a common algorithm.

6. TRMM Data Processing

TSDIS is the TRMM Science Data and Information System. TSDIS is responsible for three important functions: supporting TRMM instrument operations planning, science data processing, and the transfer of the TRMM science data products to the Earth Observing System Data and Information System (EOSDIS) and the TSDIS Science Users (TSUs). The TSUs consist of the TRMM science algorithm developers (U.S. Science Team and all PR algorithm developers) , the TRMM Project Scientists (both U.S. and Japan), the TRMM data quality scientists, and the TRMM instrument scientists. TSDIS is responsible for only the TRMM rain instruments, which are the TMI, the VIRS, and the PR. The CERES and the LIS instruments are the responsibility of scientists at the NASA Langley Research Center (LaRC) and Marshall Space Flight Center (MSFC), respectively.

TSDIS comprises three segments: the Science Data Operations Center (SDOC), the Science Operations Control Center (SOCC), and the Remote Science Terminals (RSTs). The function of the SDOC is to receive, process, and manage science data. It generates the science data products, delivers the data products to the TSUs, and it sends the data products to the EOSDIS for permanent archive. The SDOC also provides support to the TRMM algorithm developers for testing and maintenance of the science algorithm software. The SDOC provides support for the ingest and processing of surface-based rainfall data from the TRMM Ground Validation (GV) sites.

The SOCC is the interface between the TRMM instrument scientists (TMI, VIRS, and PR) and the TRMM Mission Operations Center (MOC). All support for instrument planning and scheduling is handled by the SOCC. The RSTs are the interface between the TSUs and TSDIS. They provide a user-friendly means to access the TSDIS services.

TSDIS will be developed prior to TRMM launch. It will participate in pre-launch testing, including TRMM Ground Segment end-to-end testing, to ensure that it is ready when the TRMM data start to flow. TSDIS will provide support during early orbit checkout of the rain instruments, and it will support TRMM science algorithm checkout. TSDIS will process TRMM satellite and GV data throughout the life of the TRMM mission and through the final reprocessing of all TRMM data at the end of the mission.
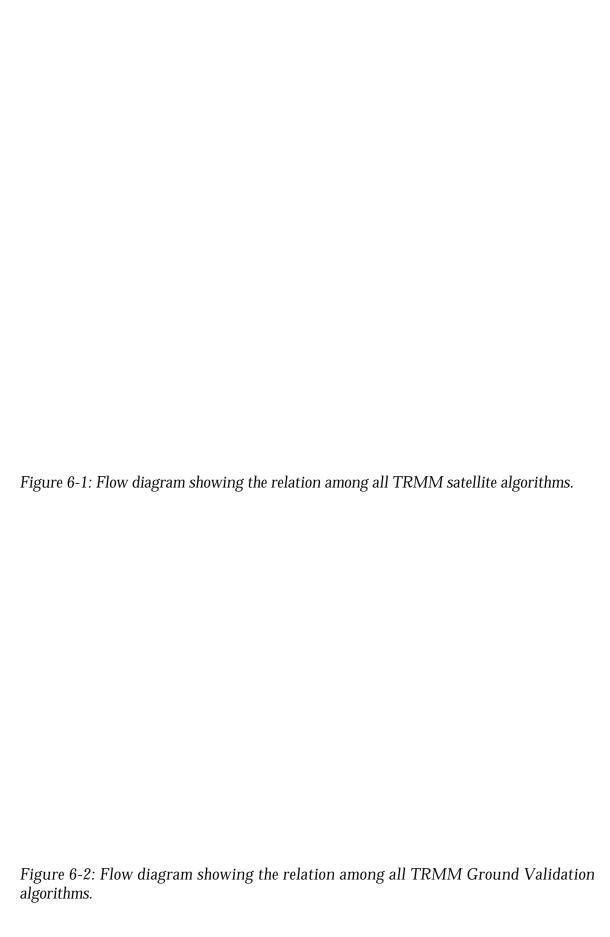
6.1 TRMM At-Launch Algorithms

The TRMM science algorithms are the heart of TRMM, since they are used to generate the science data products which will be used by science investigators, both within and beyond TRMM. The Level-1 algorithms for the TMI and the VIRS are provided by their respective instrument scientists to TSDIS, which will code the algorithms. NASDA/EOC will code the Level-1 algorithms for the PR

and provide the codes to TSDIS. The GV Level-1 algorithm codes will be provided to TSDIS by the TRMM Office (TO).

The Level-2 and Level-3 algorithm codes are developed by members of the TRMM Science Team and provided to TSDIS in four deliveries. The first version of the algorithms provides a description, without computer code. It indicates the input and output parameters, the size of the code, the size of the data products, and other information which provides TSDIS with an initial understanding of the algorithm. TSDIS produced the initial file specifications for each algorithm from version one. The second delivery consists of working code with most, but not all, of the final functionality. These version two algorithms allow TSDIS an opportunity for hands-on experience with the algorithm codes and a chance to refine the file specifications. Both the first and second algorithm deliveries also provide TSDIS with sizing information which is useful for hardware selection. The third delivery is working code including the TSDIS toolkit, with all or nearly all of the final functionality of the algorithm. For many algorithms, this will represent the at-launch code and a fourth delivery of the code will not be necessary. For others, only minor modifications will be made, which will be included in the fourth delivery.

The TRMM algorithms have been described in chapters 3 and 5 of this document. A flow diagram showing the interaction of these algorithms is presented in Figure 6-1 for the satellite products and Figure 6-2 for the Ground Validation products. It is expected that by TRMM launch, TSDIS will have tested and integrated a working algorithm code or a proxy code for each algorithm shown in the figures.

Figure 6-1: Flow diagram showing the relation among all TRMM satellite algorithms.

Figure 6-2: Flow diagram showing the relation among all TRMM Ground Validation algorithms.

6.2   Science Algorithm Testing and Integration Plan

TSDIS will use the TRMM science algorithm codes for the routine generation of science data products. However, as TRMM data become available, algorithm developers are expected to test, improve and modify their algorithms at yearly intervals.   TSDIS will support algorithm development by providing TRMM data to the algorithm developers, and by providing a computing environment for testing their codes.

The TSDIS Integration and Testing Environment (ITE) will be used for testing science algorithm codes. The ITE is a computing environment which is distinct from the computing environment used by TSDIS for routine data processing and for data reprocessing. It will have much of the functionality of the routine processing environment, but less computing capacity. Testing in the ITE will be coordinated with the schedule for data reprocessing. Approximately six months prior to the next scheduled reprocessing event, some science algorithms will be approved for testing in the ITE. Approval of algorithms is not the responsibility of TSDIS, but rather it is the joint responsibility of the TRMM Project Scientists from the United States and Japan.

Barring egregious errors for which algorithms must be reprocessed immediately, the reprocessing of algorithms will occur once at the end of the checkout period (if necessary), and then at approximately annual intervals (from launch). At the end of algorithm checkout (i.e., about six months following instrument checkout), all TRMM data will be reprocessed back to launch. Scheduled reprocessing events will occur at twice the rate of routine data processing (i.e., two days of data reprocessed every day) and data will be reprocessed back to TRMM launch to ensure a complete, consistent dataset. The reprocessed data products will be archived at EOSDIS and they will be labeled as a new version of the products. The old version of the same data products in the EOSDIS archive will be deleted by EOSDIS after six months.

6.3 Science Data Processing

The TSDIS SDOC will process all TRMM science data from Level-0 to Level-1A through Level-3B products. In addition to generating science data products, TSDIS will also generate metadata and browse images. The metadata will describe attributes of each science data product and can be used in database searches for processing data product orders. TSDIS will generate two types of metadata: EOSDIS core metadata and product-specific metadata. The EOSDIS core metadata contain attributes which are required by EOSDIS. Since EOSDIS provides the permanent archive for TRMM data, TSDIS is obligated to use their core metadata. The product-specific metadata contain additional product attributes, not found in the core metadata, which are desirable for describing the

products. They are defined jointly by TSDIS and the science algorithm developers. One of these metadata attributes is a data product quality indicator. TSDIS will insert a default value in the metadata when each product is generated. Each algorithm developer is responsible for evaluating his/her data products and providing TSDIS with updated quality indicators. TSDIS will deliver the updated quality indicators to EOSDIS, where they will be inserted in the archived product metadata.

TSDIS will also use the TRMM definitive orbit data to determine coincidence between the TRMM observatory and each of the GV radar sites. The coincidence information will be stored in the TSDIS database for the life of the mission. The coincidence information will also be stored in a separate ASCII file. This file will be used primarily by the P.I.s at the Special Climatology GV sites for generating their coincidence data products.

TSDIS will produce one browse product for each science algorithm. For the Level-1 and Level-2 TRMM products, TSDIS will produce daily browse images (i.e., all orbits for one day are included). To reduce clutter, all ascending portions of each orbit and all descending portions of each orbit will be grouped together in separate images. All of these browse images will use degraded horizontal resolution, to reduce their size. For Level-3 TRMM products, the browse images will be displayed at full resolution. Since these products are spatially averaged over cells which are much larger than the instrument pixel sizes, they will not be large.

TSDIS also will produce browse images for the Ground Validation radar data. Each image will consist of a horizontal scan of radar reflectivity or a higher-level derived data product displayed at degraded horizontal resolution. All browse images will be produced once per hour for each TRMM GV radar which provides data to TSDIS.

For all TRMM algorithms, the TRMM Science Team is responsible for defining the horizontal resolution of the browse images (as specified in the TRMM Science Requirements document). Each algorithm developer will specify what data fields the browse image should depict, the details of the color table, and other pertinent information.

6.3.1 TRMM End-to-End Data Flow

Figure 6-3 depicts the end-to-end data flow for the TRMM Ground Segment. The data flow begins with the transmission of science and housekeeping (H/K) data from the TRMM Observatory to the Tracking and Data Relay Satellite System (TDRSS). There will be one 20-minute contact per orbit. During that contact, one orbit of stored data will be downlinked along with realtime housekeeping data. The data are received at the White Sands Complex (WSC) in New Mexico, USA.

These data are forwarded to the Sensor Data Processing Facility (SDPF) and the TRMM Mission Operations Center (MOC) at NASA's Goddard Space Flight Center (GSFC) in Maryland, USA. The NASA Communication (Nascom) Network is used for the data transfer between these and other ground system facilities.

Figure 6-3: TRMM end-to-end data flow

The SDPF receives observatory data and processes them to a Level-0 data file. This is accomplished by first removing block transmission overhead and performing error correction decoding. The data, received in Consultative Committee for Space Data Systems (CCSDS) packets, are placed into time-ascending order based on header, time code, and sequence counter information. The packets are quality checked, redundant packets are removed, and missing packets are identified. Quality information is appended as part of each Level-0 data file. A detached Standard Format Data Unit (SFDU) header file is provided with each Level-0 data file. Level-0 data sets are essentially in the same form as when the packets were collected from the instrument on board the observatory.

The SDPF also distributes observatory ephemeris data produced by the Flight Dynamics Facility (FDF), located at GSFC. The FDF receives tracking data from the WSC and generates long and short duration ephemerides. These ephemerides contain both definitive and predictive orbit information. The SDPF distributes the FDF ephemeris information to the TSDIS, to the Marshall Space

Flight Center (MSFC) and Langley Research Center (LaRC) DAACs (Distributed Active Archive Centers), and to NASDA. These facilities use these data to develop geolocation parameters associated with the collected science data.

The SDPF will deliver the Level-0 datasets (including science and housekeeping data) and the TRMM definitive and predictive orbit data to the TSDIS SDOC, the MSFC DAAC, the LaRC DAAC, and the NASDA interface point once per day. All Level-0 datasets will consist of a single 24-hour dataset, except for the PR Level-0 dataset which will consist of four 6-hour datasets, at the request of NASDA. The Level-0 datasets will be kept online for 5 days to assure that each customer can complete its data transmission. Each customer will be able to request a retransmission, if needed. As a backup, the SDPF will archive all raw TRMM telemetry for up to two years.

The SDPF will also provide some observatory data as Quick-Look. Each Quick-Look dataset will consist of the data downlinked from one TDRSS contact, which corresponds nominally to one orbit. Only minimal processing will be performed on Quick-Look data. These data are distributed by the SDPF to TSDIS, LaRC, MSFC, and NASDA within two hours of receipt from the WSC.

TSDIS will ingest the TMI, VIRS, and PR Level-0 data once per day. The Quick-Look data for each of these instruments will be ingested when they are available (up to four times each day). Non-TRMM data products (such as SSM/I Level-1B data and NMC global analyses) which are needed for data processing will be provided by EOSDIS, except for one product which will be provided by a member of the TRMM Science Team. TSDIS will then process the data using the TRMM algorithm codes and deliver the data products to the TSUs, according to their requests. TSDIS will also ingest GV data and data products as they arrive from the GV sites. They will be sent on tape cartridges and delivery is expected to be irregular. TSDIS will process the GV data, as appropriate.

All TRMM data products, including GV products, will be sent to EOSDIS for archive. All TRMM data products will be archived at the GSFC DAAC.

For a data reprocessing event, EOSDIS will provide the necessary TRMM and non-TRMM data at the rate of two days of data per day. After TSDIS reprocesses the data, the new data products will be delivered to EOSDIS for archival.

6.3.2 TRMM Data Processing

TSDIS will begin processing a science algorithm once all of its necessary data inputs have been received. These data inputs will consist of Level-0 data for the TMI, the VIRS, and the PR, calibration data for the PR, and non-TRMM data. NASDA/EOC will send the PR calibration data to TSDIS approximately every 2-4 weeks. Non-TRMM data will be available daily from EOSDIS.

TSDIS allows up to 24 hours to complete Level-1 processing after the Level-0 data are received. Similarly, up to 24 hours are allowed to complete Level-2 processing after Level-1 processing is completed. This processing includes the production of metadata and browse images. TSDIS will begin to fill data orders as soon as the data products and their metadata are completed. Intermediate products generated by each algorithm code will be made available to the algorithm developers for a specified period of time and then they will be deleted from TSDIS disk storage.

Level-3 data products are accumulated over either 5 days or a month. These data products will be available at the end of the averaging period, with the possible exception of the two TRMM and Others algorithms. This is due to the expected long delay (three or more months) in obtaining two of the non-TRMM data inputs. The TRMM & Others data products will be made available once their algorithm codes can be fully processed. Intermediate products generated by each algorithm code will be made available to their algorithm developers.

Quick-Look data are collected primarily for the benefit of the TRMM instrument scientists, who will perform anomaly analyses of their instruments. There will be three scheduled Quick-Look datasets each day for the TMI, the VIRS, and the PR. The TRMM instrument scientists are also permitted to request one additional, unscheduled Quick-Look dataset per day. (The limit of only one unscheduled Quick-Look is due to limited disk storage capacity at the SDPF). All Quick-look data will be processed through Level-1B (Level-1C for the PR). Quick-Look data will be processed by TSDIS within one hour after receipt from the SDPF.

The instrument scientists have requested that they only occasionally receive Quick-Look data products after the initial instrument checkout, following TRMM launch. Therefore, Quick-Look data products will be distributed only upon request, and they will not be included in standing orders.

6.3.3 Ground Validation Data Processing

There will be two types of Ground Validation radar sites: Primary, or Direct Data (DD) sites and "Special Climatology" or Direct Product (DP). The principal distinction between these types of sites is that TSDIS receives Level-1C through Level-3 data products from the DP sites (no data processing is required) and Level-1B radar reflectivity from the DD sites.

A Principal Investigator (PI) is assigned to each DP site. Each PI is responsible for obtaining the GV data (radar, raingauge, and disdrometer) and processing them through Level-3 using the same algorithm codes as those used by TSDIS. Each PI is also responsible for delivering their data products and their metadata

to TSDIS. Once they are received at the TSDIS SDOC, TSDIS will catalogue the products, ingest the metadata, and produce browse images.

Currently, there are expected to be four DD sites. These sites will send radar data to TSDIS for processing from Level-1 through Level-3. TSDIS will also generate product metadata and produce browse images. Raingauge and disdrometer data will be sent directly from the DD sites to the TRMM Office. The TRMM Office will process these data to Level-2 and deliver the data products and their metadata to TSDIS. TSDIS will catalogue these data products and ingest their metadata. No browse images will be produced for raingauge and disdrometer data products.

TSDIS, the TRMM Office, and the Ground Validation Group have agreed to limited pre-operational processing by TSDIS for GV data. This gives TSDIS experience in GV processing and assures that the data flow will be stable by TRMM launch. The pre-operational system will begin data processing two years before launch. Initially there will be two DD sites. This will expand by two additional DD sites 1 year before launch. All TRMM GV data products will be generated, but without browse images. No sophisticated database or distribution system will be used.

Level-1 Data Processing will be performed by TSDIS only for radar data from DD sites. The data will be processed through Level-1C, which involves applying Quality Control (QC) procedures to the data. The Level-1 GV algorithms will be supplied to TSDIS by the TRMM Office.

Level-2 and Level-3 Data Processing will be performed by TSDIS only for radar data from DD sites.   The data will be processed using the GV science algorithms, which are supplied to TSDIS by the TRMM Office.

6.3.4 Data Archive and Short-Term Storage

Quick-Look data products, which are intended primarily as a tool for the instrument scientists to assess their instrument's behavior, will be maintained in local storage at TSDIS for 72 hours, then they will be deleted. Quick-Look products will not be archived.

All routine and reprocessed data products which are generated using the TRMM science algorithms will be sent to the permanent archive at EOSDIS. Metadata, browse images, a copy of each algorithm code, and other descriptive information about each algorithm will also be saved in the EOSDIS archive. All TRMM products which reside at EOSDIS are available, without restriction, to the general user community. The only exception will occur during instrument checkout and algorithm checkout (following launch), when access to TRMM data products will be restricted to TSDIS personnel and the TSDIS Science Users.

TSDIS will maintain copies of all of the routine and reprocessed data products for three days in local on-line storage. This will give TSDIS adequate time to satisfy user requests for data products. In addition, TSDIS will maintain copies of all product metadata and browse images in local storage for the life of the mission. This will assist TSUs in performing data product searches and product ordering.

All GV data and data products are expected to arrive at TSDIS on 8 mm tape cartridges. After TSDIS has completed data ingest from the GV tapes, they will be sent to the TRMM Office at GSFC for storage for the life of the mission.

6.3.5 Data Browse and Ordering

Remote Science Terminals
   The Remote Science Terminal is the optimal means for accessing TSDIS services. Physically, the RST is a Unix workstation or X-terminal which is provided by each TSU. The computing platforms which will be supported by TSDIS are SGI (Silicon Graphics), HP (Hewlett Packard), and Sun. TSDIS will provide computer code to each TSU which optimizes the interface with TSDIS. It is expected that a client/server approach will be used. The RST code consists of a graphical user interface (GUI), which is convenient and user-friendly. TSDIS is planning to use World Wide Web software as the basis for the RST. The RST will be useful for many purposes, including browsing and ordering data, checking on TSDIS system status, sending and receiving instrument planning and scheduling information, checking the status of data orders, and communicating with the ITE. Display pages, with on-line help, will be available to support all of the RST's functions.

Standing Orders and Data Distribution Model
   TSDIS users will receive most of their requested data products using standing orders. These are requests for data products which are placed before the data products are created. TSDIS will fill the standing orders without requiring any further intervention by the users. Any standard TRMM data products and any non-TRMM data used by TSDIS (e.g., SSM/I Level-1B data, NMC global analyses) can be ordered using standing orders and many delivery frequencies will be available (e.g., daily, once per week, once per month, etc.). Reprocessed data products can also be ordered using standing orders. TSDIS will deliver most data products using 8 mm tapes. Small datasets will be available for FTP access.

Special Orders
   Special orders are non-routine orders which are placed by TSUs after they have identified data which they want to receive. TSDIS will provide two capabilities for identifying data of interest: database searches and browse

image displays. Database searches will consist of scanning metadata for key parameters (e.g., instrument name or GV coincidence), which are identified by the TSUs. The RST will also provide a capability for spatial searches within latitude and longitude limits supplied by the TSUs. Browse images will provide a means for visual evaluation of data. Once data products are identified, TSUs will place special orders with TSDIS. When the requested data products reside in local storage at TSDIS, TSDIS will fill the order. If the data products have been deleted from local storage, then TSDIS will forward the special orders to EOSDIS for completion. EOSDIS will be responsible for sending the data products to the TSUs according to its procedures and policies. TSDIS will monitor the status of the orders until they are completed. TSDIS will also make order status available to TSUs, upon request.

6.4 TRMM Instrument Planning, Scheduling, and Monitoring

6.4.1 MOC Operations

The TRMM Mission Operations Center (MOC) is responsible for commanding, health and status monitoring, mission planning and scheduling, network scheduling, and coordinating functions for day-to-day spacecraft and instrument operations. The MOC receives command requests from the TRMM instrument scientists, assembles and formats the commands for transmission to the observatory, and verifies their subsequent execution. The MOC receives real-time and playback housekeeping data which it uses to monitor spacecraft and instrument performance. The MOC monitors the playback science data to identify missing frames and to initiate commands for retransmission of missing frames when needed. Trend and performance analysis is performed using the housekeeping data from the observatory and its instruments. Additionally, real-time health and safety status of the observatory is monitored through display of the real-time telemetry.

6.4.2 SOCC Description

The Science Operations Control Center (SOCC) is the TSDIS segment which is responsible for supporting the instrument scientists for the TRMM rain instruments (for the PR, NASDA/EOC is the instrument scientist). The principal function of the SOCC is to serve as an intermediary between the instrument scientists and the MOC. This is necessary because neither the instrument scientists, nor any other TSUs, are permitted to make a direct electronic connection to the MOC, for security reasons. Thus, the SOCC has a direct, secure link to the MOC on MODNET, and a separate link to the instrument scientists via internet or a GSFC Local Area Network (LAN).

The TRMM instrument scientists are responsible for the operation of their instruments. They provide command requests to the MOC (via the SOCC for the PR, TMI, and VIRS), which issues the commands to the spacecraft. The CERES and LIS instrument operations groups interface directly with the MOC. A list of command procedures, which will be routinely performed, is provided to the MOC. These procedures are specified prior to launch, although they can be amended anytime after launch. These command procedures can include infrequently performed tasks, such as calibrations at three week intervals. The instrument scientists need only provide the details to the MOC (exact date and time, beam orientation, etc.) at the appropriate time.

It is the responsibility of TRMM instrument scientists to notify the SOCC of temporary changes to the routine commanding for a particular instrument, or to identify special, short term events. The SOCC will forward this information to the Flight Operations Team (FOT) at the MOC. For any non-routine activity which adversely affects the collection of data from any of the TRMM rain instruments, the SOCC will coordinate instrument activities with the FOT and seek approval from the U.S. TRMM Project Scientist and the Japanese TRMM Project Scientist. (It is anticipated that final approval will be secured from TRMM Program managers in the United States and Japan).

The MOC generates many products and reports, which it makes available to the SOCC, LaRC, and MSFC. The SOCC, in turn, makes them available to the TSUs. Some of the reports and products are generated by the MOC and some of the products are generated by the Flight Dynamics Facility at GSFC. The latter products include FDF planning aids, such as the predicted ground track, and the Predicted Site Acquisition Tables (which are used to predict shadow periods, South Atlantic Anomaly approach, etc.). MOC planning aids include the integrated print (which shows the commands which are planned to be issued) and the timeline report (which contains details of the conflict-free schedule). The MOC also makes available products such as the command history (which is a listing of all issued commands), and various reports and analyses (such as for anomaly support) generated by the Flight Operations Team. All of these products are available to TSUs through the RST.

The SOCC is not responsible for monitoring TRMM instrument performance. This responsibility belongs to the TRMM instrument scientists. However, the SDOC will generate some intermediate products and reports which are specified by the TMI and VIRS instrument scientists (note: NASDA will perform its own instrument monitoring and trending activities, without levying requirements on TSDIS). These intermediate products will be made available to the appropriate instrument scientist, who will use them in evaluating instrument performance (including trending).

In the event of an instrument or spacecraft anomaly situation (including emergencies), the FOT will follow established procedures for commanding the

instrument(s) and/or spacecraft, so that they are properly safeguarded. The MOC/FOT will also immediately notify TSDIS. TSDIS will then follow procedures, established in cooperation with the instrument scientists, to notify the affected instrument scientist(s) and others, as necessary. The SOCC will channel information between the MOC/FOT and the scientists/engineers in most situations. In an emergency, the MOC/FOT may wish to maintain direct communication by telephone or facsimile with the scientists/engineers. Communication with the MOC/FOT will continue (directly or through the SOCC) until the anomaly situation is resolved. Then the MOC will generate a report regarding the anomaly. This report will be available to the TSUs via the SOCC.

7. TRMM Physical Validation

The primary goal of TRMM is to provide estimates on climate space/time scales of the profiles of latent heat released into the atmosphere by rainfall. It is absolutely essential that any quantitative estimates of latent heat and the intermediate parameters of rainfall and stratiform/cumuliform partitioning that result from TRMM have credible uncertainty values associated with them. In a traditional view, one arrives at this uncertainty by comparing the retrieved values with "ground truth" measured by conventional means. As long as it is practical to make ground truth measurements that are significantly better than the remotely sensed values, this is a straightforward and satisfying approach. For TRMM retrievals of rain rate over land surfaces, this is probably a reasonable approach. Over oceans the practical difficulties of making the desired ground truth measurements are enormous, but, on the other hand, the potential for high quality remote measurements is greatly improved both for the PR and the TMI. The experience of the TMI team members in the various algorithm inter-comparison projects using SSM/I data is that the ground truth simply isn't good enough to meet the requirements of this approach. While we expect the ground truth to be significantly better in the TRMM era, we also expect the standard of the retrievals to improve as well.

The ultimate goal of TRMM is to derive estimates of the distribution of latent heat release on climatological space/time scales. Arriving at error estimates for these latent heating profiles is also a difficult proposition. There are no "latent heat meters" that might provide latent heat ground truth. One might attempt to validate the latent heat release by comparing them with estimates from global climate models, but this raises the question of "What is validating what?". TRMM was intended to validate and help improve the climate models; we must avoid circular reasoning.

This may seem like a hopeless conundrum. However, it simply results from the fact that the remote sensing community is not accustomed to providing the best measurement of anything; there has (almost) always been some in-situ measurement that was presumed to be the "truth" that the retrievals sought. It is tautological that for any parameter that is measured, there is some best measurement. Clearly these best measurements cannot be validated by comparison with (by definition) inferior measurements.

How then are these best measurements validated and the uncertainties in the measurement determined? The key is the physical model that underlies the measurement. The model has assumptions and approximations which can be quantified. That is, an error model is developed for the measurement. Clearly, it is possible that something is left out of the interpretation and error models resulting in a bias in the result and an underestimate of the actual uncertainty. Thus, the results need to be validated against supposedly inferior measurements as a sanity check. The models also need to be examined critically by a wide

community to provide additional insurance against such mistakes. Even then, some possibility remains for an egregious error. This approach is not perfect so continuing examination is necessary, continual attempts to find better independent measurements are crucial and tests of consistency with other knowledge are prudent.

In this report we will first discuss the issues associated with estimating the latent heat release due to rainfall. Then we will discuss the issues related to the inputs to the latent heat estimates, the Radar, the Radiometer, the Ground Segment and the Sampling issues common to all of them. We will then discuss potential solutions based on existing data and describe new data required to address the issues. We will conclude with a statement of required actions.

7.1 Latent Heating Issues

The overriding goal of TRMM (Simpson 1988) is "evaluation of the four-dimensional structure of latent heating in the tropical atmosphere." The strategy to obtain the four-dimensional heating is threefold:

1) obtain the "temporal" variation of the heating by the satellite sampling on time scales ranging from diurnal to interannual.

2) obtain the "horizontal" distribution of the net latent heating through measurements of the precipitation throughout the tropics, which indicates the "horizontal" pattern of heating,

3) estimate the "vertical" distribution of the net heating through measurement and analysis of the horizontal and vertical structure of the precipitation

The last item requires some further comment. Because the latent heating in the tropics is dominated by two modes, convective and stratiform, which have distinctly different vertical distributions of heating (Houze 1982, 1989), one of the TRMM objectives is to separate the observed precipitation into its convective and stratiform components. Analysis of radar reflectivity patterns will be the basis of this separation.

To reach the goal of documenting the four- dimensional heating of the tropics, TRMM has two complementary components--a space component and a ground component (Figure 7-1). In the space component, the PR and TMI will estimate the amount and spatial structure of the precipitation. The ground component will use ground-based radars calibrated by rain gauges to do the same thing. None of the measurement approaches are perfect; the satellite payload was specifically designed so that the sensors would be complementary in that the weaknesses of one would be matched by a strength of the other. A similar

complementary relationship exists between the ground and the space components of the measurement system.

Figure 7-1: Schematic diagram of parallel paths for converting satellite and ground based measurements into the required latent hating product.

Note in Figure 7-1 that the satellite and ground components follow parallel paths to obtain the heating. The basic data are subjected to analysis algorithms, which generate "products." The products will serve as input to cloud and radiation models, which will estimate the total heating and its vertical distribution.

How do we know if the heating and its vertical distribution is correct? This is the key question in TRMM validation. Before answering this question, consider **why** we want the four-dimensional heating in the tropics on diurnal to interannual timescales: It is because we want to be able to understand and predict global climate anomalies and variations. In other words, we want to know how the atmosphere behaves in association with the heating.

Upon closer examination, it turns out the large-scale tropical circulation is not so much determined by the heating itself, but rather about the vertical *gradient* of the heating. It is clear from basic thermodynamics that temperature *differences* drive the circulation. Alternatively this may be viewed by thinking of the equations governing the large-scale flow in the atmosphere. The large-scale absolute vorticity equation describes the large-scale balanced flow in the tropics. (More generally it is the potential vorticity which describes the large-scale balanced flow, but in the tropics it simplifies to a consideration of only the vorticity. See Haynes and MacIntyre 1987.) The thermodynamic equation states that the large-scale vertical air motion is proportional the net heating (or cooling) of the air at a given altitude. The mass-continuity equation states that the vertical gradient of the vertical mass transport (proportional to the vertical gradient of

the net heating) is equal to the horizontal divergence (large-scale horizontal motions must compensate the vertical motions). The large-scale absolute vorticity equation states that the time changes of large-scale absolute vorticity are proportional to divergence (sometimes called the vortex-stretching effect). In other words, changes in the large-scale absolute vorticity (i.e. the large-scale balanced flow) are directly proportional to the vertical gradient of heating.

Since it is the vertical gradient of heating that is crucial, and since the vertical gradient of heating is proportional to the divergence, it is clear that measurements of divergence in and around regions of precipitation are critical for validation of the TRMM results. Such measurements are possible with airborne Doppler radar technology (Mapes and Houze, 1993, 1995) and by closed arrays of wind sounding instruments.

The advantages of using divergence to validate the four-dimensional heating are clear:

- Divergence is accurately measured by Doppler radar and soundings

- Vertical air velocity need not be computed; this avoids the problem of integrating the divergence vertically and thereby accumulating errors.

- Divergence (the vertical gradient of heating) is more important physically than heating per se

Since divergence measurements will not be made routinely at ground-validation sites, they will have to be a central component of special TRMM field campaigns designed to provide key validation measurements. They are in fact the most critical and basic of all validation measurements.

As noted above, the heating profiles in convective and stratiform regions in tropical precipitation systems differ fundamentally. To estimate the vertical distribution of heating in TRMM, the observed precipitation needs to be subdivided into convective and stratiform components. This split is accomplished by making use of the fact that the radar echo structure of convective and stratiform precipitation have distinctive characteristics, allowing the radar data to be used to distinguished. The local horizontal variability of the reflectivity field and the occurrence of a bright band are markers used to make this distinction.

In using the radar echo structure to distinguish convective and stratiform precipitation, we make use of radar reflectivity data as a proxy indicator of the convective and stratiform precipitation mechanisms. The radar echoes however do not *define* what we mean by convective and stratiform. The radar echo patterns are symptoms of the precipitation mechanisms, which are dynamical and physical in nature.

Houghton (1968) proposed dynamical-physical definitions for convective and stratiform precipitation. According to these definitions, convective precipitation is produced by vertical air velocities at least as large as the terminal velocities of ice particles, while stratiform precipitation is produced by vertical velocities much smaller than the hydrometeor terminal velocities. The strong air motions in the convective case favor ice-particle growth by riming. These air motions and rapid growth processes produce a highly variable reflectivity pattern. In contrast, the weaker air motions in stratiform areas favor growth of ice particles by vapor deposition and the sedimentation, aggregation, and melting of ice particles to form a concentrated melting layer. The reflectivity pattern in stratiform regions is more uniform in the horizontal and *sometimes* exhibits a bright band in radar reflectivity data.

Different approaches to using the radar reflectivity data to separate convective and stratiform radar echoes have been intercompared by the TRMM Ground Validation Team. Different results arise from the different techniques, but there is no absolute test routinely available to determine which method works the best. Since the radar reflectivity data are used to distinguish the convective from the stratiform radar echoes, the test must be independent of the radar reflectivity field. Since the definitions of convective and stratiform are based on the vertical air motion strength in the precipitating cloud, the appropriate test is to measure the vertical air motions throughout regions identified on the basis of reflectivity patterns as convective or stratiform. These measurements can be provided by ground- based dual-Doppler radar. Steiner et al. (1995) made such a test for one case of Florida precipitation. Since the required dual-Doppler radar data are not routinely available, they must be provided as part of a TRMM field campaign in order to conduct further tests of convective-stratiform separation methods.

In addition to dual-Doppler radar measurements, airborne and/or balloon-borne measurements of ice particle types and sizes in convective and stratiform regions are needed. By distinguishing whether the particles develop by riming or vapor deposition, these airborne measurements will determine whether the observed ice-particle characteristics are consistent with the vertical air motions observed by Doppler radar. Polarimetric radar measurements may provided further clues as to the ice-particle growth mechanisms.

7.2 TRMM Precipitation Radar Issues

In order to provide accurate rainfall data to fulfill the TRMM scientific objectives, the error structure of the data products obtained by the TRMM Precipitation Radar (PR), both systematic and random, must be quantitatively assessed through a vigorous calibration/validation program.

The error sources in rain profile retrievals from spaceborne radar measurements are primarily the sources of uncertainties associated with the forward models with which the meteorological parameter retrieval algorithms are based. So far as the TRMM PR is the concerned, the key forward models are those associated with radar return power measurements, rain reflectivity, and rain attenuation.

The return power measurement is a function of the transmitted power, the range to the observation volume, the antenna gain function, the reflectivity of the hydrometeors in the volume, the attenuation along the path between the radar and the observation volume and an empirical calibration constant for the radar. The reflectivity and attenuation are functions, in turn, of the radar wavelength, the distribution in size, shape and phase of the hydrometeors, the dielectric properties of liquid water and ice, and the distribution of absorbing gasses such as water vapor and molecular oxygen. Finally, the rain rate in the observation volume is a function of the drop size distribution, the terminal velocity of the raindrops, and any up- or downdrafts. The retrieval algorithm attempts to interpret measurements of the return power in terms of the reflectivity and attenuation and then to infer rain rate from these inferred parameters. Uncertainties in any of the links in the chain result in uncertainties in the inferred rain rate.

The key error sources can be identified as the follows:

- vertical profile of drop size distribution,
- radar beam filling,
- drop size, shape and orientation,
- radar calibration constant and antenna radiation pattern
- algorithm limitations.

7.2.1 Vertical profile of drop size distribution

Because of their dynamic and varying nature, it is difficult to find precise descriptions on the size distributions of the various atmospheric species at different altitudes. Although it has been shown from land-based distrometer measurements that the raindrop size distribution at the earth surface fits reasonably well by a Gamma function, the fitted parameters of such function using data sets collected at various locations and for various rain events exhibit large variations. The lack of reliable drop size measurements at higher altitudes and over ocean complicates the problem even further. To remedy this problem, extensive analysis of existing data as well as aggressive field campaigns for data collection during both the TRMM pre-launch and post-launch periods will be needed.

7.2.2 Radar beam filling

Radar beam filling problem arises due to the relatively large radar beam extent with respect to the spatial scale of rain homogeneity. The key error contribution of beam filling is that the surface reference technique, the baseline TRMM PR profiling algorithm, would in general produce erroneous estimates of the surface cross-section of the raining area, which in turn would produce errors in rain attenuation and rain rate estimation. The extent of this problem is currently being investigated by various research groups through computer modeling with existing data sets collected with airborne rain radars. Two existing airborne rain radars, the NASA/JPL Airborne Rain Mapping Radar and the CRL Airborne Rain Radar, are best suited for tackling this problem because of their fine spatial resolutions and TRMM PR-like viewing configurations. The deployment of such airborne instrumentation during the TRMM era would help to establish error bounds for different rain types and to validate the PR data.

7.2.3 Drop size, shape and orientation

It is well known that radar backscattering cross-section is a function of the size, shape, and orientation of the scatterers relative to the incident electromagnetic field, particularly at Mie scattering regime at which the size of the scatterers are comparable to the radar wavelength. At the TRMM PR frequency of 13.8 GHz, it is expected that the radar return power would be sensitive to the raindrop size, shape and orientation. However, this is a well-defined problem and mature analytical works have been established. Further work in collecting and analyzing 13.8 GHz rain backscatter measurements would appear to be the next logical step in fine-tuning the TRMM forward models.

7.2.4 Radar calibration constant and antenna radiation pattern

Variability in radar system parameters, such as transmit power, system gain, system temperature, etc., will introduce uncertainties in the radar calibration constant. The TRMM PR has incorporated an extensive internal calibration scheme to measure these set of system fluctuations. External calibration experiments has also been planned to validate such measurements. Furthermore, specific calibration sites (e.g., Amazon Rain forest) have been identified in which routine experiments to monitor the antenna pattern stability will be carried out.

7.2.5 Algorithm limitations

Because the number of TRMM radar observables (range-gated radar return power measurements) will be less than the number of rain parameters of interest (range-gated reflectivity and attenuation), the retrieval algorithm must make

use of certain assumptions in order to convert radar measurements into rain rate. Although such assumptions are based on our current understanding of the nature of precipitation, they surely will not be valid in some rain events to be observed by the TRMM PR. Depending on the extent that the underlining assumptions are valid, certain level of ambiguity will result during the rain rate profile retrieval process. This, together with the noisy nature of the radar measurements, will introduce additional error in rain rate estimates. Once again, analyses using data acquired by airborne rain radar instruments in conjunction with other airborne and ground-based sensors would be extremely valuable in testing out some of these assumptions.

7.3 TRMM Microwave Radiometer Issues

The orderly development of an error model implemented as a calibration standard, which could be used to evaluate any given precipitation retrieval algorithm, has several prerequisites. It is essential to understand the assumptions and simplifications that are inherent to the calibration procedures, to carefully prescribe all the component parts of the underlying forward radiative transfer model, and to fully stipulate all the "data realizations" that the error model would have to accommodate in numerical runs.

Since the underpinnings of such a calibration system consists of a high resolution, fully explicit microwave radiative transfer model (MW RTE model) that accounts for detailed absorption, scattering, and emission processes for any microphysically complex environment, it will be important to first prescribe what the RTE model will not address, i.e. the nature of the simplifying assumptions. The standard approximations required to avoid unwieldy problems consist of: (1) invoking the far field approximation in conjunction with the single scattering calculations (i.e. no particle-particle EM far-field interactions, thus avoiding totally arbitrarily decisions on proximity relationships), (2) assuming steady-state microphysics (i.e. the calibration model need not account for the effect of high frequency fluctuations of the microphysical state), (3) considering only aerosol-free hydrometers (this is of negligible consequence at microwave frequencies, and (4) applying the Rayleigh-Jeans (RJ) approximation. Only the later assumption can lead to non-negligible errors, and those would only occur for cold sources at the higher MW frequencies. In fact, the RJ approximation is not essential for a calibration model, although it has its utility. Table 7.1 summarizes the severity of impact of making these assumption with respect to the calibration model and assesses the degree of difficulty in overcoming the various simplifications if such steps were deemed necessary.

Table 7.1: Standard approximations used for MW RTE models.

	Assumption	Severity of Problem	Degree of Difficulty in Overcoming Problem
1.	far-field approximation	minor	high
2.	steady-state microphysics	minor	low
3.	clean hydrometeors	minor	high
4.	Rayleigh-Jeans approximation	conditionally moderate	trivial

Insofar as RTE model design is concerned, there are 8 key components. These are summarized in Table 7.2, along with assessments of the degree of difficulty in modeling these components, the generally accepted state-of-the-art component models, and the level of accuracy of these component models vis a' vis a calibration-level modeling system. It is clear from Table 7.2 that the different modeling components present a range of difficulties from minor to major. Most model components are well in hand, however, there are remaining serious problems such as modeling surface emissivity (particularly for land surfaces). There are also modeling components for which it is unclear how well we are doing with the state-of-the-art techniques, suggesting that part of the effort in developing a calibration system must concentrate on careful sensitivity testing of all model components to better understand the imperfections and shortcomings. This would be particularly true for such issues as treating variable instrument viewing geometry and its interaction with the related problems of beam filling and 3-dimensional complexities of cloud shape (as well as their internal microphysical structures). It should also be noted that there are limits to what can be done with arbitrary particle shapes for purposes of single scatter calculations. Even in the case of the discrete dipole approximation (DDA) technique (in which particle shapes are built up from point dipole sources), there are computational limits which prevent specification of arbitrarily complex hydrometeor shapes (such as occurs with ice aggregates). Computational overhead is also a relevant issue for multiple scattering models, since the reverse Monte Carlo technique is the only current technique that can address any arbitrarily specified 3-dimensional medium, and any Monte Carlo technique is, by nature, computationally limited. Nevertheless, it appears that with the exception of modeling the surface emissivity of a land background, if state-of-the-art modeling techniques were employed, a reasonably accurate calibration model is within reach. Since this exercise is primarily relevant to oceanic rainfall retrievals, the land limitations are not germane.

Table 2: Foremost RTE model components.

	RTE Model Component	Severity of Problem	State-of-Art Model	Model Accuracy & Precision
1.	dielectric constant	small for liquid water moderate for ice	theory for liquid water observations for ice	good for liquid water moderate for ice
2.	mixed phase representation	moderate structure	matrix	good
3.	absorption coefficients H_2O & O_2 lines & H_2O continuum	minor for line/ empiricism for continuum	QM theory for line/ moderate for continuum	good
4.	radiometer noise	minor	pre-launch: NE T's post-launch: Autocorrelation functions	good
5.	surface emissivity	moderate	none	poor
6.	instrument view geometry	large	trigonometry	imperfect
7.	single scatter properties	moderate	DDA	excellent but restricts
8.	multiple scattering process	moderate	reverse MC	good (computer time)

The final leg of the calibration system involves developing a robust database which contains enough meteorological and microphysical realizations that the entire physical domain of the precipitation process could be explained and understood in terms of its accompanying microwave radiation signatures. Table 7.3 summarizes the individual pieces of the "realization" component, along with assessments of how much the current lack of definition of these quantities is having on precipitation retrieval. Also included are evaluations of the likelihood that such "realization data" could be obtained from either model simulations or measurements. For most of these quantities, there are reasonably sound modeling or observational solutions. This is particularly true for the beam filling problem, for which both high resolution cloud models, and multiparameter radar data present excellent sources from which to represent a wide range of realizations. There are also glaring deficiencies in the "realization" area, such as prescribing both microscale and macroscale topographic features for land surfaces, or the roughness properties of sea surfaces. There is also a dearth of methods to get at realistic renditions of the vertical distributions of liquid and ice hydrometers, and the rain-cloud water ratio. In general, cloud models do not simulate such quantities all that well, and aircraft experiments have not been very successful in acquiring such information in any meaningful detail.

Table 7.3: Foremost RTE model components.

	Required Realizations	Severity of Problem	Modeling Prospects	Observational Prospects
1.	beam filling (hor. & vert.)	large	good	excellent
2.	T-q profiles	small	good	good
3.	vertical liquid/ice distributions	large	poor-good	poor & few opportunities
4.	liquid/ice particles size, shape, & orientation distributions (hor. & vert.)	moderate	good	good
5.	profile of rain-cloud water ratio	moderate	poor-good	poor & few opportunities
6.	surface temperature	minor	good	good
7.	surface characteristics & micro/macro topographic representations	moderate	poor	poor
8.	macro cloud geometry	large	good	good but difficult
9.	cloud rainout	moderate	good	good
10.	cloud heating	large	good	poor

However, the few shortcomings vis a vis "realizations" are not serious enough to inhibit the development of a calibration error model. In fact, the prospectus that the beam filling problem could largely be resolved with a calibration model, is reason enough to warrant pressing ahead with such a project.

7.4 TRMM Sampling Error

All the measurements performed by the space segment of TRMM and many of the ground based measurements are instantaneous in nature and all are of limited spatial extent. However, the latent heat release estimates must be "totals" for some time period. Thus, we must estimate the contributions for the

times not observed. The error in this estimate ("sampling error") will be a significant portion of the total error budget and must be carefully estimated.

Errors in the monthly averaged rain rate in a 5° grid box can have two sources: 1) the satellite views a grid box only when the instrument swath intersects the box during an overflight, and it may view only part of the box; 2) Even when the satellite is viewing the box, the algorithm estimates rain rates imperfectly. The first source of error will be referred to as sampling error, the second will be referred to as retrieval error.

Sampling error for gridded, monthly-averaged rain rate depend upon a number of factors:

• Satellite coverage. TRMM sampling increases at higher latitudes. A rough measure of the amount of information collected by TRMM during a month is

$$S = \sum_{i=1}^{N} A_i / A$$

where A is the area of the grid box and A_i is the area seen by the satellite during the overflight i. There are N overflights during that month. The value of S for TRMM at latitude 30 degrees is more than twice the value of S at the Equator.

• The variability of rain in the area. The amount of variability can depend on local climatology, and there may be systematic changes in the amount of rain depending on the time of day and the presence of large scale effects such as ENSO or the phase of the Madden/Julian oscillation, if present.

The sampling error for TRMM sampling of GATE-like rain has been much studied, and values of the sampling error, expressed as the ratio of the standard deviation of the error to the mean rain rate for the area, range from 8 to 12%. A recent study by Oki and Sumi (J. Appl. Meteor., 1994) showed that sampling error over Southern Japan could vary significantly with the time of year. Studies of sampling error over other sites and climatologies need to be carried out.

A number of studies using SSM/I data show that sampling error (relative to the mean) decreases with rain rate in the area. Theoretical considerations suggest that this behavior can be captured by an equation of the form

$$\frac{\sigma_{sampling-error}}{R} \approx Const \cdot R^{-x} \cdot (A\,S)^{1/2}$$

where R is the mean rain rate in the grid box area A. The exponent x is expected to be around 1/2. The box-average rain rate R serves as a simple measure of the climatology in different regions and time periods. The inverse power relationship reflects the increased likelihood of TRMM missing rain when it

occurs only rarely and R is small, so that the relative sampling error gets large. The formula seems to describe much of the changes in sampling error with region and time, and, after some tuning of the constant and exponent x, should serve to provide error estimates for each grid box estimate provided by TRMM, for both the PR and TMI averages. [In progress] This should produce by launch time a candidate formula for the error in monthly averaged, gridded TRMM data. It will need to be returned after sufficient TRMM data are collected.

• Diurnal cycle: TRMM views a given grid box at different times of the day as the month progresses, there is a possibility that the average of its observations may be biased because it may observe different phases of the diurnal cycle unequally during the month. This is especially true at higher latitudes, where TRMM visits during a portion of the day at the beginning of the month are not repeated until 6 weeks later.

This possibility has been looked at by a few researchers. Oki and Sumi (1994), mentioned above, found that random sampling error was much larger than the possible diurnal cycle bias in monthly averages. The study needs to be repeated to compare the diurnal bias relative to the mean rain rate (rather than to the random sampling error). Soman et al. (1995) looked at Darwin rain gauge data and found that sampling approximating that of TRMM would not produce a significant diurnal bias, though perhaps this study should be confirmed with a more realistic TRMM orbit.

Diurnal bias error, if it is a problem, can be reduced after TRMM has collected enough data to estimate diurnal cycles in rain rates. The monthly means can then be corrected for the average bias expected to occur using the TRMM-derived diurnal cycles. This technique, though relatively straightforward, should be flushed out by 1998 so that it can be implemented and used to improve the accuracy of the TRMM averages during reprocessing.

• Bias due to aliasing from a diurnal cycle superimposed on a long term cycle like the Madden/Julian oscillation or even rapid seasonal change (monsoon onset?). TRMM views an area at different times of day at different times of the month. A strong diurnal cycle in rain rate superimposed on a variation of the likelihood of rain with a time scale of the order of a month could produce a bias in the TRMM average. This could be studied if a GCM with adequate representation of both the longer-time scale cycle and the diurnal cycle could be found. It could also be studied if a long series of rain gauge data from a region where such a phenomenon is observed could be used to characterize the amplitudes of the two cycles.

• Correlation of retrieval errors: It has generally been argued that if the retrieval error in each footprint is independent of the others, then sampling error will dominate the error in monthly averages, because the retrieval errors in the thousands of footprints will average out to very small values. Some recent

studies of SSM/I data raise the possibility that this assumption may be incorrect. If retrieval errors are correlated from footprint to footprint, retrieval errors will not average to zero as well, and may contribute substantially to errors in monthly averages. (Sampling error, however, will still contribute significant amounts to the error budget.) Possible approaches to getting quantitative estimates of how big an effect this may be include the simplified approaches used by North and Colleagues (need ref.) or 3-d model output of retrieval errors.

7.5 Ground Segment Issues

Nature produces hydrometeor fields with vertical and horizontal spatial structure spanning a continuum of scales from the order of meters (fine scale turbulence), to kilometers (convective cells), to hundreds of kilometers (fronts, mesoscale convective systems, etc.). At close ranges (a few kilometers or less) previous radar studies have found good agreement between theory, which predicts a power law relation between radar reflectivity (Z) and rainfall rate (R), and observations of effective reflectivity (Ze; a transformation of received power via the radar equation) and R from rain gauges.

It can be shown that under ideal conditions the fundamental variability in Z-R relations is due to variability in the raindrop size distribution (DSD). Competing microphysical processes such as coalescence, break-up, aggregation, melting and evaporation determine the DSD. The dominant process varies within and between rain producing clouds, introducing variability in the Z-R relation and errors in radar-rainfall estimation. Also, radar illuminates hydrometeors within a scattering volume whose size increases with range from the radar. The range dependent resolution of the radar scattering volume results in beam filling errors as the radar beam encompasses increasing hydrometeor variability at increasing ranges. In addition, for a fixed elevation angle, as range increases, the height of the scattering volume increases, introducing effects of vertical structure and systematic range dependent errors. Attenuation by intervening rain and cloud water introduces additional range dependent errors. Besides the above sources of variability in radar - rainfall estimation, radar calibration introduces additional sources of uncertainty. A well calibrated radar may be within 1 - 2 dBZ, introducing rainfall rate errors of 15 - 35 %. As a result, the estimation of surface rainfall from radar observations is generally pursued by a combined strategy of first principles (Z-R relation) backed up by empiricism (adjustment to in situ rain gauge observations). Rain gauge networks over land provide the primary source of validation for radar estimation of rainfall, despite their own limitations.

Conventional wisdom and experience indicate that high resolution, instantaneous radar rainfall rates are accurate to only within a factor of two. The objectives of most techniques are first to reduce the bias in retrieved rainfall rates for some large space-time domain and second to use some statistical or empirical methods to reduce smaller scale random errors.

7.6 Solutions Employing Existing Data

From the above discussion, it is clear that several sources of error are significant for more than one of the measurement schemes. Two such sources of algorithm uncertainty were examined in detail and found to have (at least partial) solutions based on existing data and models. The use of existing data to solve sampling problems is discussed within the Sampling section above.

Source of uncertainty: Beamfilling
Severity of problem: Large for radiometer, moderate for spaceborne radar,
                          minor for ground-based radar. Opportunities with
                          models/ existing data: Excellent

The variability of rainfall within a pixel is by far the dominant term in modifying the radiance field from that pixel. because of the non-linearity in rainfall-radiance relationships, this uncertainty in the variability causes uncertainties in the radiance interpretation. For a comprehensive error analysis, two quantities are required. The mean variance of the rain rate (V) , and the standard deviation (SD) of V. The mean variance must be known to remove biases in the retrieval. The SD of V will introduce random errors into the retrievals.

Since the effect of beamfilling is most severe for radiometer retrievals, its effect will be studied first. Very similar techniques, however, can be applied to PR data. For attenuation based inferences of rainfall with the PR, the beamfilling error is equivalent to the beamfilling error for TMI except that the relevant area is smaller due to the better spatial resolution of the radar.

There is very little known about the global distribution of V. It is expected, however, that the TRMM Precipitation Radar will help significantly in obtaining global distributions. In the meantime, it is possible to examine radar data from various locations around the world to obtain V and SD of V. If no other information is known, then the range of V from one location to another may be a good indicator of the possible biases. To study random errors introduced by SD of V, it is possible to take the largest value from observations as an initial estimate. This is likely to occur in the tropics.

Ground-based radar data will be analyzed on representative resolutions for various instruments. For each radar data set, histograms of V as a function of rainfall rate will be compiled. From these histograms, it is possible to compute V and SD of V. In parallel, each value of V for a corresponding rainfall rate will be matched with existing cloud model output having a similar rainfall rate and V Radiative transfer calculations will be made to examine the effect of various radiative transfer assumptions. (i.e., plane parallel, plane parallel indep. pixel and 3-D Monte Carlo). For each method, a TB-bias and a TB-random noise will

be computed based upon the real 3-D cloud radiative profile. Using Tb-bias and Tb-random noise will enable algorithm developers to simulate the corresponding potential bias and random errors in their algorithms. The TRMM passive microwave team will actively look into this problem over the next 6 months. While most of the data to carry out these experiments exists, some aircraft underflights of TRMM over a ground-based radar will eventually be needed to verify that all the radiative transfer assumptions are correct.

Source of uncertainty: Convective/Stratiform nature of rainfall
Severity of problem: Has a large impact upon latent heating
                         uncertainty. Opportunities with models/
                         existing data: Good

The heating profile is very different between convective and stratiform rainfall. Although many cases are obvious, there is no well established quantitative distinction between the two for borderline cases. Indeed the dichotomy between the two may be too simple and we may need to go to a continuous measure such as updraft velocity. Thus, even the problem is not, at this point, fully defined.

There is uncertainty about the consistency of the various definitions and marker parameters for "convective" and "stratiform" cloud regions. The most promising approach is to use existing or new cloud simulations from a state-of-the-art three-dimensional numerical cloud model to quantify the qualitative model upon which the convective/stratiform distinction is based. First, the model clouds should be categorized according to the dynamical definition, identifying typical structures for each region (particularly reflectivity texture and bright band behavior). The parameters to be considered include vertical velocity, hydrometeor distribution, and latent heating profile. This step ignores the intermediate zone between the two regimes, allowing a clean determination of the respective structures. Second, the various parts of the cloud excluded by the dynamical definition must be examined to determine whether their properties are sufficiently similar to "convective" or "stratiform" conditions that they may be included in one region or the other.

It is likely that part of the intermediate zone will resist easy classification into convective or stratiform. A decision will be required either to accept a wider error bar on "typical" structure, or to retain a third "intermediate" region in the conceptual model. In either case, some estimate must be made of the variability in the typical structures for each region. As part of this exercise, it will be necessary to understand the possible errors resulting from the use of model output.

This work is best done by a group with good access to a state-of-the-art three-dimensional numerical cloud model, as well as expertise in the remote sensing issues that require this information. There will be voluminous data processing required, together with extensive manual intervention in the analysis process.

The cost should be modest, particularly to the extent that existing archives of appropriate model runs can be used.

Source of uncertainty: Hydrometeor distributions/habit (phase, size, shape, cloud water)
Severity of problem: Severe for PR and GV radars, serious for TMI
                         Opportunities with models/existing data: Few

A persistent problem in both radar and radiometer retrievals is that particle habits and distributions are rarely measured. There are currently no measurements from which to derive mean microphysical states and their expected departure from the mean. Thus solutions to this problem area must be left to the TRMM field campaigns section (Section 8).

8. TRMM field campaigns

The Intensive Field Experiments (IFE) must serve three key functions:
1) To validate and, if necessary, calibrate the TRMM observations as discussed in chapter 2.
2) To obtain measurements and thereby increase confidence in the parameters that drive the error models as discussed in chapter 7.
3) To validate the models used to convert the TRMM observables into ultimately the most important of the TRMM objective (i.e. the climatology of the four dimensional heating of the tropical atmosphere)

Because the details of the required field experiments have not been finalized, it is premature to discuss logistics at this time. Instead, this section presents the rationale for the various observations that must ultimately be made once the details of available instruments and sites, as well as possible collaborations with other existing field experiments crystallize over the next year.

8.1 Simulating TRMM satellite measurements with aircraft instrumentation

The TRMM operational GV sites will employ ground-based radars and rain gauge networks to provide independent estimates of the TRMM variables, which the TRMM satellite will also be estimating. However, the instrumentation at the operational GV sites is quite different from that on the satellite. An additional goal of the TRMM field campaigns is to obtain aircraft measurements with instrumentation similar to the TMI and PR on the TRMM satellite (Sec. 2). The NASA DC8 and ER2 aircraft support microwave sensors similar to those aboard the satellite. In addition the DC8 supports ARMAR, a prototype of the TRMM satellite radar. These aircraft, equipped with ARMAR and microwave sensors, made measurements successfully in oceanic tropical precipitation systems in COARE. They must again make these types of measurements in the TRMM GV, and these aircraft measurements will be compared with the satellite measurements themselves. These satellite-like measurements made by aircraft, to be intercompared with the satellite data, will be carried out in the context of the TRMM field campaigns so that the extensively enhanced surface-based and other aircraft measurements will provide validation for them as well as for the satellite data.

8.2 Algorithm error models

When the largest sources of uncertainty described in section 7 are examined, a great deal of commonality emerges. All algorithm groups are concerned with the typical distribution and range of distributions of hydrometeors according to phase, size and shape in three dimensional space. It has become customary to

separate the horizontal variability under the rubric "beam-filling". So that by "distribution of hydrometeors" we will refer primarily to distribution in the vertical. Although both aspects are important, this vertical sense seemed to be the more important across the board although the "beam-filling" error was considered to be the most important for the passive microwave estimates. From a measurement point-of-view it is convenient to consider the two together. We must measure 3-dimensional fields of hydrometeor properties.

Dual polarized ground based precipitation radars can be used to gain information on the size and phase of hydrometeors at useful (3 dimensional) resolutions over rather wide areas (ca. 200 km radius) At least two such systems are planned for the TRMM validation network, Darwin and Kwajlein. The Darwin system is currently operational.

In some measure, appropriate measurements of hydrometeors can be accomplished by vertically pointing VHF radars such as the MU-Radar of Kyoto University in Japan. These have the advantage that it is possible to have many hours of observing time. This is balanced by the disadvantage that such systems are essentially immobile and view more-or-less directly overhead; they can only sample the range of conditions occurring at their location which is generally on land.

These observations can be complemented by airborne observations. The mobility of aircraft can be exploited to seek out a variety of weather conditions, particularly those over water which are more relevant to this physical validation exercise. Aircraft can carry a variety of instruments to directly measure the size and shape (from which phase can generally be inferred) of hydrometeors. Similarly aircraft can carry radars such as the ARMAR (JPL) or the new TRMM PR simulator of CRL to sample a larger volume of hydrometeors and to provide 3-D data sets with better resolution than is possible with ground based systems. Ideally, aircraft observations would at least partially coincide with both types of radar observations to provide a basis for combining the very dissimilar data types. The same logic suggests that measurements of the hydrometeor microphysics should be complemented by ground based distrometers.

To validate the vertical gradient of heating, divergence measurements must be made by airborne Doppler radar and a closed sounding array. To validate the accuracy of convective-stratiform separation of radar echo patterns, Dual-Doppler radar observations are required to determine the distribution of vertical air velocity with precipitation regions at high spatial resolution and airborne and/or balloon-borne microphysical data are needed to verify the microphyscial growth mechanisms implied by the vertical air motions. Polarimetric radar data could also help verify the microphysical regimes.

A properly designed airborne experiment campaign would also provide measurements to help quantify uncertainties in several other areas. It can be

used to measure the variability of the ocean surface reflectivity used in surface reference PR algorithms and in an underflight mode to verify the calibration of the spaceborne sensors. If dropsondes are deployed from the aircraft, data on the thermodynamic variables needed for the radiometric algorithms can be obtained.

The TRMM space segment itself will provide data which will be useful for the physical validation effort. Since the PR has a better spatial resolution than does the TMI, it can be used to approximate V, the variance of the rain rate over the radiometer fields of view. These approximate values of V can be used as a transfer standard to fill in the areas between the determinations of V based on higher resolution measurements.

A persistent problem in microwave radiometry over land has been the screening of surfaces that have scattering and emission signatures similar to those of rainfall. Current refinements of techniques appear limited due to the lack of good validation data. The TRMM PR, however, should be able to generate a significant database from which it will be possible to improve the screening techniques as well as quantifying the probability of misclassification.

In a related problem, passive microwave instruments have historically had a difficult time retrieving rainfall over land correctly when ice-phase hydrometeors are absent (such as in shallow orographic rainfall). The TRMM PR should again serve as an invaluable tool to generate a database of where and how often these conditions exist. This database can be used in conjunction with radiometer retrievals to assign expected errors due to rainfall that is formed without an ice phase.

In order to arrive at error models for the retrieval algorithms a number of actions must be taken. Many of these are relatively small actions using existing data and/or models. Participation in this workshop has motivated the relevant researchers to pursue these studies so no recommendation is needed here. Larger efforts, especially those requiring additional data, do need to be highlighted.

Since the scientific end item of TRMM is latent heat profiles, we need some way of getting an independent estimate of this very elusive quantity. As was discussed in the Latent heat issues section of this report, measurement of the wind divergence can be used to infer the latent heat released by rainfall (or at least the gradient thereof). Several experiments need to be performed using dual doppler radar (probably airborne) to make such measurements. The measurements need to be accompanied by the rainfall remote sensing measurements that will provide the inputs to a TRMM latent heat retrieval model.

An overarching issue in all the remote sensing algorithms is the vertical distribution of drop sizes, phases and shapes. There is very little data in hand to determine the range of variability of these parameters. In some measure these can be obtained by vertically pointed VHF radar's such as Kyoto University's MU radar and by ground based precipitation radars with polarization diversity capability (eg. Darwin) These data need to be collected systematically. However they are not enough. It will be important to make some airborne measurements embedded within the measurement space of the ground based radar. The aircraft must carry a precipitation physics payload (primarily PMS probes), a TRMM-like radar (candidate systems from JPL and CRL), upward viewing microwave radiometers and dropsondes. The mobility of the aircraft can be used to seek out the weather extremes and thereby extend the range in parameter space. It will also be very important to involve the modellers in the airborne experiment from the earliest experiment design phase.

Beam filling is another overarching issue. Largely, this can be satisfied using existing data. It is important that the existing data be organized in a manner that will be useful to the community and that they be associated with a set of radiative transfer models. This pairing would amount to a test bed for algorithms. This is a large effort beyond what can reasonably be absorbed into a single investigator's ongoing research. It will require some coordination through the TRMM instrument teams to be implemented. As the data set is organized, shortcomings will inevitably be discovered. Additional measurements to cover these shortcomings will need to be included in aircraft campaigns.

Multiple airborne experiments must be performed. It has been suggested that the Japanese may be able to mount an experiment before the launch of TRMM. This would get a very useful head start on many of the analyses. Coordination with the MU radar would be a natural element of a Japanese organized airborne experiment. It is critical that there be an aircraft experiment after the launch of TRMM. The divergence experiment described in the Latent heating section needs to be performed in a TRMM underflight mode. Other measurements of the hydrometeor distribution would be most useful if performed within the TRMM observations. This is by no means the total requirement for measurement campaigns; each of the TRMM teams will have their own requirements which will overlap these requirements but are not redundant with them.

8.3 Filling in the missing links in achieving TRMM goals

The operational GV sites will make measurements day after day throughout a two-year period prior to launch and continue to do so during all the years that the TRMM satellite flies. As discussed in chapter 5, these products directly address the TRMM objectives by providing an independent means of estimating the same parameters sought by the TRMM satellite and as such providing a check on the satellite estimates.

Although the GV products listed in Table 5-2 address the three objectives listed in table 5-1, they do not directly achieve TRMM goals. Nor do the products based on TRMM satellite measurements directly achieve these basic objectives. Rather they provide information that allows the TRMM variables (i.e., the climatology of the four-dimensional heating of the tropical atmosphere) to be estimated via models or calculations based on physical assumptions. Special field data will provide the additional key information required to link the operational GV and satellite products to theory, so that the TRMM data (both GV and satellite) can actually lead to achievement of the larger goals of TRMM. As such, the field campaigns are an essential element of the TRMM validation methodology. We consider now how field campaigns will add the physical linkages required to use the TRMM GV and satellite products with confidence in achieving TRMM goals.

Another way to put this is that the TRMM GV products themselves need to be validated. The convective/stratiform maps (products in Table 5-2c, addressing objective I of Table 5-1) are based on the structure of radar echoes. However, convective and stratiform precipitation refer to distinctly different precipitation mechanisms. The field campaign data must validate whether or not the convective and stratiform regions computed from the radar echo patterns indeed are regions where convective and stratiform dynamics and microphysics predominate. The vertical structure products (in Table 5-2d, addressing objective II of Table 5-1) are actually input data to computations of the vertical gradient of latent heating. The field campaigns must provide data to directly evaluate the vertical gradient of latent heating. The rain maps (products in Table 5-2e, addressing objective III of Table 5-1) are based on highly empirical conversions of radar reflectivity data to equivalent rain rates and they represent the net latent heating (Sec. 5.1.6). The field campaigns must provide data that independently confirm the rain amounts and relate them directly to atmospheric heating. The following subsections indicate how the TRMM GV field campaigns will fill in these missing links not provided by operational GV data products.

8.3.1 Validating the algorithm for convective/stratiform separation by means of kinematic and microphysical measurements

The product 2A-54 [Table 5-2(c)] subdivides the precipitation patterns observed by operational GV site radars into convective and stratiform regions. Radar echo patterns are the sole basis of this subdivision. The premise is that the echo patterns are symptomatic of the distinctly different air motions and precipitation growth processes characterizing the two precipitation types. Special additional field measurements must determine if the algorithm based on radar echo structure actually distinguishes the physical processes in an optimum way.

Figure 8-1: Characteristics of stratiform precipitation. (a) Characteristics of convective precipitation. Shading shows higher intensities of radar echo, with hatching indicating the strongest echo. In (b) cloud is shown at succession of times $t_0,\ldots,t_n$. The growing precipitation particle is carried upward by strong updrafts until t_2 and then falls relative to the ground, reaching the surface just after t_5. After t_5, the cloud may die or continue for a considerable time in a steady state before dissipation sets in at t_{n-1} and t_n. The dashed boundary indicates an evaporating cloud. (From Houze 1981.)

Figure 8-1 illustrates schematically the physical processes in stratiform and convective precipitation regions. Stratiform precipitation [Figure 8-1(a)] occurs when upward air motions are present and sufficiently strong and persistent to condense vapor onto existing precipitation particles but are, at the same time, weak enough that they allow precipitation ice particles to drift downward. In other words,

$$|w| << |V| \tag{1}$$

where V is the terminal fall velocity of snow particles (Houghton 1968; Houze 1993). Since the fall velocity of snow is $\sim$ 1-3 m s^{-1}, this velocity condition implies that the general in-cloud vertical air motion in cloud-producing stratiform

precipitation does not exceed a few tens of centimeters per second. Under this condition, ice particles in the upper levels of the clouds must fall; air motions are too weak to suspend them aloft or carry them upward. At upper levels, the only viable growth mechanism is vapor deposition; air motions are too weak to produce sufficient liquid water particles to support much growth by riming. When the ice particles falling and growing by deposition descend to within about 2.5 km of the 0°C level, the ice particles may (under certain conditions) begin to aggregate and form large, irregularly-sshaped snowflakes. The particles may also grow by riming, since at these warmer levels the vertical air motions of a few tens of centimeters per second are sometimes strong enough to maintain a small amount of liquid-water drops in the presence of the falling ice particles. Aggregation becomes more frequent within about 1 km of the 0°C level. Aggregation, of course, does not add mass to the precipitation but rather concentrates the condensate into large particles, which, upon melting, become large, rapidly falling raindrops. When it becomes well developed, the layer in which the large snowflakes melt may be marked on radar by a bright band of intense echo in a horizontal layer about 1/2 km thick located just below the 0° C level [Figure 8-1(a)].

Convective precipitation differs sharply from the stratiform process in two important respects. Firstly, w is large; in contrast to the condition of the stratiform case;

$$w = 1\text{-}10 \text{ m s}^{-1} \tag{2}$$

Secondly, the time available for the growth of precipitation particles is short; often rain reaches the ground within half an hour of cloud formation. So little time is available for growth that the precipitation particles must originate and begin growing not far above cloud base at the time the cloud forms [time t_o in Figure 8-1(b)]. It is possible for the growth to begin at that time since updrafts are strong enough to carry the growing particles upward until they become heavy enough to overcome the updraft and fall relative to the earth [see the particle trajectory in Figure 8-1(b)]. The only microphysical growth mechanism rapid enough to allow the particles to develop this fast is accretion of liquid water. Since the strong updrafts carrying the particles upward during their growth phase condense large amounts of liquid water, the larger particles (whether they be liquid or ice) in the rising parcels of air grow readily by collection of cloud liquid water. Since the strong updrafts in convective clouds are usually narrow (typically ~1 km or less in width; Lemone and Zipser 1980; Yuter and Houze 1995a), radar echoes from precipitation associated with active convection form well-defined vertical cores of maximum reflectivity, which contrast markedly with the horizontal orientation of the radar bright band seen at the melting level in stratiform precipitation [compare the reflectivity patterns in Figure 8-1 (a,b)].

In the dissipating stages of precipitating convective clouds [after time t_5 in Figure 8-1(b)], strong upward motions cease and no longer carry precipitation particles

upward or suspend them aloft. The fallout of the particles left aloft by the dying updrafts can take on a stratiform character, including a radar bright band. Real data, however, show that often the bright band is not readily apparent in the early stages of the stratiform stage of development; the vertical velocity weakens and the radar echoes exhibit a stratiform structure when the whole echo volume is viewed statistically (via CFADs) before the bright band becomes apparent in individual echo cross sections (Yuter and Houze 1995). For this reason an algorithm that asserts that precipitation is stratiform if and only if a radar bright band is present is bound to underestimate the stratiform areas and overestimate the convective areas.

To validate the algorithm used to generate convective/stratiform maps (product 2A-54) from operational GV radar echo patterns, in situ measurements must establish that the physical processes in the convective and stratiform regions are physically consistent with the above descriptions. The field campaigns for TRMM GV must provide the following in situ measurements.

The required field measurements are:

i) *High-resolution vertical air motion field within mesoscale precipitation systems.* Dual-Doppler radar measurements by ground- or ship-based radars must be available to provide vertical velocity fields. We will run the algorithm for product 2A-54 on the radar reflectivity field from these radars and then use the dual-Doppler velocity fields to verify whether conditions (1) and (2) apply, respectively, in the stratiform and convective regions identified by the algorithm. If so, then we will have validated the algorithm. If not, we will have to modify the algorithm. Steiner et al. (1995) validated the algorithm in this manner for a case study of precipitation in the vicinity of the Melbourne, Florida GV site. They plotted CFADs of both vertical velocity and reflectivity in the convective and stratiform regions and found that the vertical velocity data verified the occurrence of conditions (1) and (2) in the stratiform and convective regions, respectively. The field campaigns must test a much larger sample of data in this manner to validate product 2A-54.

ii) *In situ measurements of the ice-particle types and size distributions in the upper levels of mesoscale precipitation systems.* Airborne measurements with particle measuring system probes carried out within the region of dual-Doppler radar measurements will verify whether or not the ice-particle growth mechanisms within the areas designated stratiform and convective by product 2A-54 are physically consistent. This test will show that the algorithm generating product 2A-54 is valid if the airborne measurements show that 1) in regions identified as stratiform ice-particles grow predominantly by deposition and the downward-settling particles systematically form large aggregates as they approach the 0° C level, and 2) in convective regions ice particles grow predominantly by collection of liquid water droplets (as evidenced by the

occurrence of graupel). If the measurements do not show evidence to this effect, we will have to revise the algorithm.

8.3.2 Obtaining a more direct measure of the vertical gradient of heating

The GV products listed in Table 5-2(d) (vertical structure of radar reflectivity) are to provide data which will <u>help</u> achieve the TRMM goal of determining the vertical distribution of latent heating. They do not actually determine the vertical distribution of heating. Models must be employed to do that, and observations of the vertical structure of radar reflectivity provide some partial input to calculations of the vertical distribution of heating.

The TRMM field campaigns must provide direct measurements of the vertical gradient of heating. The large-scale balanced flow in the tropics adjusts to the vertical derivative of the heating (Haynes and MacIntyre 1987; Mapes and Houze 1992, 1993, 1995). The vertical derivative of the heating in the tropics is proportional to the vertical gradient of vertical velocity, which is in turn equivalent (through mass continuity) to the large-scale convergence (negative of the divergence) of the horizontal wind. Most of the horizontal convergence in the tropics occurs in precipitating cloud systems. A single Doppler radar measures this convergence accurately, if the radar is surrounded by precipitation. One way to obtain such measurements is with a tail Doppler radar such as those aboard the NOAA P3 and NCAR Electra aircraft. Flying such an aircraft in a small circular flight track (called a "purl") leads to a vertical profile of the convergence (Figure 8-2). Mapes and Houze (1993, 1995) analyzed vertical profiles of convergence obtained in this way for ~250 purls obtained in precipitating mesoscale cloud systems over the tropical ocean in EMEX and COARE. These results show distinctly different convergence profiles in stratiform and convective regions, and Mapes and Houze (1995) used these convergence profiles as input to a set of spectrally decomposed linear primitive equations to show how the large-scale environment responds differently to the heating in convective and stratiform regions.

Figure 8-2: "Purl" flight pattern. (a) Horizontal flight track with purl (loop). As aircraft flies around loop, Doppler radar beams point outward from flight track. Velocity components along the beams allow the horizontal divergence of the wind to be computed for a circular region (e.g., the 15 km radius circle shown) centered on the purl. (b) Vertical cross section showing that the radar beam scans vertically through a sequence of elevation angles (alpha) so that the divergence can be determined as a function of height when the aircraft flies in a purl such as that in (a).

The TRMM GV field campaigns will provide convergence profiles from purl flight patterns as a direct indication of the vertical distribution of heating in convective and stratiform regions, and these empirical data on the vertical gradient of heating will be an independent comparison data set for model calculations using vertical structure of radar echoes as partial input. Since the convergence profiles reflect the vertical gradient of total (i.e., latent plus

radiative) heating, it will be necessary to measure also the radiative heating in the precipitating cloud systems. Aircraft with full suites of radiation sensors will participate in the field campaigns to provide this information.

The divergence profile may also be measured by ground-based radars. A single Doppler radar provides the profile if the radar is completely surrounded by precipitation. Dual-Doppler radar provides the profile if precipitation is in the limited zone where beams cross at angles > 20 deg. Unfortunately, the chances that a single radar is surrounded by rain or that precipitation is in the dual-Doppler zone is so small that the sample size obtained in a field experiment of any reasonable duration will usually be too small to be statistically meaningful.

8.3.3 Providing heat and moisture budget constraints on precipitation estimates

The GV rain map products [Table 5-2(e)], if corrected for evaporation from the surface, represent the net (vertical integrated total) latent heat released into the atmosphere at the location of an operational GV site. The net convergence of heat into the region surrounding a site provides an independent check on this total heating. A closed array of soundings of atmospheric temperature, humidity, pressure, and wind provides the opportunity to compute this net convergence and estimate the net latent heat release as a budget residual (e.g., Yanai et al. 1973; Johnson 1976; and many others). This estimate of the latent heat is validation for the rain amount determined from radar and rain gauge data within the region of the array. Each TRMM GV field campaign will employ surface meteorological measurements and upper-air soundings to provide this independent validation of the rain map algorithms. The sensor array will also require estimates of radiation and surface evaporation to close the budgets.

8.4 TRMM Field Campaign Planning (Report from the first TRMM Field Experiment Planning Group Meeting of 1-2 March 1996 -- Summary

Algorithm developers, and indeed most U.S. TRMM scientists, will be inundated with data for some time after launch. Many of the critical individuals are the same ones needed to plan and carry out field programs. The human resources available to TRMM are simply not sufficient to do what is necessary in the U.S. during the post-launch period and at the same time prepare for a field program outside the U.S. with all its inevitable complications. Therefore, our strong recommendation is to defer *any* major land and ocean campaigns outside the U.S. until 1999.

We believe that the field campaigns outlined below are in the best interests of TRMM:

1. 1998: While postponing major campaigns outside the U.S. until 1999, there are opportunities during 1998 to accomplish several important objectives for TRMM. Within the first several months after launch, there are requirements for TRMM underflights for instrument calibration and physical validation of algorithms. To get the most scientific benefit for TRMM from these periods of potential-to-likely aircraft availability for TRMM, we have one recommendation and one suggestions.

   1a: We recommend a low risk, high payoff, limited expense campaign focused on the Florida and Texas GV sites. The ER-2 is requested for April-June 1998. The time period is appropriate for the underflights mentioned above, and there is a very high probability of deep convective systems in the vicinity of Florida, Texas, or both (see below)

   1b: If resources permit, we suggest that it would be useful for TRMM to participate in the SCSMEX experiment in a limited way. The DC-8, equipped with ARMAR, together with likely Japanese aircraft experiments with CAMPR, along with an existing ship radar, with supplemental rain gauges on nearby islands, would provide a very useful database. However, we are concerned that the human and financial resources available for TRMM field campaigns may not be sufficient for the participation with both an aircraft and a radar program.

2. Major Land Campaign: We recommend a 6-week period during January and February 1999, the wet season in Brazil, for TRMM's tropical land campaign. The ER-2 is requested because it can overfly the huge Amazon thunderstorms. The success of this campaign is dependent upon securing certain facilities from sources other than TRMM (see below).

3. Major Ocean Campaign: We recommend that Kwajelein be the location for TRMM's tropical oceanic campaign, for a 60-day period during June-August 1999. The DC-8 is requested; the ER-2 would be desirable but probably most impractical and we are quite prepared to do this campaign without it. Details follow below.

8.4.1 Discussion of major issues.

GV Team Leader Houze stressed (and all agreed) that there were two principal reasons for investing resources in the field campaigns: (1) Strengthen the weak points in the assumptions of the various algorithms; (2) Address 4-dimensional latent heating of the tropical atmosphere by combined use of models and observations.

The convective-stratiform separation of precipitation is fundamental. Therefore it is important to validate those algorithms. The most troublesome regions are "intermediary", which are typically in the process of transition from convective to stratiform. The issue is not a semantic one, but one of learning the relative speed of transition as determined *by the algorithm* (which uses the radar reflectivity

structure) and by the decay of the convective vertical velocity field (which requires dual-Doppler radar to estimate accurately). The models which will be used to estimate diabatic heating must be validated against measurements of both fields.

In all TRMM field campaigns, other things being equal, one would request both the DC-8 and the ER-2. The scientific requirements for these missions is the verification of algorithms including flights over and through convective and intermediary regions of mesoscale convective systems. Long experience over the tropical oceans has demonstrated that the DC-8 can often penetrate such regions at its normal flight altitudes. However, it is well known that at similar altitudes in the operative weather situations in Texas, Florida and the adjacent Atlantic and Gulf of Mexico, and in the Amazon, very high supercooled liquid water contents, hail, strong electrification, and severe turbulence are likely. If flight safety considerations make it unlikely that these areas could be penetrated (and the DC-8 could not get high enough to top them), we consider it wise to decline to request that aircraft. Of course, that does not preclude the use of the DC-8 for selected calibration or physical validation flights, but this report deals solely with the coordinated field experiments.

The convective-stratiform separation is a separation of the radar echo into volumes of space in which the operative precipitation growth mechanism is collection of cloud liquid water (convective) or vapor diffusion (stratiform). An important additional and independent verification of the convective-stratiform separation is therefore *in situ* particle image data at a wide range of ambient temperatures (0° to -40°C). These data are most important in those regions not obviously convective or stratiform, but again in the intermediary regions. An aircraft with PMS probes can obtain the required data. The main problems in so doing will be logistic, not scientific.

An independent estimate of the diabatic heating can be made by direct measurements of the divergence field, best accomplished by aircraft equipped with scanning Doppler radar such as on the NOAA WP-3 or the NCAR Electra. It is understood that the absence of radar scatterers outside precipitation over water creates some difficulties in measuring the divergence, especially in very low and very high levels, so supplementary wind measurements should be planned to account for these problems, but the Doppler aircraft are essential.

It is highly desirable to calculate the atmospheric water vapor flux divergence as a function of height, and thereby obtain an independent estimate of the rainfall via the water budget method over a suitable time-space volume as part of the validation of the TRMM estimates. In Section 8.3.3 of the TRMM SOP it is stated as a requirement for all TRMM field campaigns (!). If we believed that resources would permit such an estimate to better than 30-40%, we would agree. However, unless we are convinced otherwise, it is our conclusion that such accuracy cannot be achieved in the vicinity of Kwajalein, and is unlikely in any

other GV site with the possible exception of Florida and Texas. We recommend, with reluctance, that *TRMM FCs should abandon the "water budget" objective*, because expending major resources for such an inaccurate estimate would be an unwise, wasteful decision. That does not mean that augmented soundings are not essential; they are. What they are essential *for* is to provide frequent (usually 3-hr) initialization data for the linked mesoscale, cloud, and radiative transfer models which are essential components of the algorithm testing and GV programs. For each FC, such soundings should be made at a minimum of two sites, preferably more.

8.4.2 TExas-FLorida UNderflights (TEFLUN1998):

This program meets several important requirements in a timely manner. The instrument teams require TRMM underflights in the time frame of 2-6 months after launch. Some of these could be done in clear skies over water and over land; others require precipitation but these flights would be far more useful if there were also ground validation (GV) data at the same time. Planning these flights for desired weather conditions is not simple, especially if the GV sites are to supplement with specialized observations such as radar scans and soundings. The radar at Texas A&M will be made available to obtain customized scans synchronized with TRMM overpasses; it is highly desirable if a radar could be found to do the same in Florida. By specifically incorporating these disparate needs into a coherent program, it will be possible to achieve far more.

During April, May, and June, there are precipitation, thunderstorms, and mesoscale convective systems, some severe, are frequent occurrences at the Texas and Florida GV sites. Further, it is rare that *both* Texas and Florida would be without precipitation for many days. Therefore, by basing the ER-2 about halfway between TX and FL, its efficient use is assured. We believe that 5 flights of 3 h on-station time at each site are required, plus 5 fair weather flights not necessarily over GV sites for calibration. Adding ferry time and contingencies, 90 h of ER-2 time are requested.

The efficient scheduling of the aircraft, and ancillary measurements, requires that a modest forecasting and operations center be established for the Spring of 1998.

By obtaining several case studies of MCSs over TX and FL early in the mission, it will be possible to exercise the algorithms on the basis of cloud and radiative transfer models, using high quality radar data and underflight data. These tests will be invaluable for building confidence in the algorithms. The models require accurate profiles of temperature, humidity and wind for initialization and for validation, leading to the additional observational requirement for 3-hourly soundings at and near the GV sites. Capability for obtaining such data from TX and FL will be important from time to time throughout TRMM, so assuring its availability during the early months of TRMM will have continuing benefits.

Summarizing the requirements for the 1998 Florida and Texas FC:

- ER-2, 90 hours, based about halfway between FL and TX GV sites
- Augmented soundings from at least 2 sites in TX and 2 sites in FL
- Texas A&M Doppler radar available for customized scans for overpasses; Doppler radar for dual Doppler desirable; additional Doppler radar for Dual-Doppler pair with Melbourne site desirable
- Operations center (modest) for forecasts and aircraft and radar scan coordination

8.4.3 Amazonia, January-February 1999:

Meteorologically, we consider the Amazon basin representative of the interior of tropical continents, with heavy seasonal precipitation, the most important unsampled region of the tropics for TRMM purposes. No TRMM GV site is in the interior of Africa or South America; Darwin and Thailand, however valuable, have much of their precipitation controlled by monsoon circulations, orography, or land-sea circulations. We believe that the existence of several planned scientific field campaigns in Brazil argues strongly that the highest priority for a TRMM FC in a tropical continent is in Amazonia. In addition to international programs in chemistry, hydrology, and ecology, the Brazilian Government and Universities are planning to implement sounding systems and radars of great importance to TRMM, further justification for the decision to recommend Brazil. The wet season is between December and April; the rains are so reliable during January and February that our recommendation is to deploy for a 6-week period, about 5 January - 20 February 1999.

Details of the resources required for this program are necessarily sketchy because we have not yet obtained sufficient information on what facilities are to be provided by others in connection with the LBA and other programs. We are assuming that the site would be the one selected by the ecologists and hydrologists in Rondonia near Ji-Parana. (However it is too soon to rule out the site in Para near Maraba, selected by the atmospheric chemists.) Chris Kummerow is taking the lead in the endeavor of securing more information. Based on the best available estimates at this time, our recommendation for the main resources to be available for the TRMM FC in Brazil (source not necessarily TRMM) include:

- ER-2, probably based in Manaus, from which either site could be reached in a reasonable ferry time, for about 80 research hours (10 flights @ 6.5 h plus contingency time)
- One research quality Doppler radar; a second Doppler radar is desirable; polarization diversity on at least one of the radars is desirable
- Lear Jet or equivalent for cloud microphysical sampling from 0°C to -40°C

- Augmented soundings from at least 2 sites, every 3 h on operational days
- Augmented lightning network
- Augmented rain gauge network
- Surface data, fluxes, and boundary layer profiling capability

8.4.4 Kwajalein, June-August 1999

This is the only scientifically viable ocean location among all the TRMM GV sites for both physical validation and algorithm validation. The TRMM science team has already endorsed this site as the highest priority of all TRMM GV sites, and despite some significant difficulties, we recommend that the ocean TRMM FC should take place at Kwajalein.

We discussed at length what our "fallback" position would be, should some of the required observations and facilities prove logistically difficult or impossible. We reiterate our recommendation that we do whatever is possible to maximize the database at Kwajalein, because we cannot find an acceptable alternative. If we are *forced* into compromising the requested observations at Kwajalein, we would devise a revised scientific plan which would obtain the specific missing observations at another GV site, and apply that knowledge to interpreting the Kwajalein results, rather than move the entire tropical ocean FC to any other site.

We recommend that the TRMM Kwajelein FC take place during the most likely period for reliable heavy rains (June-Nov.) and within that period we recommend a 60 day period sometime during June-August, because university people are more available then, and because other things being equal, we would rather not delay this FC any later in the satellite's lifetime than necessary. Resources required include:

- NASA DC-8 with ARMAR and as complete a complement of TMI-like sensors as possible; operating from Kwajalein or Majuro for 60 days; estimate 100 research flight hours (15 flights @ 6 h plus contingency).
- Dual Doppler radar, surface-based (one radar in addition to the Kwajalein radar). This second radar should be located about 30 km distant from the Kwajalein radar, preferably on a ship to the south where more rain is expected
- Aircraft with Doppler radar (Electra) for divergence purls, several other objectives; 100 research hours
- Aircraft for microphysics at low levels and high levels (could be Doppler aircraft at low levels and DC-8 at high levels)
- Augmented soundings at Kwajalein, Majuro, perhaps other atolls, at 3 h intervals during MCSs and aircraft operations
- PBL T, q, wind, probably from tethered balloon
- Polarization diversity added to existing Kwajalein radar
- Augmented lightning network

- Oceanographic measurements
- Lear Jet for additional high level microphysics measurements

8.4.5 Closing remarks on resource allocation.

During the next several months, information will be obtained that will determine logistic feasibility, and allow cost estimates for the FCs that have been recommended. We have intentionally been modest in our ambitions to the extent possible while still addressing the important TRMM goals. We explicitly recognize that the centerpiece of the GV program for TRMM is not the one-time FCs, but the 3-year database obtained at the GV sites. Therefore, we emphasize that those making final resource decisions (from the MO & DA budget) should be open to the possibility that the wisest course for TRMM's success may be to allocate some fraction of those resources to ensuring the viability of the data from the GV sites. The FCs are essential, but not at the expense of the climatological database from the GV sites.

9. Modeling and Analysis

The United States Modeling group for the Tropical Rainfall Measurement Mission (TRMM) has interests ranging from cumulus ensemble models to the climate models. Precipitation validation on time scales of few hours to monthly and seasonal time scales are areas of relevant interest. Figure 9-1 provides a schematic outline of the modeling group's interest. The centerpiece of this activity would be the Goddard Cloud Ensemble Model, Tao and Simpson (1993), which will play a key role in providing useful information on the vertical distribution of heating to the modeling community. The thrust of the GARP Atlantic Tropical Experiment (GATE) experiment provided the refinements and developments of cumulus parameterization schemes such as those of Arakawa Schubert (1974), Kuo (1974), Betts and Miller (1986), and Tiedke (1984). None of these schemes had the benefit of observational verification of the modeled vertical distributions of the cumulus scale heating. The prospect of TRMM is to provide radar based measurements of the vertical distribution of hydrometeors. That together with the Goddard Cloud Ensemble Model (GCEM) holds the promise for the determination of the vertical distribution of heat sources.

Figure 9-1: A schematic diagram of he proposed U.S. modeling for TRMM on different space-time scales.

9.1 Goddard Cloud Ensemble Model

The modeling activities for TRMM would rely on the data sets from the precipitation radar and the TRMM microwave instrument. This model is designed to make use of the hydrometeor distribution as seen from the precipitation radar and provide measures of the vertical distribution of heating via the Goddard Cloud Ensemble Model. Tao and Simpson have run this model over a variety of tropical environments. They have noted that it is possible to provide statistical relationships among the hydrometeors and heating rates thus providing a practical utility for the data sets from the TMI and precipitation radar.

The GCEM can improve TRMM's capability both by helping derive rainfall algorithms as well as by helping to validate and correct them. In addition, several convective and stratiform partitioning techniques for TRMM heating retrieval algorithms will be evaluated using Tropical Ocean Global Atmosphere Coupled Ocean Atmosphere Response Experiment (TOGA COARE) data and model results. This effort will also provide an archive of hydrometeor and heating profiles associated with the convective systems for different geographic locations. The work under this initiative has so far been the only source of latent heating/cooling retrievals.

Rainfall and its variability is a key link in the hydrologic cycle as well as the primary heat source for the atmosphere. The vertical distribution of convective latent-heat release modulates the large-scale circulations of the tropics and their impacts upon mid-latitude weather. Furthermore, changes in the moisture distribution at middle and upper levels of the troposphere as well as the radiative responses of cloud hydrometeors to outgoing longwave and incoming short-wave radiation are a major factor in assessing climate change. Present day large-scale weather and climate models simulate cloud processes only crudely, reducing confidence in their predictions on both global and regional scales. The GCEM is nested in a mesoscale model, which will result in better initialization and representation of rain processes and their impacts on larger scales. They are continually using observations of convective systems and enhanced computer capability to improve our model and link it with land and ocean processes.

9.2 Physical Initialization and Prediction of rainfall

The emphasis of research in this area is towards the improvement of analysis and predictions of rainfall over the tropics over various space-time scales. It is possible to enhance the tropical prediction skill over the medium range time-scale (i.e. about a week) by invoking physical initialization. That includes rain rates from a mix of surface (rain gauge) and space Outgoing Longwave Radiation (OLR) and Special Sensor Microwave Imager (SSM/I) based

observations, (Krishnamurti et al., 1993, and Goirola and Krishnamurti, 1992). Use of such rain rate input via physical initialization in a very high resolution global model (horizontal resolutions (T213) provides a very high skill for the nowcasting of the initial rainfall. The analysis of rainfall begins with the Florida State University (FSU) mixed algorithm, which includes a sharpened OLR as a first guess and the data sets include SSM/I based rainfall over oceans and raingauge over the land areas. Figure 9-2 illustrates what we can do currently towards making global models accepting rainrates as derived from satellite measures and the global surface raingauge network. The top panel shows rainrates based on such observations, the middle panel illustrates what we can teach the model to include in its initial state via what we call physical initialization. The middle panel of Figure 9-2 illustrates the rainfall as derived from the physical initialization and the bottom panel of Figure 9-2 shows what we obtained from a simple application of the so-called nonlinear normal mode initialization with physics. It is clearly apparent that we can initialize rainfall from the SSM/I to a high degree of accuracy. This would be one of the components of the model improvement we shall bring about in the proposed studies.

Figure 9-2: (a) Observed (based on SSM/I, OLR and rain gauge) rainfall for a 24-hour period. (b) Physically initialized rain for the same 24-hour period. (c) Control experiment based rain for the same period. Units: mm/day.

Figure 9-3: (a) Correlation of predicted and observed rain over the tropical belt for FSU model (based) on physical initialization for day 0; also shown is the skill of NMC/GDAS rain compared to observed rain. (b) Correlation of predicted and observed rain over the tropical belt, 30°S to 30°N for the FSU (physically initialized and control), NMC and ECMWF models for the one-day forecast.

Figure 9-3 illustrates from such a month-long experiment the skill that one finds from use of physical initialization compared to that from the use of diabatic normal mode initialization. Skill is here measured from a correlation of observed versus predicted rain over 6 hour bins covering transform grid squares in space. It is apparent that physical initialization carries a very high nowcasting skill for the rainfall. That is also reflected in the one day rainfall forecasts where the physical initialization carries a skill of around 0.6 (correlation of 'observed' versus predicted rainfall) as against roughly 0.35 for the various operational models and for the experiments that do not invoke physical initialization. The major problem arises as one proceeds from day 1 to day 2 of forecast, a sharp drop in rainfall forecast skill is noted. That drop is apparently due to many factors: the phase errors of predicted disturbances starts to increase after day 1 of forecast, physical parameterization algorithms are deficient in describing the heating moistening and rain rates during the forecast. The physical initialization builds up a local meso-scale structure, Krishnamurti et al. 1995, that describes the vertical distributions of heating, the humidity variable, the divergence field and the surface pressure field. The TRMM data sets may provide us with the means

to improve the mesoscale vertical structures. Many research groups e.g. the Florida State University (FSU), (Krishnamurti et al., 1991, 1994), the Australian Bureau of Meteorological Research Center (BMRC), (Puri and Miller 1990, Puri and Davidson 1992), and others (Kasahara et al., 1994, Donner and Rasch 1989) are engaged in this important area of research to improve the analysis and forecasts from numerical weather prediction models.

The modeling approach at FSU utilizes a primitive equation spectral model in the sigma-coordinate system. It can be integrated with different horizontal resolutions, ranging from a low T-42 to a high T-213 resolution, and has 16 vertical levels extending from earth's surface to about 50 mb. It includes a complete array of parameterization for various physical processes.

The Australian Bureau of Meteorology Research Center (BMRC) Modeling group expects to provide a validation of TRMM data via regional and global modeling. The Global Assimilation and Prediction system (GASP) has been used for operational analysis and prediction in the Australian Bureau of Meteorology since September, 1990. Predictions have been run out to five days ahead from both 0000 UTC and 1200 UTC.

This model currently includes a physical initialization based on rainfall and diabatic heating estimates from the Japanese Geostationary Meteorological Satellite the GMS, Davidson and Puri (1992). This model also incorporates a comprehensive moisture analysis scheme based on Infra Red (IR) satellite signatures from the Japanese geostationary satellite.

An operational version, the Tropical Analysis and Prediction System (TAPS), was implemented in November 1992, and it runs with a horizontal resolution of 95 km and 19 vertical levels over the domain 45°N to 40°S and 85°E to 178°E. A detailed description of the tropical numerical system is given by Puri et al. (1992) and Davidson and Puri (1992). It is a hydrostatic, primitive equations model with a sigma vertical coordinate and semi-implicit time differencing. The physical parameterizations package is the same as that used in GASP. Boundary conditions are taken from the GASP system for real-time predictions.

The relatively poor analysis of the divergent part of wind is a reason for the common problem of spin-up. Inaccuracies in the divergence can lead to incorrect initiation of convection in a model. In order to reduce such problems, the convective parameterization (generally the Kuo scheme) is replaced by a specified diabatic heating distribution during the initialization period of nudging. The heating distribution is derived from six-hourly GMS infrared imagery, such that the peak heating rate is linearly related to the cloud-top temperature. The vertical profile for the imposed heating is fixed and it is consistent with observed heating rates in the tropics. This results in BMRC tropical numerical system to have minimal spin-up problems, with useful estimates of precipitation over the Asia-Pacific region (Puri and Davidson, 1992).

This model is also used for operational analysis and prediction by the Bureau of Meteorology in the Australian tropics, particularly to support tropical cyclone forecasting. The system therefore provides a valuable base for assimilation and modeling research for TRMM.

The focus of the U.K. Meteorological Office is in improving the hydrological cycle in the Numerical Weather Prediction (NWP) model. The emphasis is on studying the biases and errors in moisture observations from radiosondes and TIROS Operational Vertical Sounder (TOVS) as well as the model. Plans are in hand to extend this to SSM/I data and after its launch to Advanced TIROS Operational Vertical Sounder (ATOVS), and studying Cloud liquid water derived from SSM/I measurements. Future research plans include conducting experiments to assimilate SSM/I precipitable water using data assimilation which is being planned for 1995. This would lead on to using cloud and rainfall, and a 4-dimensional variational assimilation scheme should be ready for experiments by the launch of TRMM in 1997.

TRMM research will focus towards providing guidance on ways in which the radar data can be used to improve retrieval by TRMM Microwave Instrument (TMI). This group sees the need for close collaboration with the passive microwave group in comparing SSM/I and TMI retrievals towards improved use of TRMM data sets.

9.3 Organization of Tropical Rainfall and Convective Systems and their Interaction with the Large-Scale Circulation

A National Aeronautical and Space Administration (NASA) Goddard group (W. Lau, Arthur Hou, C.H. Sui and S. Schubert) proposed research on the analysis, modeling and application of TRMM data focusing on the relationship between rainfall, latent heating and the large scale circulation and their roles in the tropical water and energy cycles. TRMM and TRMM-related satellite and ground based data, and models are utilized. The research tasks are broadly divided into four areas: regional analysis, global analysis, cumulus ensemble modeling and Four Dimensional (4-D) assimilation. Specific research tasks were proposed within each of the above areas. Results obtained from the ongoing research and availability of current data have enabled us to better formulate and refine research tasks from the previous investigation and to initiate new tasks.

During the 1991-93 period, the following milestones were reached by this group. A major effort has been devoted to implementing an efficient radiation routine and a sophisticated microphysics package in the Goddard Cumulus Ensemble Model (GCEM). A series of experiments to study the tropical water and energy cycles and their sensitivity to climate feedback have been conducted. Significant results regarding the importance of evaporation and moisture recycling as a thermostat of Sea Surface Temperatures (SST) were found.

Preliminary results on the possible mechanism for westerly wind burst and its relationship to latent heating from analysis for TOGA-COARE data have been obtained. A significant milestone is the completion of an atlas detailing daily synoptic situations during the entire intensive observation period of COARE. The atlas serves as a reference guide to all COARE researchers and is being distributed worldwide. Dr. Lau and his co-workers examine the time history of a number of surface parameters along with the rainfall regions. These are studied on seasonal time scales. Figure 9-4, from one of their recent studies, illustrates what was possible to obtain during the recent TOGA-COARE. Here they illustrate the behavior of the IR measurements from GMS ocean temperature and surface fluxes during a sequence of wet and dry episodes. Similar computations during TRMM hold the promise of obtaining better relationships between rain rates and surface fluxes over several time scales over the tropical oceans.

Figure 9-4: Time series during TOGA COARE of various parameters identified at the top of each panel. Based on Lau, Sui and Schubert.

They have completed the first phase of a TOGA-COARE 4-D assimilation using the Goddard GEOS-1 Data Assimilation System (DAS) and have carried out intercomparison studies with other operational assimilation systems.

A rainfall ground truth validation and diagnostic study using rain gauge, radar and GMS satellite data study over Darwin, Australia has been carried out. The objective is to explore the utilization of an OLR based rainrate technique similar to Global Precipitation Index (GPI) on short time scales and in delineating the interaction of the diurnal, synoptic and low frequency variability using TRMM ground truth data.

We have initiated a satellite rainfall intercomparison task which focuses on space-time evolution of climate scale rainfall derived from TRMM or related rainfall algorithms in parallel with model rainfall intercomparison under the Atmospheric Model Intercomparison Project (AMIP).
Some of Research Results are:

The preliminary assimilation product, albeit somewhat crude, can provide useful information shedding new light on the mechanics of the large scale atmospheric controls and probable causes for the westerly wind bursts (WWB) and rainfall variability over the warm pool of the tropical western Pacific.

Based on the comparative model diagnostics, a consistent picture of large scale evolution and multi-scale interaction during TOGA-COARE emerges:

The Propagation of the Madden Julian Oscillation (MJO) into the western Pacific from the Indian Ocean region foreshadows the establishment of WWB events over the COARE region. The maritime continent appears to play a critical role in separating the circulation and convection between the two regions, allowing only occasional but relatively rapid transmission of OLR and wind signals via the MJO, from the Indian Ocean the western Pacific.

The maintenance of the WWB during TOGA-COARE is related to the establishment of large scale east-west pressure dipole between maritime continent and the equatorial southern Pacific near the dateline. This pressure dipole can be identified in part with the ascending (low pressure) and descending branch (high pressure) of the MJO in the near equatorial western Pacific and Indian Ocean region.

Accompanying the development of WWB over the Intensive Flux Array (IFA) and crucial to its maintenance is a strong meridional circulation, with strong cross-equatorial flow and rising motion near the entrance region of the WWB and sinking motion in the extratropical northern hemisphere.

The mature phase of the WWB is associated with enhanced extratropical cyclonic activities along the East Asian wintertime storm tracks. Surface pressure and wind surges related to cold air outbreak off the East Asian continent may play a role in the rapid build up and termination of the WWB during TOGA-COARE.

References

Adler, R.F., G.J. Huffman, and P.R. Keehn, 1994: Global rain estimates from microwave-adjusted geosynchronous IR data. *Remote Sens. Rev.*, **11**, 125-152.

Arakawa, A. and W.H. Schubert, 1974: Interaction of a Cumulus Cloud Ensemble with the large- scale environment: Part I. *J. Atmos. Sci.*, **31**, 674-701.

Arkin, P.A., and B.N. Meisner, 1987: The relationship between large-scale convective rainfall and cold cloud over the Western Hemisphere during 1982-1984. *Mon. Wea. Rev.*, **115**, 51-74.

Atlas, D., D. Rosenfeld, and A. R. Jameson, 1995: Evolution of radar rain measurement methods; Steps and Mis-steps. Keynote paper. Proc. III International Symposium on Hydrological Applications of Weather Radars, Sao Paolo, Brazil, Aug 20-23.

Austin, P. M., 1987: Relation between measured radar reflectivity and surface rainfall. *Mon. Wea. Rev.*, **115**, 1053-1070.

Betts, A.K. and M.J. Miller, 1986: A new convective adjustment scheme. Part II: Single Column Test Using GATE-Wave BOMEX, ATEX and Arctic Airmass Data Sets. *Quart. J. Roy. Meteor. Soc.*, **112**, 693-710.

Birrer I. J., E. M. Bracalente, G. J. Dome, J. Sweet, and G. Berthold, 1982: ^{0} signature of the Amazon rain forest obtained from the Seasat Scatterometer," IEEE Trans. Geos. and Remote Sens., GE-20, 11-17.

Braun, S. A., and R. A. Houze, Jr., 1995: Diagnosis of hydrometeor profiles from area-mean vertical-velocity data. *Quart. J. Roy. Meteor. Soc.*, **121**, 23-53.

Davidson, N.E. and Puri, K., 1992: Tropical prediction using dynamical nudging, satellite-defined convective heat sources, and a cyclone bogus. *Mon. Wea. Rev.,* **120**, 2501-2522.

Donner, L.J. and P.J. Rasch, 1989: Cumulus initialization in a global model for numerical weather prediction. *Mon. Wea. Rev.* **117**, 2654-2671.

Garstang, M., H. L. Massie, Jr., J. Halverson, S. Greco, J. Scala, 1994: Amazon coastal squall lines. Part I: Structure and kinematics. *Mon. Wea. Rev.*, **122**, 608-622.

Goirola, R.K. and T.N. Krishnamurti, 1992: Rain rates based on SSM/I, OLR and raingauge data   sets. *J. Meteorol. Atmos. Phys.*, **50**, 165-174.

GPCC, 1992: Monthly precipitation estimates based on gauge measurements on the continents for the year 1987 (preliminary results) and future requirements. WMO/WCRP and DWD, Rep. No. DWD/K7/WZN-1992/08-1, 20 pp.

Haynes, P. H., and M. E. MacIntyre, 1987: On the evolution of vorticity and potential vorticity in the presence of diabatic heating and frictional or other forces. *J. Atmos. Sci.*, **44**, 828-841.

Houghton, H. G., 1968: On precipitation mechanisms and their artificial modification. *J. Appl. Meteor.*, **7**, 851-859.

Houze, R. A., Jr., 1982: Cloud clusters and large-scale vertical motions in the tropics. *J. Meteor. Soc. Japan*, **60**, 851-859.

Houze, R. A., Jr., 1989: Observed structure of mesoscale convective systems and implications for large-scale heating. *Quart. J. Roy. Meteor. Soc.*, **115**, 425-461.

Houze, R. A., Jr., 1993: *Cloud Dynamics*. Academic Press, 573 pp.

Houze, R. A., Jr., and A. K. Betts, 1981: Convection in GATE. *Rev. Geophys. Space Phys.*, **19**, 541-576.

Houze, Jr., *R.* A., C.-P. Cheng, C. A. Leary, and J. F. Gamache, 1980: Diagnosis of cloud mass and heat fluxes from radar and synoptic data. *J. Atmos. Sci.*, **37**, 754-772.

Huffman, G.J. R.F. Adler, B. Rudolf, U. Schneider, and P.R. Keehn, 1995: Global precipitation estimates based on a technique for combining satellite-based estimates, rain gauge analysis, and NWP model precipitation information. *J. Clim.*, **11**, to appear.

Iguchi, T., and R. Meneghini, 1994: Intercomparison of single frequency methods for retrieving a vertical rain profile from airborne or spaceborne data. J. Atmos. Oceanic Technol., 11, 1507-1516.

Implementation Plan: TRMM-490-003, Volume No.3, Preliminary #6 (June 9, 1994)

Johnson, R. H., 1976: The role of convective-scale precipitation downdrafts in cumulus and synoptic-scale interactions. *J. Atmos. Sci.*, **33**, 1890-1910.

Kasahara, A., A.P. Mizzi and L. J. Donner, 1994: Diabatic initialization for improvement in the tropical analysis of divergence and moisture using satellite radiometric imagery data. *Tellus,* **46A**, 242-264.

Kennett R. G., and F. K. Li, 1989a: Seasat over-land scatterometer data, Part I: Global overview of the Ku-band backscatter coefficients. IEEE Trans. Geos. and Remote Sens., GE-27, No. 5, 592-605.

Kennett R. G., and F. K. Li, 1989b: Seasat over-land scatterometer data, Part II: Selection of extended area land-target sites for the calibration of spaceborne scatterometers. IEEE Trans. Geos. and Remote Sens., GE-27, No. 5, 592-605.

Kleinschmidt, E., Ed., 1935: *Handbuch der Meteorologischen Instruments und Iher Auswertung.* Verlag von Julius Springer, Berlin, 733 pp.

Krajewski, W. F., G. J. Ciach, J. A. Smith, E. N. Anagnostou, and M. L. Baeck, 1995: A radar-rainfall estimation algorithm for climatological purposes. To be submitted, *J. Appl. Meteor.*

Krishnamurti, T.N., H.S. Bedi, G.D. Rohaly, D.K. Oosterhof, R.C. Torres, E. Williford and N. Surgi 1995: Physical Initialization. *J. Atmos. Ocean.* (To be published).

Krishnamurti, T.N., G. Rohaly and H.S. Bedi, 1994: On the improvement of precipitation forecast skill from physical initialization. Accepted for publication in *Tellus.*

Krishnamurti, T.N., H.S. Bedi and K. Ingles, 1993: Physical initialization using SSM/I rain rates. *Tellus*, **45A**, 247-269.

Krishnamurti, T.N., J. Xue, H.S. Bedi, K. Ingles and D. Oosterhof, 1991: Physical initialization for numerical weather prediction over the tropics. *Tellus*, **43AB**, 53-81.

Kuo, H.L., 1974: Further Studies of the parameterization of the influence of cumulus convection on large-scale flow. *J. Atmos. Sci.*, **31**, 1232-1240.

LeMone, M. A., and E. J. Zipser, 1980: Cumulonimbus vertical velocity events in GATE. Part I: Diameter, intensity, and mass flux. *J. Atmos. Sci.*, **37**, 2444-2457.

Li F. K., L. Durden, E. Im, A. Tanner, W. Ricketts, W. Wilson, R. Meneghini, T. Iguchi and K. Nakamura, 1993: Airborne rain mapping radar and preliminary observations during TOGA/COARE, Proc. of IGARSS'93, pp. 832-834

Mapes, B. E., and R. A. Houze, Jr., 1992: An integrated view of the 1987 Australian monsoon and its mesoscale convective systems. Part I: Horizontal structure. *Quart. J. Roy. Meteor. Soc.,* **118**, 927-963.

Mapes, B. E., and R. A. Houze, Jr., 1993: An integrated view of the 1987 Australian monsoon and its mesoscale convective systems. Part II: Vertical structure. *Quart. J. Roy. Meteor. Soc.*, **119**, 733-754.

Mapes. B. E., and R.A. Houze, Jr., 1995: Diabatic convergence profiles in western Pacific mesoscale convective systems. *J. Atmos. Sci.*, **52**, 1807-1828.

Morrissey, M.L., and J.S. Greene, 1991: The Pacific atoll raingauge data set. Planetary Geosci. Div. Contrib. 648, Univ. of Hawaii, Honolulu, HI, USA, 45 pp.

NCDC, 1995: Surface Reference Data Center operations and products. NCDC/SRDC, Ashville, NC, USA, 15 pp.

Puri, K. and Davidson, N.E., 1992: The use of infrared satellite cloud imagery data as proxy data for moisture and diabatic heating in data assimilation. *Mon. Wea. Rev.*, **120**, 2329-2341.

Puri, K., Davidson, N.E., Leslie, L.M. and Logan, L.W., 1992: The BMRC tropical limited area model. *Aust. Meteor. Mag.*, **40**, 81-104.

Puri, K. and Miller, M.J., 1990: The use of satellite data in the specification of convetive heating for diabatic initialization and moisture adjustment in numerical weather prediction models. *Mon. Wea. Rev.*, **118**, 67-93.

Raymond, D. J., 1994: Convective processes and tropical atmospheric circulations. *Quart. J. Roy. Meteor. Soc.,* **120**, 1431-1455.

Rosenfeld, D., D. B. Wolff, and D. Atlas, 1993: General probability-matched relations between radar reflectivity and rain rate. *J. Appl. Meteor.*, **32**, 50-72.

Rosenfeld, D., D. B. Wolff, and E. Amitai, 1994: The window probability matching method for rainfall measurements with radar. *J. Appl. Meteor.*, **33**, 682-693.

Simpson, J. (Ed.), 1988: *TRMM: A Satellite Mission to Measure Tropical Rainfall, Report of the Science Steering Group.* National Aeronautics and Space Administration, Goddard Space Flight Center, Greenbelt, Maryland 20771, 94 pp.

Steiner, M., R. A. Houze, Jr., and S. E. Yuter, 1995: Climatological characterization of three-dimensional storm structure from operational radar and raingauge data. *J. Appl. Meteor.,* **34**, 1978-2007.

Takahashi N., H. Kumagai, H. Hanado, T. Kozu and K. Okamoto, 1995: The CRL airborne multiparameter precipitation radar (CAMPR) and the first observation results, Preprints of the 27th Conference on Radar Meteorology, pp. 83-85

Tao, W.K., and J. Simpson, 1993: The Goddard Cumulus Ensemble Model. Part I: Model description. *Terrestrial, Atmospheric and Oceanic Sciences*, **4**, 35-72.

Tiedtke, M., 1984: The effect of penetrative cumulus convection on the large-scale flow model. *Beitr. Phys. Atmoph.*, **57**, 216-239.

Wilheit, T., R. Adler, A. Chang, C. Kummerow, S. Avery, W. Berg, J. Ferriday, E. Barrett, C. Kidd, D. Kniveton, P. Bauer, N. Grody, S. Goodman, R. Spencer, A. Mugnai, W. Olson, G. Petty, A. Shibata, and E. Smith, 1994: Algorithms for the retrieval of rainfall from passive microwave measurements. *Remote Sensing Reviews*, **11**, 1-32.

Xie, P., and P.A. Arkin, 1995: Analyses of Global Monthly Precipitation Using Gauge Observations, Satellite Estimates, and Numerical Model Predictions. Submitted to *J. Clim.*

Yanai, M., S. Esbensen, and J.H. Chu, 1973: Determination of bulk properties of tropical cloud clusters from large-scale heat and moisture budgets. *J. Atmos. Sci.*, **30**, 611-627.

Yuter, S. E., and *R.* A. Houze, Jr., 1995a: Three-dimensional kinematic and microphysical evolution of Florida cumulonimbus. Part II: Frequency distributions of vertical velocity, reflectivity and differential reflectivity. *Mon. Wea. Rev.*, **123**, 1941-1963.

Yuter, S. E., and R. A. Houze, Jr., 1995b: Three-dimensional kinematic and microphysical evolution of Florida cumulonimbus. Part II: Frequency distributions of vertical velocity, reflectivity, and differential reflectivity. *Mon. Wea. Rev.*, **123**, 1941-1963.

A List of Useful Acronyms

4-D	Four Dimensional
AMIP	Atmospheric Model Intercomparison Project
ARMAR	Airborne Mapping Radar
ATOVS	Advanced TIROS Operational Vertical Sounder
BMRC	Bureau of Meteorology Research Center (Australia)
CAMPR	CRL Airborne Multiparameter Precipitation Radar
CAPE	Convective Available Potential Energy
DAS	Data Assimilation System
ECMWF	European Center for Medium Range Weather Forecast
FSU	Florida State University
GAME	GEWEX Asian Monsoon Experiment
GARP	Global Atmospheric Research Programme
GASP	Global Assimilation and Prediction System
GATE	GARP Atlantic Tropical Experiment
GCEM	GODDARD Cumulus Ensemble Model
GCIP	GEWEX Continental Scale International Project
GCM	Global Circulation Model
GEWEX	Global Energy and Water Cycle Experiment
GISS	GODDARD Institute of Space Studies
GMS	Geostationary Meteorological Satellite (Japan)
GPI	Global Precipitation Index
GT	Ground Truth
GTS	Global Telecommunication System
IFA	Intensive Flux Array
IOP	Intensive Observation Period
IR	Infra-red Radiation
LAMBADA	Amazon Region Field Experiment
LIS	Lockheed Information System
MJO	Madden Julian Oscillation
NASA	National Aeronautics and Space Administration
NMC	National Meteorological Center
NOAA	National Oceanic and Atmospheric Administration
NWP	Numerical Weather Prediction
OLR	Outgoing Long-wave Radiation
PR	Precipitation Radar
SCSMEX	South China Sea Monsoon Experiment
SSM/I	Special Sensor Microwave / Imager
SST	Sea Surface Temperatures
TAPS	Tropical Analysis and Prediction System
TSDIS	TRMM Science Data and Information System
TMI	TRMM Microwave Imager
TOGA COARE	Tropical Ocean Global Atmosphere, Coupled Ocean Atmosphere Response Experiment
TOVS	TIROS Operational Vertical Sounder

TRMM	Tropical Rainfall Measurement Mission
UTC	Universal Time Coordinated
VIRS	Visible and Infra Red Sensors
VISIR	Visible and Inra Red
WWB	Westerly Wind Burst